ABCA4 STRUCTURE-FUNCTION RELATIONSHIPS:
ROLE IN STARGARDT DISEASE AND RELATED
RETINAL DEGENERATIVE DISEASES

by

MING ZHONG
B.Sc., Nanjing University, 2002

A THESIS SUBMITTED IN PARTIAL FULFILLMENT OF THE
REQUIREMENTS FOR THE DEGREE OF

DOCTOR OF PHILOSOPHY

in

THE FACULTY OF GRADUATE STUDIES
(Biochemistry and Molecular Biology)

THE UNIVERSITY OF BRITISH COLUMBIA
(Vancouver)

April 2009

ABSTRACT

ABCA4, also known as ABCR or the rim protein, is a member of the family of ATP binding cassette (ABC) proteins expressed in rod and cone photoreceptors. Mutations in ABCA4 have been linked to Stargardt macular degeneration and related retinal degenerative diseases. Studies on *abca4* knockout mice and biochemical investigations have implicated ABCA4 in the transport of retinoid compounds across the outer segment disk membrane.

This dissertation investigation describes various aspects of the structure and function relationships for ABCA4. The mechanisms by which mutations in ABCA4 lead to various retinal degenerative diseases were examined. A pull-down assay was employed to identify the retinoid substrate that interacts with ABCA4. Retinoid compounds that bound to ABCA4 were analyzed by high performance liquid chromatography and radiolabeling methods. When all-*trans*-retinal was added to ABCA4 in the presence of phosphatidylethanolamine, ~1 mol of *N*-retinylidene-phosphatidylethanolamine was bound per mol of ABCA4 with an apparent Kd of 5.4 μM. These results provided the first direct biochemical evidence for the identity of the retinoid substrate for ABCA4. To determine the role of the C-terminus of ABCA4 plays in structure and function, a series of deletion and chimera mutants of ABCA4 was expressed, purified by immunoaffinity chromatography, and their biochemical properties analyzed. Removal of the C-terminal 30 amino acids including a conserved VFVNFA motif resulted in the complete loss in

N-retinylidene-phosphatidylethanolamine substrate binding, ATP photoaffinity labeling, and retinal stimulated ATPase activity and caused retention of ABCA4 in the endoplasmic reticulum. Substitution of the VFVNFA motif with alanines also resulted in the loss in ABCA4 function and mislocalization. In contrast mutants lacking the C-terminal 8, 16 or 24 amino acids but retaining the VFVNFA motif were active. These studies indicated that the VFVNFA motif in ABCA4 is required for proper folding of ABCA4 into a functionally active protein. These results provide a molecular rationale for the disease phenotype displayed by individuals with mutations in the C-terminus of ABCA4. Co-IP studies were performed to identify novel protein interactors of ABCA4, Co-IP studies coupled to mass spectrometry were performed. Rhodopsin and arrestin (including a splice variant of arrestin, p^{44}) were identified and confirmed by western blotting techniques.

This study for the first time has identified the retinoid substrate for ABCA4, demonstrated a role for the C-terminus and has found protein partners of ABCA4.

TABLE OF CONTENTS

LIST OF TABLES

LIST OF FIGURES

LIST OF ABBREVIATIONS

ABC   ATP binding cassette

AMD   age-related macular degeneration

AMP-PNP   adenosine 5′-(β,γ-imido)triphosphates

ATP   adenosine triphosphate

BCA   bicinchoninic acid

BSA   bovine serum albumin

CFTR   cystic fibrosis transmembrane conductance regulator

CHAPS   3-[(3-cholamidopropyl)dimethylammonio]-1-propanesulfonic acid

DTT   dithiothreitol

DOPC   dioleoylphosphatidylcholine

DOPE   dioleoylphosphatidylethanolamine

ECD   extracellular domain

ER   endoplasmic reticulum

GPCR   G protein-coupled receptor

GRK   G protein-receptor kinase

HEPES   (4-(2-hydroxyethyl)-1-piperazineethanesulfonic acid)

HPLC   high pressure liquid chromatography

NBD   nuclear binding domain

N-ret-PE   *N*-ret-PE

PBS   phosphate-buffered saline

PC	phosphatidylcholine
PCR	polymerase chain reaction
PDE	phosphodiesterase
PE	phosphatidylethanolamine
ROS	rod outer segment
RP	retinitis pigmentosa
RPE	retinal pigment epithelium
RT	room temperature
TBS	Tris buffer saline
TMD	transmembrane domain

ACKNOWLEDGEMENTS

To:

my parents

CHAPTER 1: INTRODUCTION

1.1 The Eye and the Retina

The human eye is a remarkably specialized organ. Light from the outside world enters the cornea and is focused by the lens onto the retina at the back of the eye. Photoreceptor cells in the retina convert light signals to neuronal signals. This coordinated process requires accurate light focusing, transmission and sensors. Delicate supporting layers are also in place to help nourish these tissues of the eye (Fig. 1.1).

In vertebrates, the anterior segment is the front third of the eye which consists of the following structures: the cornea, iris, ciliary body, and lens (Fig. 1.1). The anterior segment chambers are filled with aqueous humor. The rest of the eye is filled with vitreous humor.

The posterior segment of the eyeball consists of three main layers: the sclera, choroid, and retina (Forrester et al., 2002; McIlwain, 1996; Rodieck, 1998). The sclera is the tough fibrous outer layer of eye that protects the intraocular contents and helps to maintain the shape of the eye. The clear and light-refracting cornea is continuous with the sclera at the front of the eye. The middle choroid layer is pigmented and contains blood vessels that nourish the outer layers of the retina. Iris and ciliary body are continuous with choroid. The iris controls the amount of light that enters the eye while the ciliary body adjusts the shape of the lens. Finally the inner most layer is the retina, where specialized neuronal cells convert light stimuli to neural impulses to be

transmitted and understood by the brain. The retina consists two primary layers: an inner neurosensory retina and the retinal pigment epithelium (RPE). Developmentally they share the same origin with the epithelial layers covering the ciliary body and posterior iris surface.

1.1.1 Neurosensory Retina

In the neurosensory retina there are three groups of neuronal cells (Fig. 1.2): the photoreceptors, including rods and cones; the intermediate neurons, including bipolar, horizontal, and amacrine cells; and the ganglion cells (Cohen, 1963; Forrester et al., 2002; McIlwain, 1996; Rodieck, 1998). Light signal is sensed by photoreceptor cells, integrated by intermediate neurons and transmitted to the brain by ganglion cells. Cell bodies of rod and cone photoreceptor cells form the outer nuclear layer. The synapses from the photoreceptors extend to the outer plexiform layer, where they establish contact with bipolar and horizontal cells. The cell bodies of bipolar cells and horizontal cells share the inner nuclear layer with those of amacrine cells and Müller cells (glial cells unique to the retina). The inner plexiform layer is the site of synaptic interactions among bipolar, amacrine and ganglion cells. The cell bodies of ganglion cells layer form another nuclear layer and their axons lead to the optic nerve via optic nerve fiber. Müller cells span several layers of the retina. They have tight junctions with plasma membranes of the photoreceptor inner segments forming the outer limiting membrane. At the other end, fused foot processes of the Müller cells form the inner limiting membrane. Outer and inner limiting membranes seal off the retinal components from

potentially harmful materials from both sides.

In the human eye, the central retina is a 5 to 6 mm diameter circular zone. The macula or macula lutea is an oval yellow spot (about 1 mm in diameter) within the center of the central retina. Near its center is the fovea or foveal pit (about 0.25 mm in diameter), a small pit that contains the largest concentration of cone cells and no rod cells, and is responsible for sharp visual acuity (McIlwain, 1996; Yamada, 1969). At the center of the foveal pit, only the cone photoreceptor layer is present, the other layers of the retina are displaced concentrically to the edge of the pit. Outside the central retina is the peripheral retina, where rod photoreceptor cells are much more abundant. This region is responsible for peripheral vision and motion detection, as well as vision in dim light.

1.1.2 Retinal Pigment Epithelium (RPE)

The RPE is a continuous monolayer of epithelial cells. (Forrester et al., 2002). On one side, it is separated from the choroid by Bruch's membrane and on the other side it is in direct contact with the outer segments of the photoreceptors. The RPE layer services and maintains the photoreceptors in five ways: (1) absorption of stray light; (2) phagocytosis of rod, and to a lesser extent cone, outer segments; (3) regeneration of visual pigments; (4) active transport and storage of metabolites; (5) provision of a selectively permeable barrier between the choroid and neurosensory retina. The RPE cells are critical for the function and survival of the photoreceptor cells.

1.1.3 Photoreceptor Cells

There are two types of photoreceptors in the vertebrate retina: the rods and cones, which are named by their shape. Rod photoreceptors are responsible for vision in dim light while cones provide colour vision and acute vision in bright light. In most mammalian retinas, rods are much more abundant than cones (rods outnumber cones 20 to 1, (Osterberg, 1935)) and easier to purify, making the processes taking place in rod cells more extensively studied than those in cones. Both photoreceptor cell types are highly polarized and can be divided into five areas (Fig. 1.3): the outer segment; the thin connecting cilium that links the outer segment and the inner segment and supports transport of molecules between the two; the inner segment which houses the biosynthetic and metabolic machinery of the cell, including the endoplasmic reticulum (ER), Golgi apparatus, and mitochondria; the cell body containing the nucleus; and the synaptic region containing synaptic vesicles and ribbon synapse for communication with intermediate neuronal cells.

1.1.4 Photoreceptor Outer Segment and Its Renewal

The outer segment of a vertebrate photoreceptor cell is a highly specialized compartment within which phototransduction takes place. The rod outer segment (ROS) contains an ordered stack of membranous disks surrounded by a separate plasma membrane (Fig. 1.3). In the cone outer segment, the disk membranes and plasma membrane are continuous. The protein composition of ROS disk membranes has been shown to differ from that of the plasma membrane (Molday and Molday, 1987). Although

4

the visual pigment rhodopsin is the major protein content (over 80%) in both membranes (Papermaster and Dreyer, 1974), proteins such as the cGMP-gated channel (Cook et al., 1989), the Na^+/Ca^{2+}-K^+ exchanger (Reid et al., 1990) and the GLUT-1 glucose transporter (Hsu and Molday, 1991) are predominately, if not exclusively, present in the ROS plasma membranes. Proteins that are unique to the disk membranes will be discussed in the following section.

The stacks of disks are constantly renewed (Young, 1971; Young, 1976), new disks are added at the base of the outer segment at the cilium. At the same time old disks are displaced up the outer segment and are shed off at the tips and engulfed by the apical processes of the pigment epithelium. The spent disks become known as phagosomes in the pigment epithelial cells, which are then broken down by lysosomal enzymes. The disks of cones are believed to be regenerated in a similar but in a slower fashion. The outer limiting membrane discussed in Section 1.2.1 seals off the outer segment, "disposable" parts of the rods and cones, from other parts of the photoreceptor.

As a consequence of aging, non-degradable molecules derived from phagocytized rod and cone membranes accumulate in the RPE cells in all normal eyes. Excessive accumulation of this material, known as lipofuscin, eventually compromises the function of RPE cells and may result in age-related macular degeneration (Young, 1987). Lipofuscin deposits are also seen in the RPE of patients with retinal diseases such as Stargardt disease (see Section 1.4.3).

1.1.5 The Disk Membrane and the Rim Region

Each disk of the ROS is believed to develop from the plasma membrane at the base of the ROS. It is then pinched off into a separately enclosed structure with two closely spaced lamellar membranes joined around the circumference with a highly curved rim (Fig. 1.4). The rim regions of the stack of disks are aligned along the margins of one or more incisures that penetrate toward the center of the disks. The disk membrane encloses a compartment called the disk lumen, the content of which, if any, is not known.

The major membrane protein in the flat region of the disks is rhodopsin. Guanylate cyclase (Liu et al., 1994) and retinol dehydrogenase (Rattner et al., 2000) are generally believed to be localized to the lamellar region. On the other hand, several protein or protein complexes are found exclusively at the rim region. These proteins include the peripherin/rds-rom-1 complex (Bascom et al., 1992; Molday and Molday, 1987; Moritz and Molday, 1996) and ABCA4 (first named as rim protein) (Illing et al., 1997; Papermaster et al., 1978). Mutations in the gene encoding the peripherin/rds subunit have been implicated in autosomal dominant retinitis pigmentosa and macular dystrophy (Section 1.4.2). ABCA4 has been linked to Stargardt disease (Section 1.4.3)

1.2 The Phototransduction Cascade

Phototransduction is a highly complex and regulated process in which the light signal is converted to neural impulses (Molday, 1998; Palczewski, 1994; Pugh and Lamb, 1993). The cascade begins when a photon isomerizes the chromophore of

rhodopsin, 11-cis retinal, to all-trans-retinal resulting in the activated (Meta II) state of rhodopsin (Fig 1.5). Meta II rhodopsin activates the heterotrimeric G protein, transducin, by catalyzing the exchange of GDP for GTP and the dissociation of the α-subunit (Tα) from the $\beta\gamma$-subunits (T$\beta\gamma$). Tα stimulates its effector, cGMP phosphodiesterase (PDE), by binding to the γ-subunit of PDE, releasing the inhibitory constraint on the $\alpha\beta$-subunits. Activated PDE catalyzes the hydrolysis of cGMP to 5'GMP. The decrease in intracellular cGMP concentration causes the cGMP gated channel to close and the rod cell to hyperpolarize. Hyperpolarization of the plasma membrane leads to decreased neurotransmitter release from the photoreceptor synapse. This change is received and integrated by bipolar and horizontal cells. The electrical signal eventually reaches the ganglion cells and is transmitted though the optic nerve to the visual cortex of the brain.

When the cGMP gated channel is closed, intracellular Ca^{2+} levels decrease as the Na^+/Ca^{2+}-K^+ exchanger continues to extrude Ca^{2+} from the outer segment (Nakatani and Yau, 1988). Photorecovery is initiated by inherent shutoff mechanisms of the visual cascade and the calcium mediated negative feedbacks. The shutoff of the visual cascade system includes the following steps: (1) deactivation of Meta II rhodopsin by phosphorylation catalysed by rhodopsin kinase (RK) and the subsequent binding of arrestin (Mendez et al., 2000); (2) hydrolysis of GTP to GDP on α-subunit of transducin, a reaction activated by a protein complex containing regulator of G protein signaling protein 9 (RGS 9), G protein β5 and membrane anchor R9AP (He et al., 1998; Hu and Wensel, 2002; Makino et al., 1999). PDE also returns to its inactive state as a result of

this reaction; and (3) re-association of the α-subunit of transducin with its $\beta\gamma$-subunits to form the inactivated transducin heterotrimer. Low intracellular Ca^{2+} concentrations lead to (i) the activation of guanylate cyclase, a process that is mediated by the calcium-binding protein GCAP (Gorczyca et al., 1995); and (ii) an increase in the sensitivity of the channel to cGMP as a result of the dissociation of calmodulin from the channel. As the cGMP concentration increases, the channels reopen and the cell is returned to its depolarized state. The increase in Ca^{2+} also converts guanylate cyclase to its inactive or basal level of activity.

1.3 The Visual Cycle

Following phototransduction, 11-*cis*-retinal must be regenerated to form rhodopsin. In the vertebrate retina, regeneration of the pigment requires the involvement of the neighboring RPE. The retinoids are transported between the photoreceptor cells and RPE cells in a process termed the visual or retinoid cycle. Regeneration of pigments is a much slower process than photolysis. In humans complete dark adaptation requires approximately 40 min, and conversion of rhodopsin to Meta II rhodopsin requires only 200 fsec (Saari, 2000). However at different levels of illumination (for rods or cones), photoreceptors maintain a steady state level of bleached visual pigments. This means the bleaching and regeneration must be taking place at an equal rate.

Several reactions are involved in regeneration of 11-*cis*-retinal (Fig 1.6). Following the photoexcitation of rhodopsin and the isomerization of 11-*cis*-retinal to all-*trans*-retinal,

all-*trans*-retinal is released from opsin and diffuses to the cytoplamic side of the disk membrane where it is reduced by all-*trans*-retinol dehydrogenase (Ishiguro et al., 1991; Rattner et al., 2000) to its alcohol counterpart: all-*trans*-retinol. All-*trans*-retinol leaves the photoreceptor cell, traverses the interphotoreceptor matrix space, and enters the RPE. In the RPE it is esterified by lecithin-retinol acyltransferase (LRAT) (Saari and Bredberg, 1989). The resulting all-*trans*-retinyl ester is hydrolyzed and isomerized to 11-*cis*-retinol by an enzyme called isomerohydrolase (Deigner et al., 1989; Rando, 1991; Winston and Rando, 1998) (which has been identified as RPE65, see Section 1.4.2). Alternatively, all-*trans*-retinyl ester must be first hydrolyzed to all-*trans*-retinol (the form that entered RPE) by a retinyl hydrolase and then isomerized to 11-*cis*-retinol. 11-*cis*-retinol from either of the two pathways is oxidized to 11-*cis*-retinal by retinol dehydrogenase. 11-*cis*-retinal is then delivered to the photoreceptor. The transport of all-*trans*-retinol and 11-*cis*-retinal in the interphotoreceptor matrix space is facilitated by interphotoreceptor retinoid-binidng protein, IRBP (Gonzalez-Fernandez et al., 2007; Gonzalez-Fernandez and Ghosh, 2008). Inside the RPE, all-*trans*-retinol binds to cellular retinoid-binding protein or CRBP (Bok et al., 1984).

1.4 Retinal Degeneration Diseases

Age-related macular degeneration (AMD) is a common disease that occurs in people over the age of 50 and estimated to affect at least 11 million individuals in the United States (Allikmets et al., 1997a). In contrast, an inherited retinal dystrophy or degeneration is rare and usually qualifies as an orphan disease (which is defined in the

United States as a medical condition affecting fewer than 200,000). Collectively inherited retinal diseases represent a major cause of untreatable vision loss and blindness.

1.4.1 Age-related Macular Degeneration (AMD)

AMD is the leading cause of blindness in the developed world. It can be classified into two forms - dry (nonexudative) and wet (exudative) (Comer et al., 2004). The dry form involves both atrophic and hypertrophic changes of the RPE underlying the macula, as well as deposits, called drusen, beneath the RPE. In wet form, abnormal blood vessels called choroidal neovascular membranes develop in and under the retina, causing fluid and blood leakage and ultimately a blinding scar in a relatively short amount of time.

While age is the primary risk factor, environmental factors are associated with AMD. Studies have shown that cigarette smoking increases risk while fish consumption and omega-3 fatty acid intake reduce risk of AMD (Seddon et al., 2006). AMD also has a significant genetic component to its etiology. Mutations in *ABCA4* (Allikmets et al., 1997a), complement factor H polymorphisms (Haines et al., 2005; Sivaprasad and Chong, 2006) and variants of the *ARMS2* and *HTRA1* gene (Jakobsdottir et al., 2005; Kanda et al., 2007; Yang et al., 2006) have been shown to increase susceptibility to AMD.

There are no proven treatments for dry AMD. For wet AMD treatment options include photodynamic therapy with verteporfin and injection of Lucentis, a humanized

anti-VEGF antibody fragment that inhibits VEGF activity by competitively binding with VEGF (Eter et al., 2006). These treatments cannot restore vision already lost to the disease; however they can help slow disease progression and prevent additional vision loss. They are suitable only for certain types of wet AMD, leaving many people with limited treatment options (Comer et al., 2004).

1.4.2 Inherited Retinal Dystrophies

Various forms of inherited macular dystrophies have been linked to specific genes and their protein products (Bessant et al., 2001; Michaelides et al., 2003) as shown in Table 1.1. The following will briefly discuss inherited retinal dystrophies associated with mutations in rhodopsin, peripherin-2 and RPE65. Stargardt disease and the role of ABCA4 will be discussed in separate sections.

More than one hundred different mutations of the gene encoding the visual pigment, rhodopsin, have been identified. Most of these mutations are associated with autosomal dominant retinitis pigmentosa (RP) (Bessant et al., 2001; Kennan et al., 2005). These mutations are mapped to different regions of the rhodopsin molecule according to a three-dimensional model derived from high-resolution crystallography (Palczewski et al., 2000; Teller et al., 2001). One phenotype-genotype study reported patients with mutations affecting the C-terminal region of rhodopsin have the fastest average rates of decline of visual field area and ERG amplitude. These clinical data support that the C-terminal tail is a key region for proper targeting of rhodopsin to rod outer segments (Sung et al., 1994; Tam et al., 2000). Gene delivery of ribozymes has

been used in a rhodopsin animal mutant to rescue and slow photoreceptor loss and to improve retinal function (Lewin et al., 1998).

Mutations in the *peripherin-2/rds* gene result in a variety of retinal dystrophies, including autosomal dominant RP (Keen and Inglehearn, 1996). Naturally occurring *rds* mice homozygous for the disrupted gene fail to develop outer segments and heterozygous mice produce highly disorganized disk structures (Sanyal and Jansen, 1981; Travis et al., 1989). The protein encoded by this gene was later identified as a protein already known as peripherin-2 (Connell et al., 1991), a membrane protein specifically localized to the rims and incisures of both rod and cone photoreceptor disks (Arikawa et al., 1992; Molday et al., 1987). The discovery of peripherin-2 and rom1 (another disk rim specific protein) forming a oligomeric complex (Bascom et al., 1992; Goldberg and Molday, 1996) provided a molecular-based rationale for the digenic disease inheritance pattern of one specific type of RP requiring a coinheritance of defects in the unlinked *peripherin-2/rds* and *rom-1* alleles (Kajiwara et al., 1994). Further detailed biochemical investigations (Loewen and Molday, 2000; Loewen et al., 2001) revealed peripherin-2 containing tetamers are required for proper targeting of the protein complex to the outer segment, the failure of which cause RP. Peripherin-2 was also shown to interact with the cGMP-gated channel, which is in the plasma membrane (Poetsch et al., 2001). These studies revealed the role of peripherin and rom-1 as key structural proteins critical for the morphogenesis and stability of photoreceptor outer segments. Hope for treatment is also on the horizon for peripherin associated visual loss,

as investigators have found that diseased animals show improved photoreceptor structure and function using gene therapy with *Prph2* (Ali et al., 2000; Schlichtenbrede et al., 2003).

The RPE65, an RPE specific protein, was independently discovered and reported by two groups in 1993(Bavik et al., 1993; Hamel et al., 1993). A few years later, mutations in RPE65 were reported to cause recessive childhood-onset severe retinal dystrophy (Gu et al., 1997) and Leber's congenital amaurosis (LCA) (Marlhens et al., 1997). The latter, an autosomal recessive condition, is the earliest and most severe form of inherited retinopathy, usually characterized by blindness at birth (Foxman et al., 1985; Leber, 1869). *RPE65∕* mice lack rhodopsin, but not opsin apoprotein. In these mice all-*trans*-retinyl esters over-accumulate, whereas 11-*cis*-retinyl esters are absent (Redmond et al., 1998). These results suggested that RPE65 is required for regeneration of 11-*cis*-retinol as part of the visual cycle. In 2001 gene therapy on a naturally occurring animal model *RPE65∕* dog was successfully carried out with a recombinant adeno-associated virus carrying wild-type *RPE65* (Acland et al., 2001). More recently, RPE65 was identified as the long-sought isomerohydrolase in the retinoid visual cycle, which hydrolyzes and isomerizes all-*trans*-retinyl ester into 11-*cis*- retinol (Moiseyev et al., 2005; Moiseyev et al., 2006). In 2008 adeno-associated virus-2-based *RPE65* gene replacement therapy on three young adults with *RPE65*-LCA demonstrated dramatic, albeit imperfect, recovery of rod- and cone-photoreceptor-based vision (Cideciyan et al., 2008; Hauswirth et al., 2008).

1.4.3 Stargardt Disease

Stargardt disease (also known as fundus flavimaculatus or Stargardt macular dystrophy) was first described by Karl Stargardt in 1909. This disease is the most common form of inherited juvenile macular degeneration, affecting approximately 1 in 10,000 children. Inherited as an autosomal recessive trait, it is clinically characterized by a progressive loss in central vision beginning in late childhood and eventually leading to legal blindness (Allikmets et al., 1997b; Gelisken and De Laey, 1985; Stargardt, 1909). Early in the disease course, patients show delayed dark adaptation but otherwise normal rod function (Fishman et al., 1991). Histologically, Stargardt disease is associated with lipofuscin deposition in the RPE layer beneath the macula (Fig. 1.7). These deposits appear as yellowish-tinted flecks. In advanced Stargardt disease, the buildup of lipofuscin causes atrophy of the macula and the underlying RPE. Lipofuscin deposition in RPE cells is also seen in AMD (Kliffen et al., 1997) and some cases of RP (Kolb and Gouras, 1974).

In 1997 as a result of an international collaboration of several groups, researchers identified *ABCR* (later named *ABCA4*) as the gene responsible for Stargardt disease (Allikmets et al., 1997b). *ABCA4* encodes a retinal specific adenosine triphosphate (ATP) binding cassette transporter which is expressed in photoreceptors (Illing et al., 1997). Since then the mechanism of the disease and the role of ABCA4 have been extensively studied with genetic, biochemical and cell biology techniques.

1.5 The Superfamily of ABC Transporters

The ATP-binding cassette (ABC) transporters comprise a superfamily of proteins found in all phyla from bacteria to humans (Higgins, 1992). These transmembrane proteins utilize the energy of ATP hydrolysis to the transport a wide variety of molecules, such as amino acids, peptides, ions, metabolites, vitamins, fatty acid derivatives, steroids, organic anions, phospholipids, and drugs, across extra- and intracellular membranes. (Molday, 2007).

The human genome is known to contain at least 49 genes that encode ABC transporters (Dean and Allikmets, 2001; Dean and Annilo, 2005). These transporters have been organized into seven subfamilies (ABCA-ABCG) based on the amino acid sequence and organization of their NBDs.

1.5.1 ABC Transporter Domain Organization

Proteins are classified as ABC transporters based on the presence of the ATP binding cassette in their nucleotide binding domains (NBDs). Each cassette contains characteristic Walker A and B motifs, separated by approximately 90–120 amino acids, as well as an additional signature (C) motif, located just upstream of the Walker B site (Schneider and Hunke, 1998) (Figure 1.8A). As membrane transporters, this class of proteins contains transmembrane domains (TMDs). Usually each TMD contains 6 or more membrane-spanning α-helices. The functional protein typically contains two NBDs and two TMDs. The two TMDs form a pathway for the translocation of compounds

across the membrane and also provide the specificity for the substrates. The NBDs are located in the cytoplasm and hydrolyze ATP to supply energy for the transport of substrates across the membrane.

A typical prokaryotic ABC transporter has the two TMDs and two NBDs in separate polypeptide chains: two integral membrane proteins each having six transmembrane segments and two peripheral proteins each bearing the ABC unit. These four components as well as a periplasmic (or lipoprotein) substrate binding protein together form a functional transporter (Fig. 1.8B).

Eukaryotic ABC transporters are usually organized either as full transporters containing two NBDs and two TMDs or as half transporters containing only one NBD and one TMD. Examples of full transporters include CFTR (Riordan et al., 1989), P-gycoprotein (Chen et al., 1986), ABCA4 (Illing et al., 1997) and multidrug resistance protein Pdr5p of *Saccharomyces cerevisiae* (Tutulan-Cunita et al., 2005) (Fig. 1.8C). Half transporters must form either homodimers or heterodimers to form a functional transporter. Examples include the peptide transporters involved in antigen presentation - TAP1 and TAP2 (Monaco et al., 1990), and the transporters encoded by the *Drosophila genes* white (*w*), brown(*bw*), and scarlet (*st*), which are involved in the transport of guanine and tryptophan (precursors of the red and brown eye pigments) (Ewart et al., 1994).

1.5.2 Mechanism of Transport

Since 2001 the crystal structures of more than half a dozen intact ABC transporters have been solved, all of which are bacterial ABC transporters made up with two integral membrane proteins (TMDs), two peripheral proteins (NBDs) and a periplasmic substrate binding protein. These ABC transporters include the lipid A-flippase MsbA from *Escherichia coli* and *Vibrio cholerae* (Chang, 2003; Chang and Roth, 2001; Reyes and Chang, 2005; Ward et al., 2007), *E. coli* vitamin B_{12} transporter BtuCD (Hvorup et al., 2007; Locher et al., 2002), and the exporter Sav 1866 bacterial ABC transporter from *Staphylococcus aureus* (Dawson and Locher, 2006), the putative metal-chelate-type ABC transporter encoded by genes HI1470/71 of *Haemophilus influenzae* (Pinkett et al., 2007), putative molybdate transporter ModBC from *Archaeoglobus fulgidus* (Hollenstein et al., 2007), the maltose uptaking system MalFGK of *Escherichia coli* (Oldham et al., 2007), and the high-affinity *E. coli* methionine uptake transporter MetNI (Kadaba et al., 2008). These structural studies have contributed greatly in establishing the basic molecular architecture of ABC transporters and providing a mechanistic scheme that rationalizes ATP-driven transport.

These structures were either found in an extracellular (outward) facing conformation of the TMDs coupled to a closed conformation of the NBDs, reflecting the ATP-bound state, as exampled by Sav1866 (Dawson and Locher, 2006) or in a cytoplasmic (inward) facing conformation of the transmembrane domains coupled to an nucleotide-free and open conformation of the nucleotide-binding domains, as exampled

by ModBC (Hollenstein et al., 2007). Four X-ray structures of MsbA trapped in different conformations, nucleotide bound or nucleotide free, were determined (Ward et al., 2007). Structural comparison of homologous ABC transporters trapped in different conformation and study of the conformational changes between the different states of MsbA, suggest a common alternating access and release mechanism.

The simplest scheme of the transporter mechanism invokes two states (Fig.1.9): an inward-facing conformation with the substrate binding site accessible from the cell interior, and an outward-facing conformation with an extrusion pocket exposed to the external medium. These structural data revealed that tight interaction of the NBDs in the ATP-bound state is coupled to the outward-facing conformation of the TMDs. Hydrolysis of ATP is expected to return the transporter to an inward-facing conformation, again granting access to the binding site from the cell interior. ABC transporters may thus use an "alternating access and release" mechanism first postulated for major facilitator transport proteins (Guan and Kaback, 2006; Jardetzky, 1966).

Key features in this "alternating access and release" model had been already proposed earlier in an "ATP switch model" (Higgins and Linton, 2004), based on a large amount of biochemical data and fewer crystal structures available. These include: (1) ATP binding induces dimerization of NBDs and drives the power stroke for transport; and ATP hydrolysis and release P_i and ADP facilitate dissociation of NBDs to an open dimer; (2) the two NBDs act in concert at a single step rather than influencing distinct steps in the transport cycle. (3) Switching between the open and closed configurations

of the dimer induces conformational changes in TMDs necessary for vectorial transport of substrate across the membrane.

1.5.3 ABC Transporters Function

Within bacteria, ABC-transporters mainly pump essential compounds such as sugars, vitamins, and metal ions into the cell. Within eukaryotes, ABC-transporters mainly transport molecules to the outside of the plasma membrane or into membrane-bound organelles such as the endoplasmic reticulum, mitochondria, etc (Higgins, 1992).

Out of the known 49 human ABC transporters, 16 have a known function and 14 are associated with a defined human disease (Borst and Elferink, 2002; Higgins, 1992). For example, mutations in the cystic fibrosis transmembrane conductance regulator protein (CFTR, ABCC7) cause cystic fibrosis (Anderson et al., 1991; Riordan et al., 1989). Several ABC transporters from different subfamilies are associated with multidrug resistance in tumors, i.e. the ability of certain cancer cells to extrude cytotoxic agents used in chemotherapy. These transporters include MDR1 (also known as ABCB1 or P-glycoportein) (Juliano and Ling, 1976), the breast cancer resistance protein (BCRP1 or ABCG2) (Doyle et al., 1998) and MRP1 (also known as ABCC1) (Keppler et al., 1998; Zaman et al., 1994). The transporter associated with antigen processing (TAP complex, ABCB2 and ABCB3) is critical for the proper functioning of the cellular immune response. It pumps antigenic polypeptides from the cytoplasm into the endoplasmic reticulum, where they are loaded onto MHC class I molecules for subsequent

presentation on the cell surface (Abele and Tampe, 1999). ABCA1, the protein closely related to ABCA4, is involved in lipid transport. Patients with mutations in this gene develop Tangier disease and familial high-density lipoprotein deficiency (Bodzioch et al., 1999; Brooks-Wilson et al., 1999a).

1.6 ABCA4 and Implication in Stargardt Disease

In 1978 Papermaster *et al.* reported the localization of a large intrinsic membrane protein to the rim region of frog ROS disks using immunocytochemical techniques (Papermaster et al., 1978). It was named the rim protein because of its specific localization in the cell. The rim protein has an apparent molecular weight of 290,000 daltons and comprises about 1-3 % of the ROS membrane mass.

After almost 20 years, the rim protein was finally identified as a member of the ABC transporter superfamily (Illing et al., 1997) and the encoding gene, *ABCA4*, was found to be the causal gene of Stargardt disease (Allikmets et al., 1997b). Mutations in this gene were also shown to be involved in AMD (Allikmets et al., 1997a). These discoveries laid the groundwork for researchers to embark on detailed molecular studies of Stargardt disease, one of the most poorly understood of the inherited macular degenerative diseases.

In 1999, Sun *et al.* investigated the ATPase activities of purified and reconstituted ABCA4 in the presence of a panel of compounds, including various geometric isomers of retinal (Sun et al., 1999). The rationale of these experiments was that the known substrates of one extensively studied ABC transporter, the P-glycoprotein, had been

shown to stimulate ATPase activities of the reconstituted transporter (Ambudkar et al., 1992; Sarkadi et al., 1992; Shapiro and Ling, 1994; Urbatsch et al., 1994). These authors identified all-*trans*-retinal as a possible substrate of ABCA4 based on its ability to stimulate the ATPase activity of ABCA4.

Shortly after, Weng *et al.* reported the generation of an *abca4* knockout mouse (Weng et al., 1999). These mice showed delayed dark adaptation (delayed regeneration of visual pigment), increased all-*trans*-retinal following light exposure, elevated PE and protonated *N*-retinylidene-PE (*N*-ret-PE, Schiff base conjugate of retinal and PE) in outer segments and accumulation of a lipofuscin fluorophore di-retinoid-pyridinium-ethanolamine (A2E) in RPE. These observations along with the clinical features of Stargardt disease, especially the accumulation of lipofuscin in RPE, suggested that ABCA4 may function as a putative flippase for *N*-ret-PE. Detailed HPLC analysis of retina from in *abca4* knockout mice and patients with Stargardt disease or AMD (Mata et al., 2000a, b; Parish et al., 1998) revealed the pathway of biosynthesis of A2E with the formation of *N*-ret-PE as the first step.

A model for the role of ABCA4 in Stargardt disease was based on these experiments previously described (Fig. 1.10). All-*trans*-retinal is released into the disk interior after photolysis of rhodopsin, most of which is cleared by passive diffusion through the disk membrane due to its hydrophobic nature. A portion of free all-*trans*-retinal reacts with the primary amine of PE in the disk membrane to form the Schiff base condensation product *N*-ret-PE. ABCA4 uses the energy from ATP

hydrolyses to flip the *N*-ret-PE to the cytoplasmic leaflet of the disk membrane. Upon translocation, *N*-ret-PE is hydrolyzed to release all-*trans*-retinal, which is then reduced to all-*trans*-retinol by retinol dehydrogenase as part of the visual cycle.

If the putative function of ABCA4 is compromised due to mutations in its gene, *N*-ret-PE may accumulate in ROS. As ROS disks is constantly phagocytosized by RPE cells, multi-step reactions in ROS and most likely one hydrolytic activity in RPE phagolysosomes convert *N*-ret-PE to A2E (Sparrow et al., 2008), the prominent constituent of lipofuscin material (Fig. 1.11). This compound accumulates in RPE cells resulting in cell death (Sparrow et al., 2003). Death of RPE causes the death of photoreceptor cells, resulting in Stargardt disease. More recently, a different type of RPE lipofuscin pigments identified as all-*trans*-retinal dimer series was shown to accumulate in even greater abundance than A2E in *abca4* knockout mouse (Kim et al., 2007).

Currently, there is no effective treatment for Stargardt disease. However, understanding of the role of ABCA4 and the disease mechanism is driving development of experimental therapies. Isotretinoin (Accutane), a drug that slows down the synthesis of 11-*cis*-retinal and regeneration of rhodopsin by inhibiting 11-*cis*-retinol dehydrogenase has been tested on *abca4* knockout mice. This compound blocked the formation of A2E and the accumulation of lipofuscin in these animals without causing any significant visual loss (Radu et al., 2003). Very recently, gene therapy trials on *Abca4⁻/⁻* mice using *ABCA4* gene carried by adeno-associated virus (Allocca et al., 2008) or lentiviral vectors (Kong et al., 2008) have shown effective gene delivery and

promising correction of the disease phenotype.

1.7 Thesis Investigation

Although biochemical studies (Ahn et al., 2000; Sun et al., 1999; Sun et al., 2000) and investigations on *abca4* knockout mice (Mata et al., 2001; Mata et al., 2000b; Weng et al., 1999) suggest that ABCA4 mediates the removal of retinoids from disk membranes, at the start of this thesis research there was no direct evidence that ABCA4 functions as a retinoid transporter. Furthermore, the identity of the retinoid substrate of ABCA4 remained to be determined.

Chapter 2 describes the development of a solid phase binding assay to identify retinoid compounds that bind to ABCA4 in the presence of phospholipid. HPLC protocols and radiolabeling methods were adapted to analyze retinoids bound to ABCA4 immobilized on a specific antibody column. Using a spectrophotometric measurement, the protonation state of the bound substrate was also determined. Part of this work has been published (Beharry et al., 2004). Data presented in Figures 2.3 C-D, 2.4, and 2.5 were obtained by Seelochan Beharry.

Chapter 3 focuses the attention on the C-terminal region of ABCA4, the function and importance of which was not fully appreciated as the more extensively studied NBDs and TMDs. C-terminal deletion mutants of ABCA1 (Fitzgerald et al., 2002) and ABCA4 (Stenirri et al., 2006) have been reported to be cause Tangier disease and retinal dystrophy, respectively. A series of 1D4 tagged C-terminal deletion mutants of ABCA4 were generated and expressed in HEK 293 cells. The effect of these mutants on

the binding of ATP and retinoid substrate, ATPase activities, and intracellular localization was investigated. This work has been published (Zhong et al., 2008). All experimental work except part of the immunocytochemistry study was performed by the author.

Chapter 4 demonstrates an all-*trans*-retinal dependant binding of rhodopsin / arrestin complex to ABCA4. Rhodopsin / arrestin complex was specifically co-purified with ABCA4 under certain conditions. The role of this interaction still remains to be elucidated. This work has been presented at the FASEB summer Conference in Snowmass Village, Colorado, June 2006.
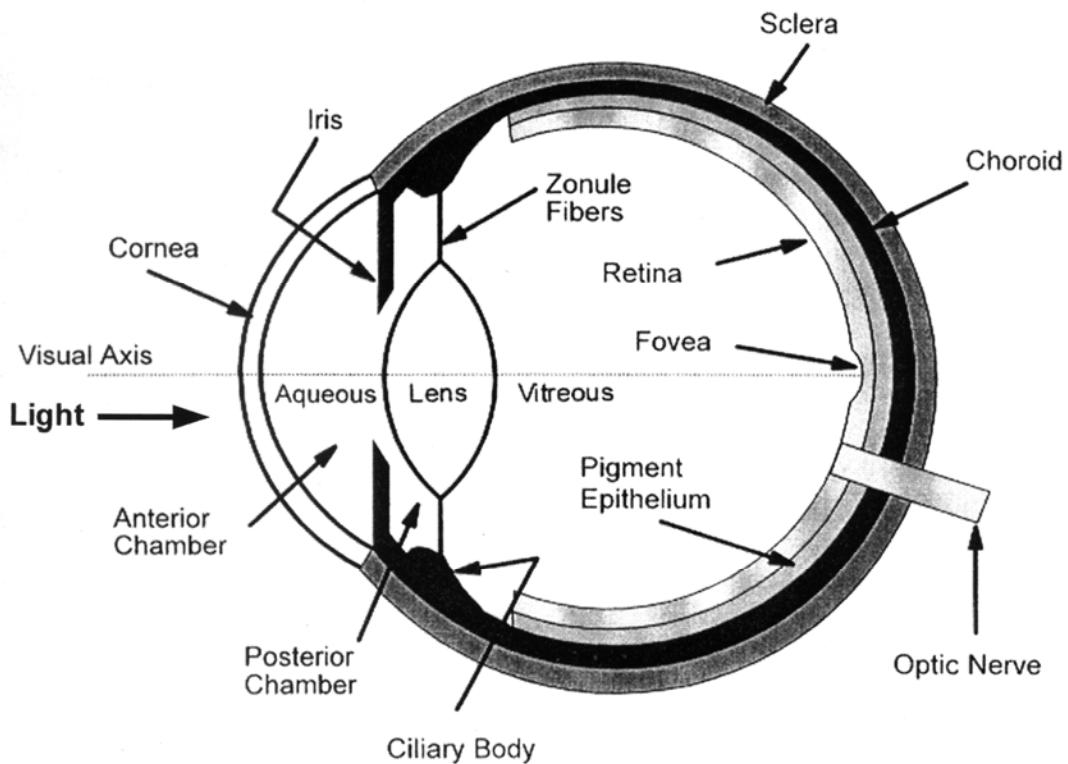
Figure 1.1. Anatomy of the vertebrate eye. Each eye is composed of three layers. The outer layer known as the sclera protects the intraocular contents and maintains the shape of the eye The middle choroid layer is pigmented and contains blood vessels that nourish the outer layers of the retina. The inner most layer is the retina, where photoreceptor cells convert light stimuli to neural impulses to be transmitted to and understood by the brain. Light must first pass through the cornea, aqueous humor, lens, and vitreous humor before reaching the retina. (Figure adapted from McIlwain, 1996.)
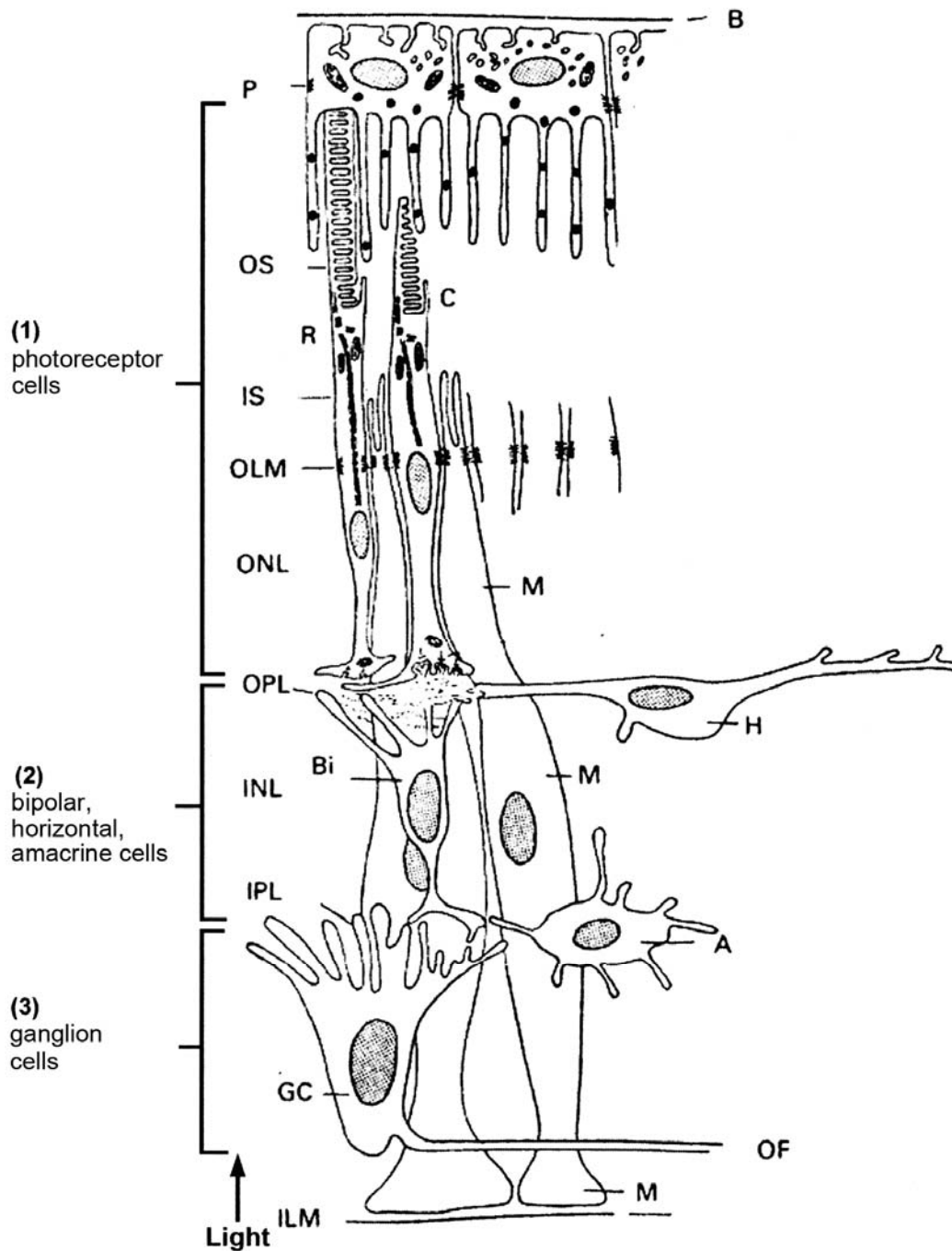
Figure 1.2. Organization of the vertebrate retina. The retina possesses three major groups of neuronal cells: the photoreceptors, including rods and cones; the intermediate neurons, including bipolar, horizontal, and amacrine cells; and the ganglion cells. The abbreviations used are as follows: ILM-inner limiting membrane, GC-ganglion cells, OF-optic nerve fiber, IPL-inner plexiform layer, INL-inner nuclear layer, Bi-Bipolar cells, A –amacrine cells; M-Müller cells, H-horizontal cells, OPL-outer plexiform layer, ONL-outer nuclear layer, OLM-outer limiting membranes, IS-inner segment, OS-outer segment, R-rod cells, C-cone cells, P-retinal pigment epithelial cells, B-Bruch's membrane. (Figure adapted from Cohen, 1963.)
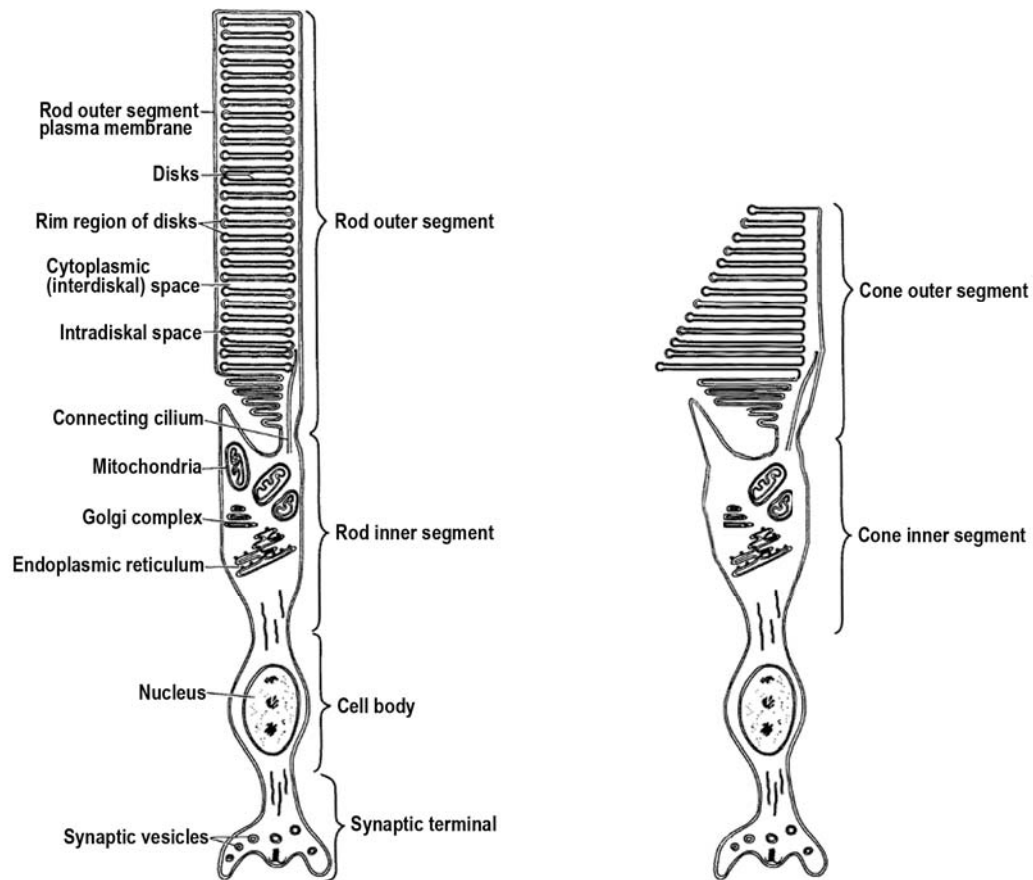
Figure 1.3. The rod and cone photoreceptor cells. There are two well-known types of photoreceptors in the vertebrate retina: the rods and cones. Both photoreceptor cell types are highly polarized and can be divided into five areas: the outer segment, the connecting cilium, the inner segment, the cell body, and the synaptic terminus. The outer segment of the rods contains an array of light sensitive membranous disks that is surrounded by a plasma membrane. The outer segment of the cones is continuous with the disk membrane. (Figure adapted from Molday 2007)
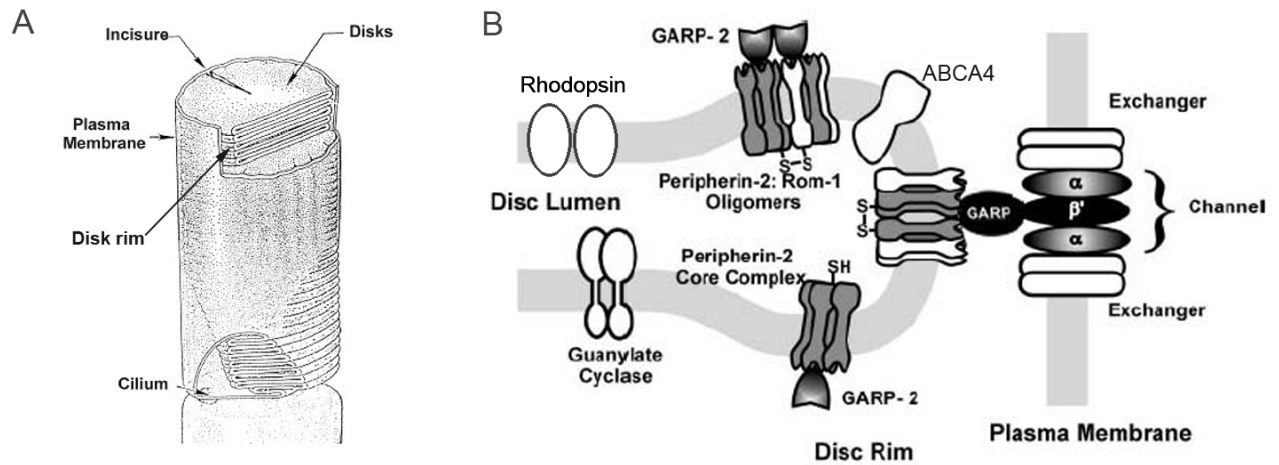
Figure 1.4. The rod photoreceptor disks and the rim region. A, The outer segment of the rods contains an array of light sensitive membranous disks that is surrounded by a plasma membrane. (Figure adapted from Molday, 1998.) **B**, Proteins like the cGMP-gated channel (*Channel*) and the Na^+/Ca^{2+}-K^+ exchanger (*Exchanger*) are predominately present in the plasma membrane. The major membrane proteins in the disks are rhodopsin, guanylate cyclase, peripherin-2-rom-1 complex and ABCA4. (Figure adapted from Poetsch et al,. 2001.)
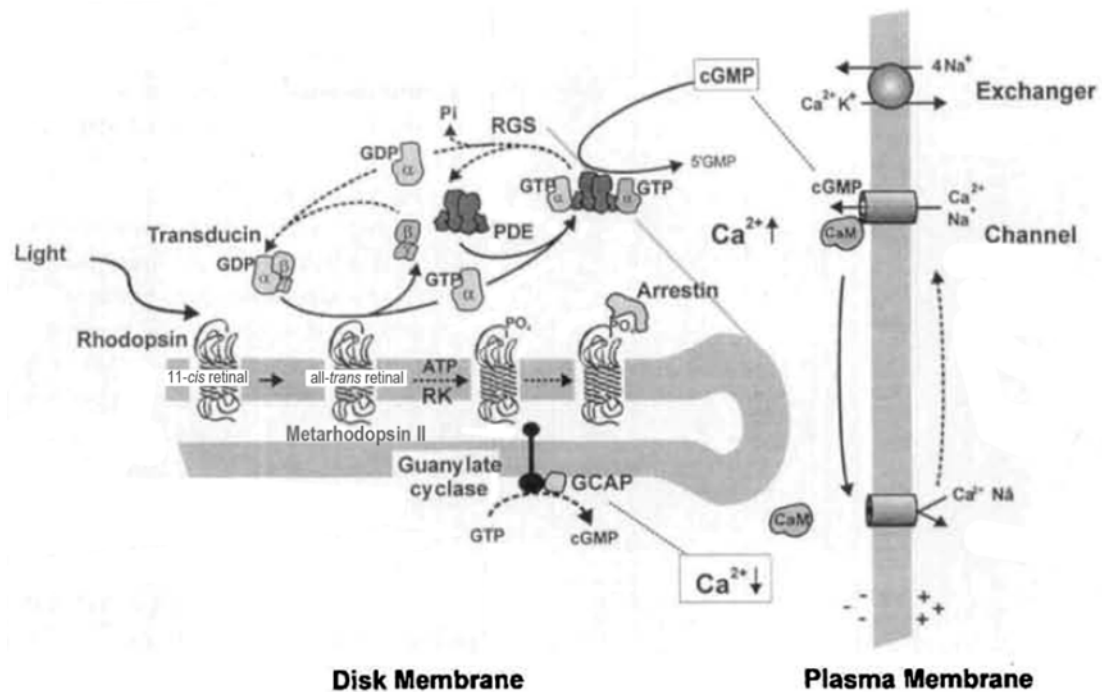
Figure 1.5. The molecular mechanism of phototransduction. A photon of light isomerizes 11-*cis*-retinal attached to rhodopsin to all-*trans*-retinal to produce metarhodopsin II, the activated form of rhodopsin. Metarhodopsin II catalyzes the exchange of GDP for GTP on transducin. The α-subunit of transducin dissociates from the $\beta\gamma$-subunit and in turn activates cGMP-phosphodiesterase (PDE) by removing PDE's inhibitory γ units. Activated PDE catalyzes the hydrolysis of cGMP to 5'-GMP. The decrease in the cGMP concentration causes the cGMP-gated channels to close, preventing Na^+ and Ca^{2+} from entering the cell and causing the cell to hyperpolarize. Intracellular Ca^{2+} concentrations decrease as the Na/Ca-K exchanger continues to extrude Ca^{2+} from the outer segment. Photorecovery is initiated by the inherent shutoff mechanisms of the visual cascade and calcium mediated feedbacks. The shutoff of the visual cascade system include the following steps: (1) deactivation of Meta II rhodopsin by phosphorylation catalysed by rhodopsin kinase (RK) and the subsequent binding of arrestin; (2) hydrolysis of GTP to GDP on α-subunit of transducin and the return of PDE to its inactive state; (3) re-association of the α-subunit of transducin with its $\beta\gamma$-subunits to form the inactivated transducin heterotrimer. Low intracellular Ca^{2+} concentrations lead to (i) the activation of guanylate cyclase via its interactions with the calcium binding protein GCAP; (ii) an increase in the sensitivity of the channel to cGMP as a result of the dissociation of calmodulin from the channel. As the cGMP concentration increases, the channel reopens and the cell is returned to its depolarized state. The solid arrows show the photoexcitation process; dashed arrows show the photorecovery process. (Figure adapted from Molday 1998.)
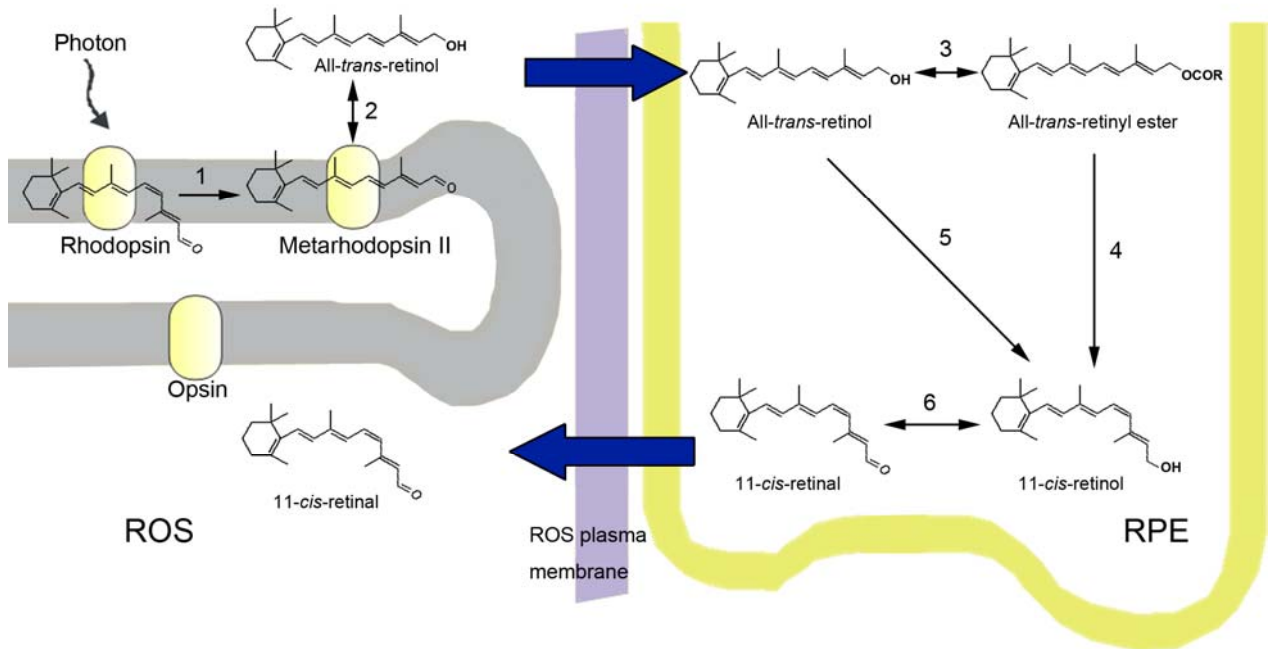
Figure 1.6. The visual cycle and the role of retinal pigment epithelium. A photon of light isomerizes 11-*cis*-retinal of rhodopsin to all-*trans*-retinal producing metarhodopsin II (*reaction 1*) All-*trans*-retinal separates from opsin and is reduced to all-*trans*-retinol by all-*trans*-retinol dehydrogenase (*reaction 2*). All-*trans*-retinol is transported to the RPE where it is esterified to all-*trans*-retinyl ester by lecithin-retinol acyltrasferase (LRAT) (*reaction 3*). All-*trans*-retinyl ester is a substrate for an enzyme called acyltransferase (LRAT) (*reaction 3*). All-*trans*-retinyl ester is a substrate for an enzyme called isomerohydrolase (RPE65), which couples the hydrolysis of the ester to the isomerization to 11-*cis*-retinol (*reaction 4*). Alternatively, the ester can be hydrolyzed back to all-*trans*-retinol (*reverse of reaction 3*) and then isomerized to 11-*cis*-retinol (*reaction 5*). 11-*cis*-retinol is oxidized to 11-*cis*-retinal by the action of 11-*cis*-retinol dehydrogenease (*reaction 6*) and then transported back to the rod outer segment, where it binds to opsin to regenerate rhodopsin. The retinoid binding proteins (CRBP and IRBP) are not shown in the figure. Figure based on (McBee et al., 2000).
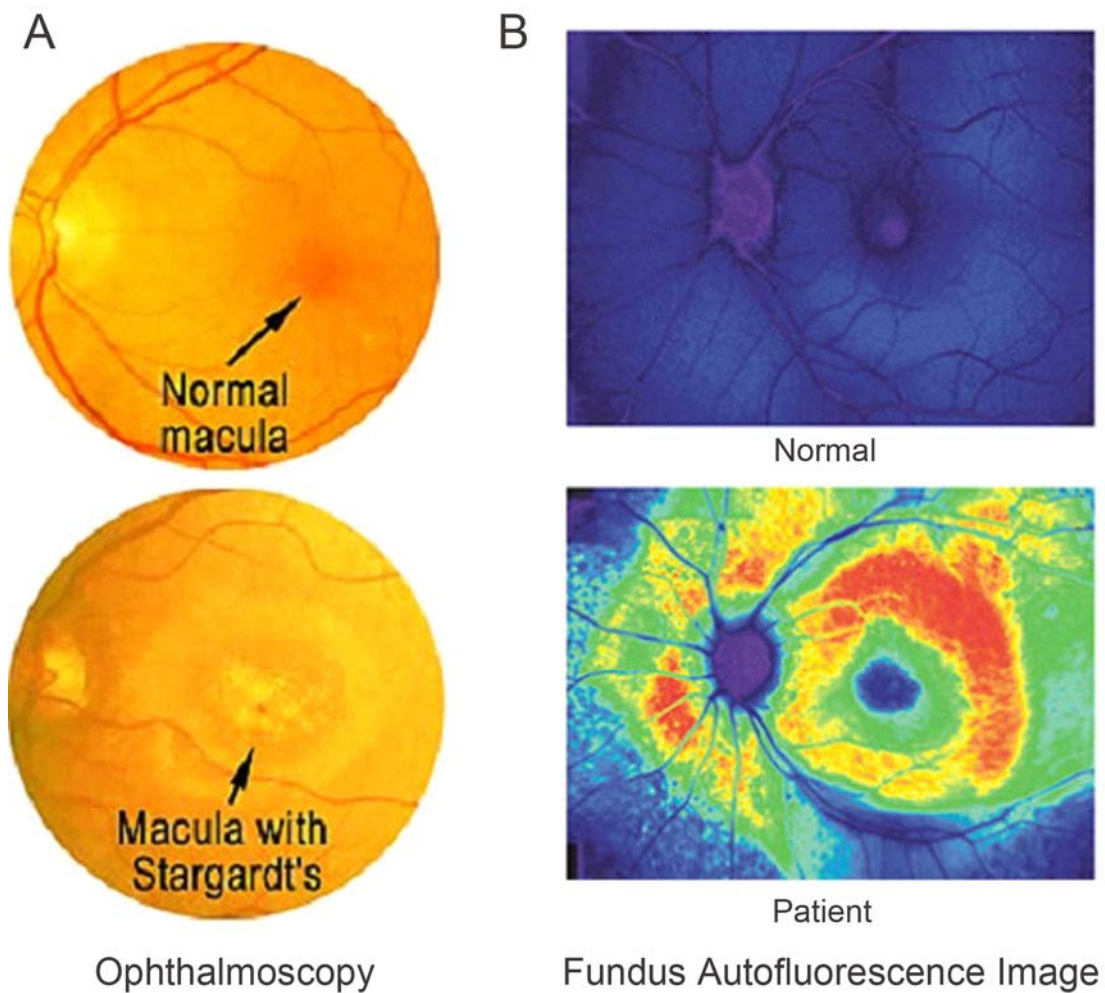
Figure 1.7. Normal and Stargardt's disease affected macula. A, The macular region of a normal individual and that of a Stargardt disease patient. One of the clinical features of Stargardt disease is the appearance of yellowish/orange deposition of lipofuscin material around the macula, as shown. **B**, The lipofuscin material deposits auto-fluoresce as shown in a fundus autofluorescence image. Diagram from (Wabbels et al., 2006).
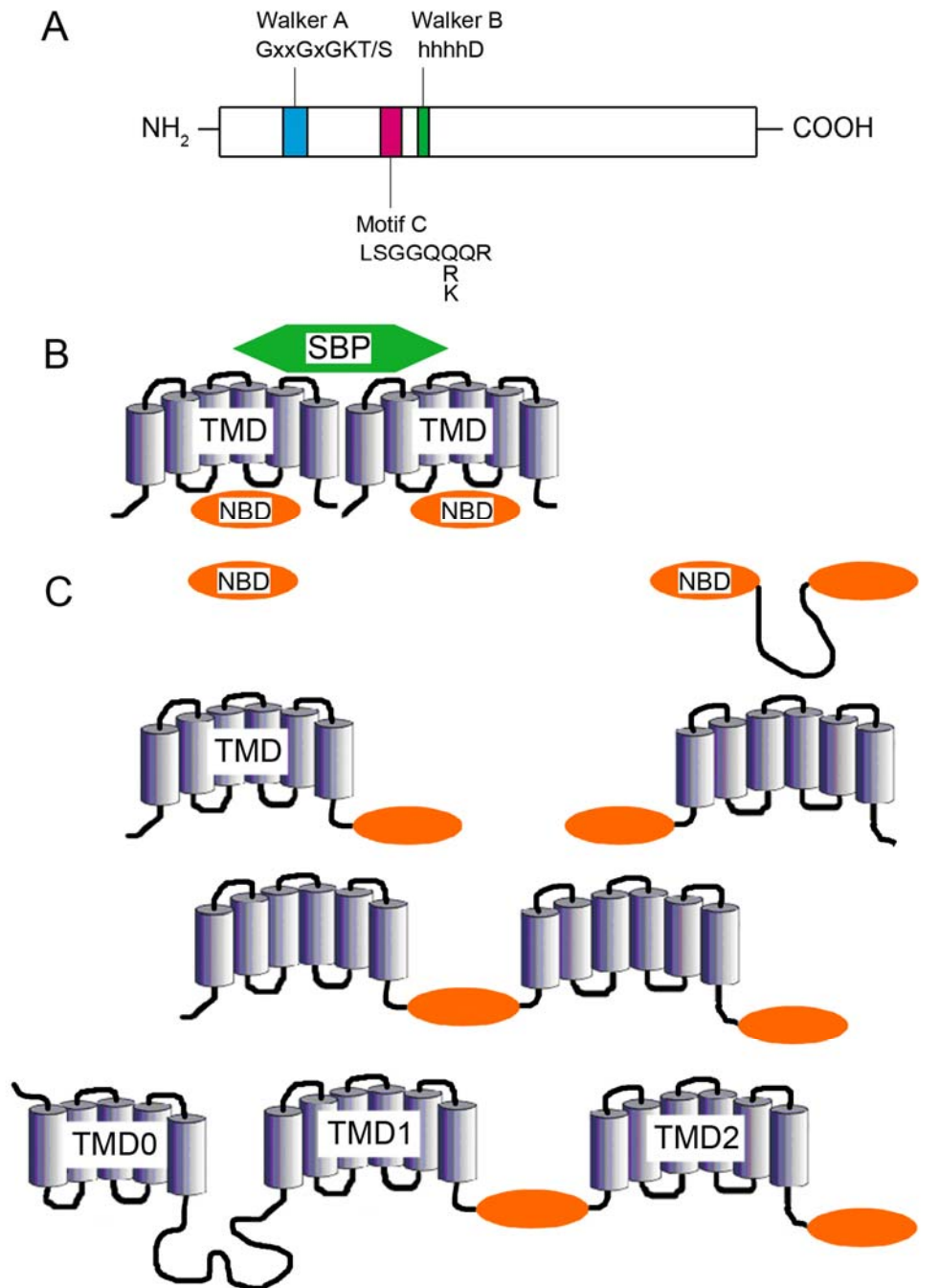
Figure 1.8. Prototype domain arrangements in ABC proteins. A, Linear representation of the nucleotide binding domain (*NBD*). Shown are the Walker A and B motifs and the signature sequence (*motif C*) of ABC transporters. The amino acids are designated by one letter code. '*h*' stands for hydrophobic amino acids and '*x*' can be varied. Figure reproduced from Schneider and Hunke, 1998. **B**, Domain organization of a typical prokaryotic ABC transporter. *SBP* stands for substrate binding protein. **C**, The different organizations of the nucleotide binding domains (*NBD*) and the transmembrane domain (*TMD*) in eukaryotic ABC proteins. The following configurations are shown: NBD, NBD-NBD, TMD-NBD, NBD-TMD, (TMD-NBD)$_2$ and TMD0(TMD-NBD)$_2$. Figure adapted from (Klein et al., 1999).
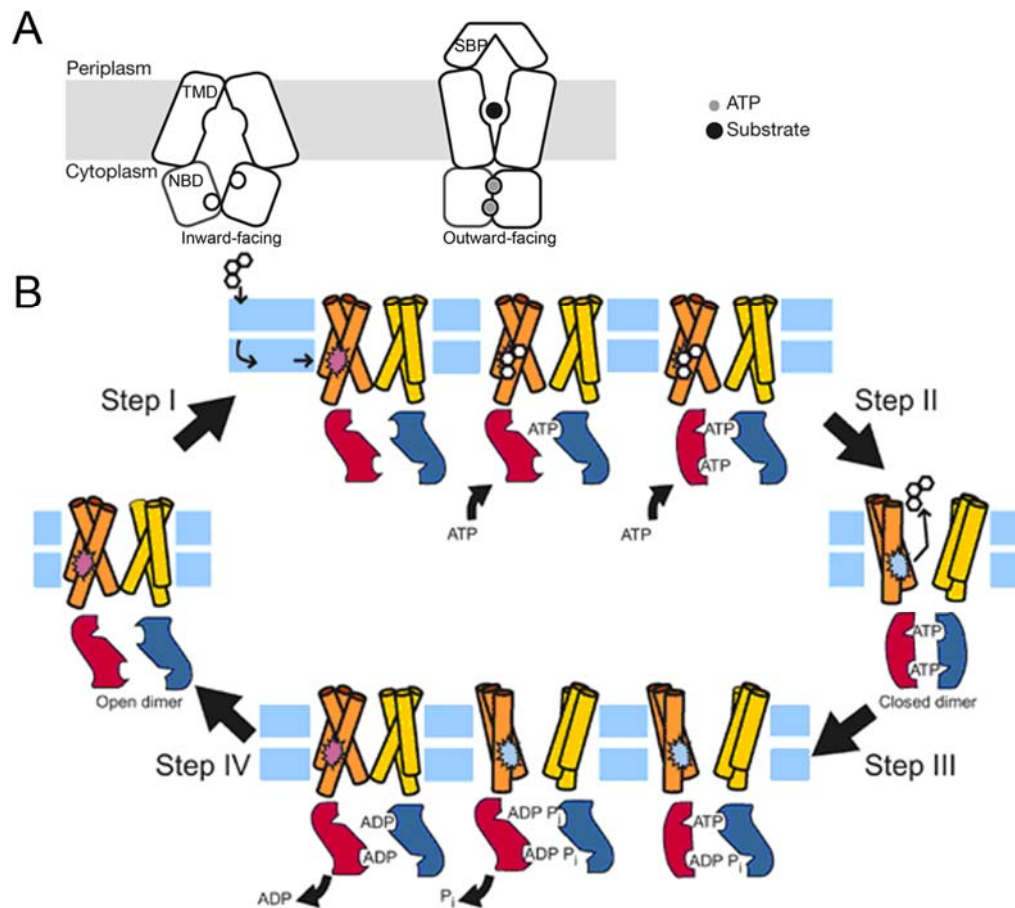
Figure 1.9. Model for mechanism of transport. A, The transport mechanism involves two states: an *inward-facing* conformation with the substrate binding site accessible from the cell interior, and an *outward-facing* conformation with an extrusion pocket exposed to the external medium. Tight interaction of the nucleotide binding domain (*NBD*) in the ATP-bound state is coupled to the outward-facing conformation of the transmembrane domains (*TMD*). Figure modified from (Oldham et al., 2007). **B**, The ATP switch model for the transport cycle of an ABC transporter. The schematic is for a drug exporter. The TMDs, shown as cylinders spanning the membrane, are viewed in the plane of the membrane. The NBDs are shown as shapes at the cytoplasmic face of the membrane and, for clarity, as if viewed from above the membrane. The transporter in its basal state has the NBDs in an open dimer configuration, with low affinity for ATP. The drug-binding site (red) is high-affinity and faces the inner leaflet of the membrane. Step I: the transport cycle is initiated by binding of substrate to its high-affinity site on the TMDs from the inner leaflet of the membrane. The affinity of the NBDs for ATP is increased, effectively lowering the activation energy for closed dimer formation. Two molecules of ATP bind, cooperatively, to generate the closed dimer. The detail here varies for different transporters. For example, in some transporters one nucleotide-binding pocket has a higher affinity for ATP than the other, whereas in other transporters, which pocket is occupied first by ATP may be stochastic. Step II: the closed NBD dimer induces a conformational change in the TMDs such that drug-binding site is exposed extracellularly and its affinity reduced, releasing the bound drug. Step III: ATP is hydrolyzed to form a transition-state intermediate. Hydrolysis of the two ATP molecules is normally sequential, although for some ABC transporters only one ATP may be hydrolyzed. Step IV: sequential release of P_i, and then ADP, restores the transporter to its basal configuration. Figure adapted from (Higgins and Linton, 2004).
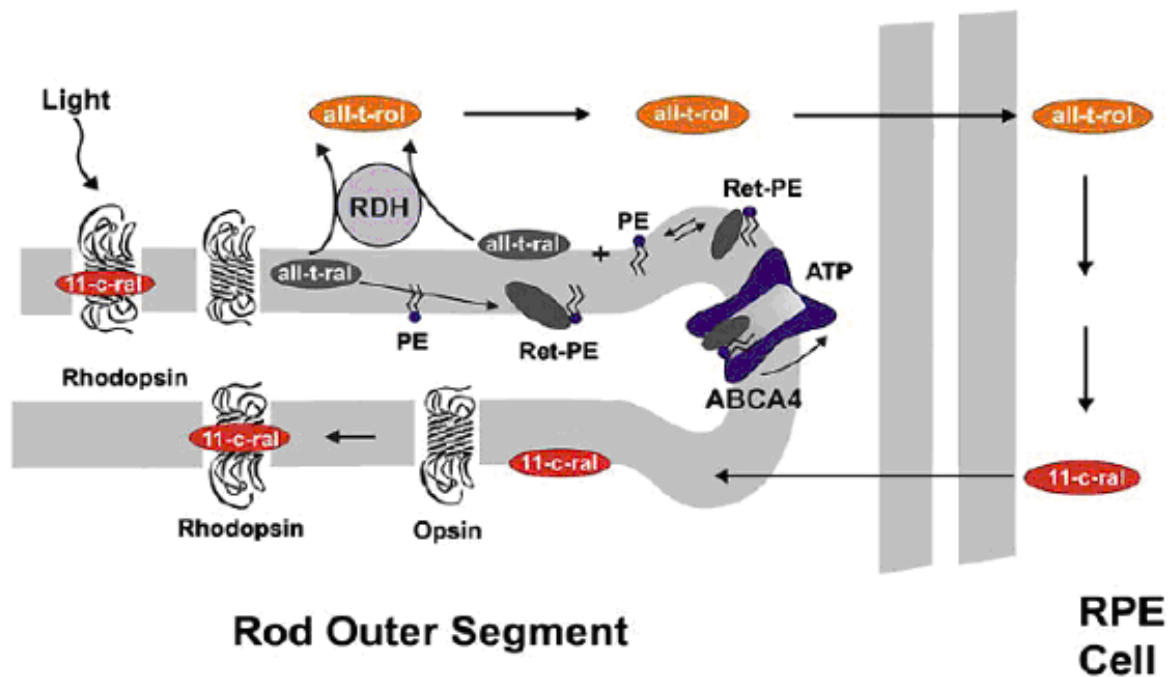
Figure 1.10. Possible functions of ABCA4. ABCA4 is proposed to transport *N*-retinylidene-PE trapped on the lumen side of the disk membrane to the cytoplasmic side where it can dissociate into all-*trans*-retinal and phosphatidylethanolamine (*PE*). All-*trans*-retinal can then be reduced by all-*trans*-retinol dehydrogenase (*RDH*) and recycled back to 11-*cis*-retinal via the visual cycle in the retinal pigment epithelial (*RPE*) cells. All-t-ral – all-*trans*-retinal; Ret-PE – *N*-retinylidene-PE; 11-c-ral – 11-*cis*-retinal; all-t-rol- all-*trans*-retinol. Figure adapted from (Molday, 2007).
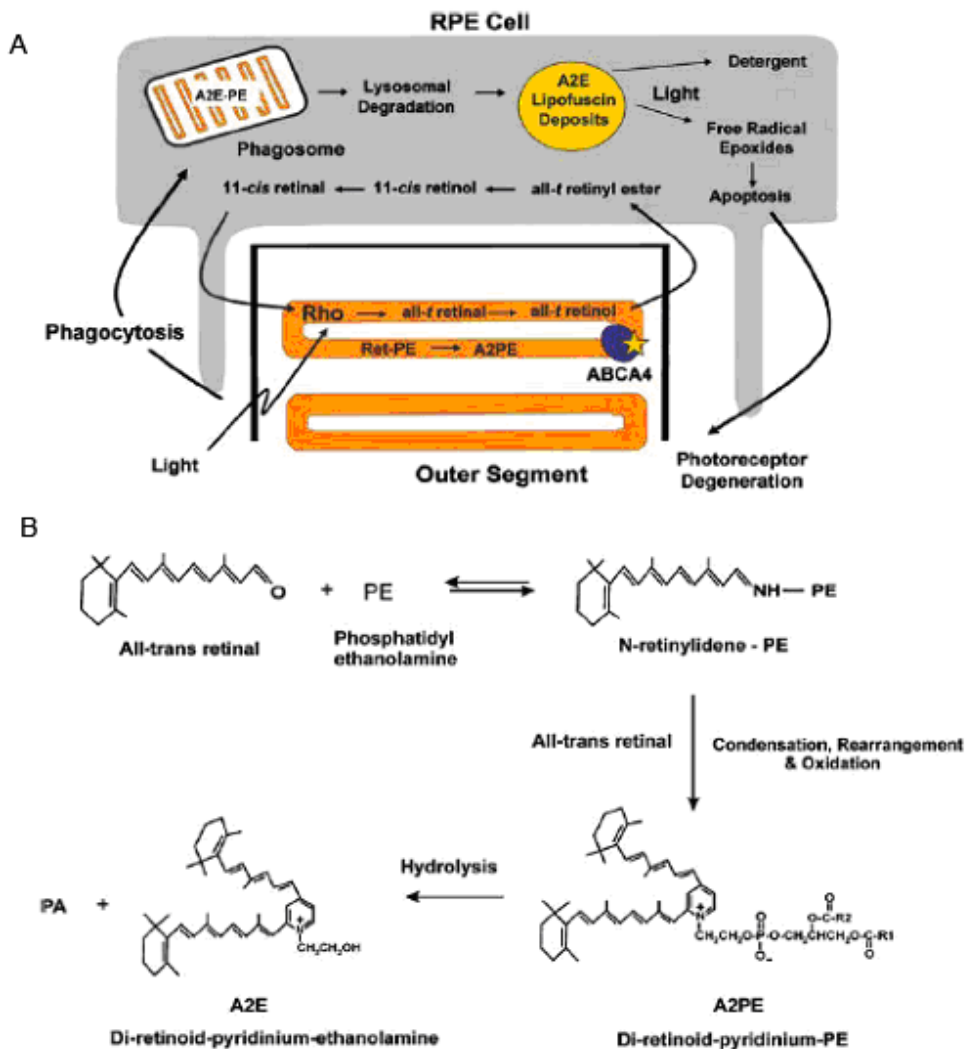
Figure 1.11. Role of ABCA4 in Stargardt's Macular Degeneration. Diagram showing the effect of mutations in ABCA4 on the processing of all-*trans*-retinal following the photobleaching of rhodopsin. All-*trans*-retinal released from rhodopsin can be recycled to 11-*cis*-retinal for the regeneration of rhodopsin through the visual cycle. However, a fraction of all-*trans*-retinal will react with phosphatidylethanolamine (PE) on the lumen side of the disk. Loss in transport activity due to disease-associated mutations, results in the accumulation of *N*-retinylidene-PE on the lumen side of the disk membrane. *N*-retinylidene-PE can react with another molecule of all-*trans*-retinal to produce the diretinoid pyridinium compound A2PE. Upon phagocytosis of the outer segment by the retinal pigment epithelial (RPE) cells, the components of the outer segment are metabolized. However, although A2PE can be hydrolyzed to A2E, it can not be degraded further. Accordingly, A2E will progressively accumulate in RPE cells as lipofuscin deposits. A2E and photo-oxidized products are toxic resulting in apoptosis of RPE cells and consequently photoreceptor degeneration and a loss in vision. B Chemical reactions of all-*trans*-retinal and PE leading to the formation of the diretinoid compounds A2PE generated in photoreceptor outer segments and A2E produced by hydrolysis of A2PE in RPE cells. Figure adapted from (Molday, 2007).

Table 1.1 Selected inherited retinal dystrophies.

Disease-Associated Protein	Inheritance Pattern	Inherited Retinal Dystropies
Phototransduction cascade		
Rhodopsin	AD	RP, congenital stationary night blindness
GNAT1	AD	Congenital stationary night blindness
Phosphodiesterase α	AR	RP
Phosphodiesterase β	AR	RP
Cyclic Nucleotide Gated Channel α	AR	RP
Recovery phase		
Arrestin	AR	Oguchi disease
Rho kinase	AR	Oguchi disease
GCAP	AD	Cone dystrophy
RetGC	AD	CRD
	AR	Leber congenital amaurosis
Structural proteins		
Peripherin	AD	RP, macular dystrophies
	Digenic	RP
ROM1	Digenic	RP
Prominin-like 1	AR	RP
Retinol (vitamin A) metabolism		
RLBP1	AR	RP
RDH5	AR	Fundus albipunctatus
RPE65	AR	Leber congenital amaurosis
ABCA4	AR	Stargardt dystrophy, CRD, RP, AMD
Transcription factors		
CRX	AD	CRD
	AR	Leber congenital amaurosis
NRL	AD	RP
NR2E3	AR	Enhanced S-cone syndrome
Extracellular Proteins		
RS1	XL	X-linked retinoschisis
TIMP3	AD	Sorsby fundus dystrophy
NDP	XL	Norrie disease

Abbreviations used: AD, autosomal dominant; AR, autosomal recessive; XL, X-linked; RP retinitis pigmentosa; CRD, cone-rod dystrophy; AMD, age-related macular degeneration. Modified from (Bessant et al., 2001) and (Michaelides et al., 2003).

CHAPTER 2: RETINOID SUBSTRATE OF ABCA4 [1]

2.1 Introduction

Biochemical studies and investigations on *abca4* knockout mice suggest that ABCA4 facilitates the removal of all-*trans*-retinal derivatives from disk membranes following photoexcitation. This prevents the formation and accumulation of toxic diretinal pyridinium side products in disk membranes in the RPE cells as a result of phagocytosis of the outer segment (Eldred and Lasky, 1993; Mata et al., 2001; Parish et al., 1998; Sun et al., 1999; Weng et al., 1999). But there is no direct evidence to date that ABCA4 functions as a retinoid transporter. Furthermore, the identity of the retinoid substrate that interacts with ABCA4 remains to be determined.

The aldehyde group of all-trans-retinal is known to react with the primary amine of PE to form an equilibrium mixture of the Schiff-base adduct, *N*-ret-PE, and free all-*trans*-retinal (Fig. 2.1A) (Ahn et al., 2000; Anderson and Maude, 1970; Poincelot et al., 1969). It has been proposed that ABCA4 may act as a flippase to translocate *N*-ret-PE from the lumen to the cytoplasmic side of the disk membrane (Sun et al., 1999; Weng et al., 1999). A number of ABC transporters have been reported to actively flip phospholipids across the lipid bilayer, for example, the multidrug-resistant proteins encoded by the mdr2 and mdr3 genes in mice (Ruetz and Gros, 1994; van Helvoort et al., 1996) and MsbA in Escherichia coli (Zhou et al., 1998) Alternatively,

---

[1] A version of this chapter has been published.

Beharry, S., Zhong, M., and Molday, R.S. (2004). N-retinylidene-phosphatidylethanolamine is the preferred retinoid substrate for the photoreceptor-specific ABC transporter ABCA4 (ABCR). J Biol Chem *279*, 53972-53979.

ABCA4 could actively extrude all-trans-retinal from the disk membranes analogous to the ATP-dependent efflux of hydrophobic compounds from membranes by P-glycoprotein (Gottesman et al., 1995).

In this study, a solid-phase assay has been developed to find potential retinoid compounds that bind to ABCA4 in the presence of phospholipids. This assay in conjunction with HPLC and radiolabeling methods shows that ABCA4 preferentially binds *N*-ret-PE in the absence of adenine nucleotide triphosphates. The specific binding to ABCA4 and ATP-dependant release of *N*-ret-PE suggests that *N*-ret-PE is the substrate that is actively transported by ABCA4.

It is also known that the Schiff-base bond in *N*-ret-PE can be protonated (Fig. 2.1A) (De Pont et al., 1970). The two forms of *N*-ret-PE have distinctive absorption spectra (Fig. 2.1B). To determine the protonation state of the substrate bound to ABCA4, spectrophotometric measurements were carried out. The absorption spectra of ABCA4 with substrate bound or the apoprotein were recorded. The difference spectrum between the two is deduced to determine the absorption of the bound *N*-ret-PE and reveal its protonation state.

The spectrophotometric assay is also used to study the quantities of and the effect of nucleotides on *N*-ret-PE bound to ABCA4. Both ATP and nonhydrolyzable nucleotide analogs, release *N*-ret-PE from ABCA4 at 22 ° C. This suggests a transport mechanism in which the binding of ATP directly triggers the translocation of the substrate.

2.2 Methods

2.2.1 Reagents and Solutions

All-*trans*-retinal, all-*trans*-retinol, soybean phospholipids, and CHAPS were purchased from Sigma (St Louis, MO). The phospholipids (DOPE and DOPC) were from Avanti Polar Lipids (Alabaster, AL). Radiolabeled sodium borohydride ($[^3H]NaBH_4$) was obtained from PerkinElmer Life Sciences (Waltham, MA) and Complete Protease Inhibitor was from Roche Applied Sciences (Indianapolis, IN). All organic solvents (chloroform, hexane, and methanol) were HPLC grade and water was distilled and deionized.

The composition of buffers was as follows: hypotonic buffer: 10 mM HEPES, pH 7.5; solubilization buffer: 50 mM HEPES, pH 7.5, 0.1 M NaCl, 18 mM CHAPS, 1 mM DTT, 3 mM $MgCl_2$, 10% glycerol, 0.32 mg/ml DOPE, and 0.32 mg/ml DOPC; column buffer: 50 mM HEPES, pH 7.5, 0.1 M NaCl, 10 mM CHAPS, 1 mM DTT, 3 mM $MgCl_2$, 10% glycerol, 0.32 mg/ml DOPE, and 0.32 mg/ml DOPC. All-*trans*-retinal concentration in ethanol was determined spectrophotometrically using an extinction coefficient of 42,900 $M^{-1}cm^{-1}$.

2.2.2 Rod Outer Segment Preparation

Bovine ROS were prepared under dim red light as follows. One hundred bovine retinas were gently inverted 60 times in 40 ml of homogenizing buffer containing 20% (w/v) sucrose, 20 mM Tris-HCl, pH 7.4, 10 mM taurine, 10 mM β-D-glucose and 0.25 mM $MgCl_2$. The retinas were put on top of a Teflon filter (300 μm mesh). The resulting

filtrate containing sheared ROS was added to 6 step gradients made up with 28% and 34% (w/v) sucrose. The samples were centrifuged in a SW 28 rotor (Beckman Instruments, CA) at 26,000 rpm for 1 hr at 4°C. The ROS band was collected from the top of the 34% sucrose layer of each gradient and washed with 30 ml of homogenizing buffer by centrifuging in a Sorvall SS-34 rotor at 10,000 rpm for 10 min. The washed ROS were resuspended in 1 ml of homogenizing buffer containing complete protease inhibitor (Roche) and pooled together. An extra 2 ml was used to rinse the centrifuge tubes. The total of 8 ml of ROS in homogenizing buffer was divided into 1 ml aliquots and wrapped with aluminum foil before freezing down in -80°C freezer. The protein concentration was determined by bicinchoninic acid (BCA) assay and was approximately 8 mg/ml.

2.2.3 Generation of 3F4 Coupled Sepharose Beads

The Rim 3F4 monoclonal antibody recognizing an epitope near the C-terminus of bovine ABCA4 was generated as described in Illing *et al.,* 1997. Approximately 2 mg of antibody per 1 ml of beads was dialyzed in three changes of borate buffer (20 mM, pH 8.4) at 4°C over night. The Sepharose 2B beads (Amersham Biosciences) were first washed three times with three volumes of water and then activated by CNBr as previously outlined (Cuatrecasas, 1970). The activated beads were washed four times with cold borate buffer by centrifugation in a clinical centrifuge for 3-5 min and subsequently incubated with the 3F4 monoclonal antibody at 2 mg/ml beads. After 3-4 hours of incubation at 4°C on a rotating wheel, the beads were centrifuged down. A_{280} of

the supernatant was measured with a spectrophotometer to determine the coupling efficiency (usually >95 % for 3F4 antibody). The 3F4 beads were washed twice with Tris buffered saline (TBS: 20 mM Tris, 150 mM NaCl, pH 8.0) and washed once more with TBS containing 50 mM glycine (in order to react and block any remaining activated sites on the beads). The 3F4 beads were stored in an equal volume of TBS and 0.01% NaN$_3$ at 4°C.

2.2.4 Synthesis and Purification of *N*-ret-PE and *N*-retinyl-PE

N-ret-PE, the Schiff base conjugate of retinal and PE, was synthesized as described (Ahn et al., 2000) with minor modifications. Briefly, 10 μmol of all-*trans*-retinal was mixed with 10 μmol PE in 0.5 ml chloroform and incubated for 3 hrs at 37 °C shielded from light. For the preparation of *N*-retinyl-PE, the reduction product of *N*-ret-PE, a 1000-fold molar excess of NaBH$_4$ was added following the initial incubation period.

To purify the product, 100 μl of the mixture was injected to a Phenomenex Primesphere 5 C18 HC column (150 × 3.2 mm) by a procedure adapted from Parish *et al.* (Parish et al., 1998). The samples were eluted using a continuous gradient of 85% methanol in water to 100% methanol over a period of 30 min, followed by isocratic elution with 100% methanol (all solvents also contained 0.1% trifluoroacetic acid), at a flow rate of 0.5 ml/min.

2.2.5 Analysis of Retinoids Bound to ABCA4 Using HPLC

For each experimental point, 12-15 mg of ROS was solubilized in 10 ml of

solubilization buffer (50 mM HEPES, pH 7.5, 0.1 M NaCl, 18 mM CHAPS, 1 mM dithiothreitol, 3 mM $MgCl_2$, 10% glycerol, 0.32 mg/ml DOPE and 0.32 mg/ml DOPC) and 0.2 mg/ml of Complete Protease Inhibitor. The solution was stirred at 4 °C for 30 min and centrifuged at 40,000 rpm for 10 min at 4 °C in a Beckman TLA100.4 rotor. The supernatant was used directly for immunoaffinity purification of ABCA4. All the above procedures were done in the dark or under dim red light.

For immunoaffinity isolation of ABCA4, 0.7 ml of gravity packed Rim 3F4-Sepharose 2B beads in a Bio-Rad Econo column (7.0 mm diameter x 4.0 cm length) was washed with column buffer. Solubilized ROS membranes (~12 ml) were added to the Rim 3F4-Sepharose matrix in a column and mixed on a rotating wheel. After 1 h at 4 °C, the column was washed extensively with column buffer to remove unbound protein. All procedures were carried out under dim lighting conditions.

The retinoid (all-*trans*-retinal, all-*trans*-retinol, or *N*-retinyl-PE) in methanol was added to the ABCA4-Rim 3F4-Sepharose beads at 4 °C under dim light to produce the desired final retinoid concentration and a methanol concentration of less than 2%. After 30 min, the column was washed with 2 ml of column buffer by low speed centrifugation in a clinical table top centrifuge. The washing procedure was repeated 5 more times. The washes from the column were retained for HPLC analysis to monitor the loss in unbound retinoid. In general no retinoid was detected after the 5th wash. The bound substrate was extracted from immobilized ABCA4 as follows. The column matrix was placed in a test tube and 2 ml of an ice-cold 1:1 mixture of chloroform and methanol was

added. The contents of the tube were gently pipetted up and down with a Pasteur pipette so as to prevent producing of bubbles and oxidation as described by Garwin and Saari (Garwin and Saari, 2000). An additional 2 ml of ice-cold hexane was added and mixed as above. After the solution was centrifuged for 3-5 min to generate a phase separation, the upper hexane phase was carefully removed and the extraction procedure was repeated twice. The hexane phases from the 3 extractions were pooled and re-extracted with 1.5 ml of ice-cold distilled and deionized water. Finally, the hexane phase was collected, dried, sealed under nitrogen, and stored overnight in the dark at -80 °C. The following day, the sample was resuspended in 300-400 µl of ice-cold methanol and 50 to 100 µl was loaded onto the same Phenomenex Prime-sphere 5 C18 HC column (150 x 3.2 mm) and eluted as described in Section 2.2.3. Bound retinoids were identified by comparison of retention time and spectra with standards run on the same column.

To ensure that we determined the specificity of retinoid binding to ABCA4 correctly, several controls were performed: 1) buffer without both solubilized ROS and retinoid substrate; 2) buffer with the retinoid substrate, but without solubilized ROS; and 3) buffer with solubilized ROS, but without retinoid substrate were added to separate immunoaffinity columns. No detectable retinoid compounds were extracted from the immunoaffinity matrix in these control samples.

2.2.6 Tritiation of All-*trans*-retinal

All-*trans*-retinal was tritiated by reduction with [^{3}H]NaBH$_4$ followed by oxidation

with MnO_2 according to a modified protocol from Garwin and Saari (Garwin and Saari, 2000). [^{3}H]NaBH$_4$ (5 mCi, 0.33 μmol; American Radiolabeled Chemicals, MO) in 100 μl of 50 mM NaOH was added to 0.13 mg or all-*trans*-retinal dissolved in 0.13 ml of ethanol. The capped tube was mixed at room temperature (RT) for 15 min. Four hundred μl of 50 mM NaOH in water and 600 μl ethanol were added to bring up the volume. The mixture was extracted with 1 ml of hexane and the extraction was repeated. The upper phases from 2 extractions were combined and mixed with 30 mg MnO_2. The contents were stirred for 15 min at 37°C. After spinning down the MnO_2 particles, products of the reaction in 2 ml hexane was dried down to 200 μl. One hundred μl of the sample was injected onto a Supelcosil LC-Si normal phase column (1.5 cm × 4.6 mm, 3 μm particle size; SUPELCO, PA). The samples were eluted isocratically at a flow rate of 1 ml/min with hexane for 5 min and then with 10% ethyl acetate in hexane for 15 min.

2.2.7 Analysis of Retinoid Bound to ABCA4 Using a Radiolabel Assay

This assay required less than one-tenth the amount of ROS and Rim 3F4-Sepharose. Each experiment was carried out in triplicate for each point determination. Approximately 60 μl of gravity packed Rim 3F4-Sepharose 2B beads were added to the inner unit of an Amicon Ultrafree MC 0.45-μm centrifugal filter device. The matrix was washed thoroughly with column buffer by low speed centrifugation. Approximately, 0.6 ml of dark-adapted, CHAPS-solubilized ROS was added to the Rim 3F4-Sepharose 2B beads. The filter device was sealed with parafilm, wrapped in aluminum foil, and placed on a rotating wheel at 4 °C for 60 min. The beads were then

washed 6 times with 0.5 ml of column buffer by centrifugation to remove unbound protein.

[^{3}H]All-*trans*-retinal (5-10 x 10^6 dpm per 0.5 ml of reaction mixture at a final all-*trans*-retinal concentration of 10 µM or as otherwise indicated) was added to the ABCA4-Rim 3F4-Sepharose. The specific activity of the [^{3}H]all-*trans*-retinal ranged from 500 to 5000 dpm/pmol. The filtration device was sealed as above and rotated at 4 or 22 °C for 30 min. Duplicate 5-µl samples were removed to determine the specific activity of the labeled sample by scintillation counting. The inner device was placed in a disposable culture test tube (13 x 100 mm) and centrifuged for 30 s in a clinical centrifuge. The inner device was then inserted into a second test tube and washed twice with 0.5 ml each of column buffer by centrifugation. For scintillation counting, 25 µl each of the combined eluate was removed. The washings were repeated 2 more times to remove the unbound labeled all-*trans*-retinal. The last wash typically showed only background counts. Each inner filtration device containing the immobilized ABCA4 with bound labeled retinoid was placed in a 13 x 100-mm culture test tube. The [^{3}H]all-*trans*-retinal was extracted from the matrix with 0.5 ml of ice-cold methanol for 5 min on ice followed by centrifugation. A second extraction with 0.5 ml of ice-cold methanol was performed and the two methanol extractions were pooled. The methanol extraction procedure was repeated 2 more times. The counts of the methanol extractions (of each sample) were determined by liquid scintillation counting. Each value is the average of triplicate experiments.

In general, the procedures were carried out under dim light to prevent any

photoreaction of the retinoids. Controls were treated in the same way except that the immunoaffinity matrix was not treated with solubilized ROS, *i.e.* had no added ABCA4. The background counts were typically less than 10% of the test sample, and subsequently subtracted to determine the amount of specifically bound retinoids.

2.2.8 UV-VIS Spectrophotometric Measurement

Immobilized ABCA4 containing bound retinoid (ABCA4 from 4 mg of ROS purified with 200 μl 3F4 Sepharose beads in the inner unit of an Amicon Ultrafree MC 0.45-μm filtration device) was eluted with 160 μl column buffer with 0.2 mg/ml 3F4 peptide. The control column was treated with 0.5 mM ATP to release bound retinoid. The elution was measured with a Cary 4000 UV-Vis spectrophotometer (Varian, Palo Alto, CA).

2.2.9 Nucleotide-dependant Release of Retinoids from ABCA4

The spectrophotometric assay was also used to determine the amount of *N*-ret-PE bound to ABCA4 using a molecular extinction coefficient of 33,800 M^{-1} cm^{-1} at 370 nm (Anderson and Maude, 1970). 0.5 mM ADP or AMP-PNP was used to replace ATP to investigate the release of retinoids from ABCA4 by these nucleotides. Immobilized ABCA4 containing bound retinoid was suspended in 0.5 ml of column buffer. ATP or other nucleotide was added to obtain the final nucleotide concentration. The filtration device was rotated for 15 min at 4 or 22 °C, after which the beads were washed four times with 0.5 ml column buffer. ABCA4 with bound substrate was eluted with specific 3F4 peptide at 0.2 mg/ml in column buffer. ABCA4 without treatment of nucleotide represented the full binding capacity. Rim 3F4-Sepharose column eluted with

no 3F4 peptide was used as zero binding.

2.2.10 SDS-PAGE and Protein Quantification

The amount of ABCA4 bound to the Rim 3F4-Sepharose matrix was determined by SDS-gel electrophoresis as follows. The immunoaffinity matrix was collected after retinoid extraction, extensively washed with column buffer, and incubated with 500 µl of SDS-PAGE loading buffer (without β-mercaptoethanol) for 20 mins at RT. The matrix was placed in a column and spun for 5 min in a clinical centrifuge to collect the eluate. An additional 500 µl of SDS-PAGE buffer was added and the elution procedure was repeated. The eluates were combined and run on an 8% SDS-polyacrylamide gel, together with bovine serum albumin standards of known concentrations. The gels were stained with Coomassie blue and densitometry was performed on a LICOR infrared imager. The concentration of ABCA4 was determined from a standard curve generated from the bovine serum albumin standards. Western blots were carried out as previously described to verify the identity of ABCA4 (Illing et al., 1997).

2.3 Results

2.3.1 Isolation of ABCA4 on a Rim 3F4-Sepharose Affinity Column

An immunoaffinity matrix consisting of the Rim 3F4 anti-ABCA4 monoclonal antibody coupled to Sepharose 2B was used to isolate ABCA4 from bovine ROS (Ahn and Molday, 2000; Illing et al., 1997). Fig. 2.2 shows a Coomassie blue-stained gel and a western blot of the ROS starting material (*lane 1*) and the fraction that selectively binds to the immunoaffinity matrix (*lane 2*). The bound fraction contained one major

stained protein that migrated with an apparent molecular mass greater than 220 kDa. The Western blot labeled with the Rim 3F4 antibody confirmed that this major protein is ABCA4.

2.3.2 Synthesis of *N*-ret-PE and *N*-retinyl-PE

N-ret-PE and *N*-retinyl-PE were synthesized and purified by HPLC. *N*-ret-PE eluted at approximately 37 min, and *N*-retinyl-PE at 49 min. *N*-Ret-PE eluted from the column as the protonated Schiff base with an absorption maximum of 450 nm. Upon deprotonation of the Schiff base by addition of 5 N NaOH, the absorption maximum shifted to 370 nm (Fig. 2.1B), consistent with earlier observations (Anderson and Maude, 1970). The absorption maximum of the *N*-retinyl-PE peak was 329 nm.

2.3.3 Retinoid Binding to ABCA4 as Measured by HPLC

All-*trans*-retinal is known to react with PE to form an equilibrium mixture of *N*-ret-PE and free all-*trans*-retinal (Ahn et al., 2000; Poincelot et al., 1969). To determine which retinoid preferentially binds to ABCA4, all-*trans*-retinal was added to CHAPS-solubilized, immobilized ABCA4 in the presence of a mixture of DOPE and DOPC phospholipids. After removal of unbound material, the bound retinoid substrate was extracted with organic solvents and analyzed by HPLC. Fig. 2.3A shows an HPLC trace of the extracted retinoids measured at 450 nm. The major peak was identified as protonated *N*-ret-PE on the basis of its retention time (in relation to standards) and absorption spectra (Fig. 2.3A).

As part of this study, the binding of all-*trans*-retinol and *N*-retinyl-PE, the reduced

form of *N*-ret-PE, was studied. As shown in Fig. 2.3C, all-*trans*-retinol did not bind to ABCA4.

Several controls were carried out to assess the specificity of retinoid binding. In the absence of added substrate, no retinoids were detected by HPLC indicating that ABCA4 from dark-adapted ROS does not contain endogenously bound retinoid. Furthermore, no retinoid compounds were detected when all-*trans*-retinal was added to the Rim 3F4-Sepharose 2B matrix lacking ABCA4. This indicates that all-*trans*-retinal and *N*-ret-PE do not bind to the immunoaffinity support.

2.3.4 Binding of Radiolabeled Retinoid to ABCA4

Due to the large quantities of ROS and Rim 3F4-Sepharose required for HPLC analysis, a more sensitive radiolabel retinoid binding assay was developed. In this procedure, [^{3}H]all-*trans*-retinal was added to immobilized ABCA4 in the presence of a DOPE/DOPC phospholipid mixture and the total amount of labeled retinoid bound to ABCA4 was measured after organic solvent extraction by scintillation counting. We first examined the binding of labeled retinoid by ABCA4 as a function of all-*trans*- retinal concentration. The binding curve and Scatchard analysis are shown in Fig. 2.4, *A* and *B*. The apparent dissociation constant for retinoid binding was determined to be 5.4 μM, which agreed with the value determined by the HPLC. A linear relationship was observed by Scatchard analysis.

2.3.5 Displacement of N-Ret-PE by N-Retinyl-PE

To determine whether *N*-ret-PE and *N*-retinyl-PE bind to the same site on ABCA4, we examined the ability of *N*-retinyl-PE to displace labeled retinoid (primarily *N*-ret-PE) from ABCA4. As shown in Fig. 2.5A, the amount of ^{3}H-labeled retinoid decreased with increasing *N*-retinyl-PE concentration. Concentration at half-maximum displacement was 10 μM *N*-retinyl-PE and essentially all labeled retinoid was lost at 50 μM. The ability of all-*trans*-retinal to displace [^{3}H]*N*-retinyl-PE was also determined. As shown in Fig. 2.5B only 20% of the bound [^{3}H]*N*-retinyl-PE was released from ABCA4 at an all-*trans*-retinal concentration of 80 μM, possibly because of the slower rate of dissociation of *N*-retinyl-PE.

2.3.6 Protonation state of *N*-ret-PE bound to ABCA4

The Schiff Base formed by the aldehyde group of retinal and primary amine group of PE can be protonated at lower pH (Fig. 2.1). To determine the protonation state of the substrate *N*-ret-PE when it is bound to ABCA4, spectrophotometric measurements were carried out. ABCA4 was immobilized on 3F4 beads with bound *N*-ret-PE substrate. Duplicate columns were prepared. One was treated with 0.5 mM ATP in column buffer so the substrate was released (background). The other was incubated with column buffer (test). ABCA4 (apoprotein or with bound *N*-ret-PE) was eluted with specific 3F4 peptide and the elution was scanned with a spectrophotometer. The difference spectrum between the test and control revealed the absorption spectrum of the bound *N*-ret-PE with absorption maximum at 370 nm (Fig. 2.6). This proves that the bound

N-ret-PE is non-protonated when ABCA4 is solubilized at physiological pH.

2.3.7 Quantitative Analysis and Effect of Nucleotides on Retinoid Bound to ABCA4

Quantitative analysis by UV-VIS spectrophotometry indicated that over 1 mol *N*-ret-PE bound to 1 mol of ABCA4. The effect of nucleotides on retinoid bound to ABCA4 was also investigated (Table 2.1). Whereas ATP released about 80% from ABCA4 at both 4 and 22 °C, ADP and AMP-PNP had relatively little effect (Table 2.1) at 4 °C. 88% of the retinoid remained bound to ABCA4 in the presence of ADP and 85% in the presence of AMP-PNP. However at 22 °C, majority of retinoid was released by ADP and AMP-PNP. 11% of the retinoid remained bound to ABCA4 in the presence of ADP and 22% in the presence of AMP-PNP.

2.4 Discussion

ABC transporters comprise one of the largest families of membrane transporters (Higgins, 1992). To date 49 genes in the human genome are known to encode ABC transporters (nutrigene.4t.com/humanabc.htm). Mutations in a significant number of these genes cause a variety of severe diseases including cystic fibrosis, Tangier's disease, familial intrahepatic cholestases, hyperinsulinemic hypoglycemia, adrenoleukodystrophy, Zellweger syndrome, and sitosterolemia (Borst and Elferink, 2002). Despite the importance of these membrane proteins in cell function, the physiological substrate is known for only a small number of ABC transporters. This is particularly true for the ABCA subfamily. In the case of ABCA4, previous ATPase assays

and studies on *abca4* knockout mice suggest that ABCA4 functions as a retinoid transporter, but the identity of this substrate and the mechanism of transport were not determined (Sun et al., 1999; Sun et al., 2000).

Using both HPLC and radiolabeling techniques, we have examined the binding of various retinoids by immunoaffinity purified ABCA4 as an essential step in determining the function of ABCA4 in photoreceptor cells. When all-*trans*-retinal was added to ABCA4 in the presence of PE, *N*-ret-PE bound to ABCA4 with high affinity. Binding was highly specific because *N*-ret-PE did not bind to the immunoaffinity matrix in the absence of ABCA4.

The binding of *N*-ret-PE to detergent-solubilized ABCA4 is strong with half-maximum binding occurring in the low micromolar range. This is consistent with the concentration of retinoid needed to stimulate the ATPase activity of ABCA4 (Ahn et al., 2000; Sun et al., 1999).

The binding of all-*trans*-retinol and *N*-retinyl-PE to ABCA4 was also investigated to further assess the specificity of ABCA4 for retinoids. All-*trans*-retinol did not bind to detergent-solubilized ABCA4 even at high concentrations, a result that is consistent with the inability of this compound to stimulate the ATPase activity of detergent-solubilized ABCA4 (Ahn et al., 2000). On the other hand, *N*-retinyl-PE strongly bound to ABCA4.

Analysis by UV-VIS spectrophotometer provided direct evidence that the *N*-ret-PE bound to ABCA4 was not protonated. Quantitative analysis indicated that close to 1 mol *N*-ret-PE bound per mol of ABCA4.

ABC transporters typically utilize energy derived from ATP hydrolysis to transport

substrates across membranes (Higgins, 1992). Therefore, we explored the effect of

hydrolyzable and nonhydrolyzable nucleotides on bound N-ret-PE (Table 2.1). At 4 °C or

22 °C ATP released essentially all of the N-ret-PE bound to ABCA4. The

nonhydrolyzable nucleotide triphosphate analogues, AMP-PNP and nucleotide

diphosphates, ADP, both release N-ret-PE from ABCA4 at 22 °C, but not at 4 °C. Since

ATP is not hydrolyzed at 4 °C and AMP-PNP and ADP can not be hydrolyzed by ABCA4,

this suggests that the simple binding of ATP to ABCA4 is sufficient to dissociate this

retinoid from ABCA4. Although transport, itself, is not measured in this study, these

results suggest a transport mechanism in which the translocation of the substrate is

induced by ATP binding but not hydrolysis. ATP hydrolysis may provide the energy input

at a different step within the operating cycle of N-ret-PE transportation.

Previous enzymatic studies have shown that ABCA4 exhibits basal and retinal

stimulated ATPase activity that generates a double reciprocal plot consisting of parallel

lines when the rate of ATP hydrolysis is measured as a function of ATP concentration

(Ahn et al., 2000; Sun et al., 1999). This behavior has been interpreted to reflect an

"uncompetitive" mode of activation or a double displacement mechanism (Sun and

Nathans, 2001). In this kinetic mechanism, ATP is proposed to first interact with ABCA4

to form a modified intermediate complex. This intermediate complex, but not free

ABCA4, binds all-*trans*-retinal (or N-ret-PE). On the basis of these and mutagenesis

studies, a complex model for ATP-dependent substrate transport has been proposed in

which ATP is first bound and "partially" hydrolyzed in NBD1 to generate a site accessible

for the binding of all-*trans*-retinal (or *N*-ret-PE). This is followed by the transport of the

retinoid and the binding and hydrolysis of a second molecule of ATP at NBD2 (Sun and

Nathans, 2001) to complete the cycle. Our studies question the validity of this proposed

mechanism. Specifically, our results clearly show that ABCA4 binds *N*-ret-PE with high

affinity in the absence of ATP. Furthermore, previous studies have indicated that ATP

binding and hydrolysis only occurs at NBD2 (Ahn et al., 2003).

Our results, together with mechanistic studies of other ABC transporters (Higgins

and Linton, 2004), suggest a possible mechanism for ABCA4 mediated transport of

N-ret-PE (Fig. 2.7). In the initial step, ATP free and inward-facing ABCA4 binds *N*-ret-PE.

The subsequent binding of ATP to NBD2 induces a protein conformational change that

enables the two NBDs to interact and converts the MSDs to outward-facing

conformation. This conformational change effectively translocates *N*-ret-PE from its high

affinity site on the lumen side of the disk membrane to a low affinity site on the

cytoplasmic side. ATP hydrolysis and dissociation of ADP serves to disengage the

NBDs and provides the energy needed to reset the transporter to its initial inward-facing

conformation. Our finding that *N*-ret-PE binds to ABCA4 in the absence of ATP is

consistent with earlier studies showing that drugs bind to P-glycoprotein in the absence

of ATP binding and hydrolysis (Ramachandra et al., 1998).

The methodology used in this study has applications for studying substrate

binding to other membrane transporters. It may be particularly useful in resolving the

uncertainties related to the putative function of ABCA1 as a mediator of cholesterol and phospholipid transport (Oram, 2002).

In summary we provided the first direct biochemical evidence for the binding of *N*-ret-PE, in particular the non-protonated form, to ABCA4. This result, together with the finding that ATP binding and hydrolysis promotes the dissociation of *N*-ret-PE from ABCA4, provides strong support for the role of ABCA4 in the transport of *N*-ret-PE across the photoreceptor outer segment disk membranes.
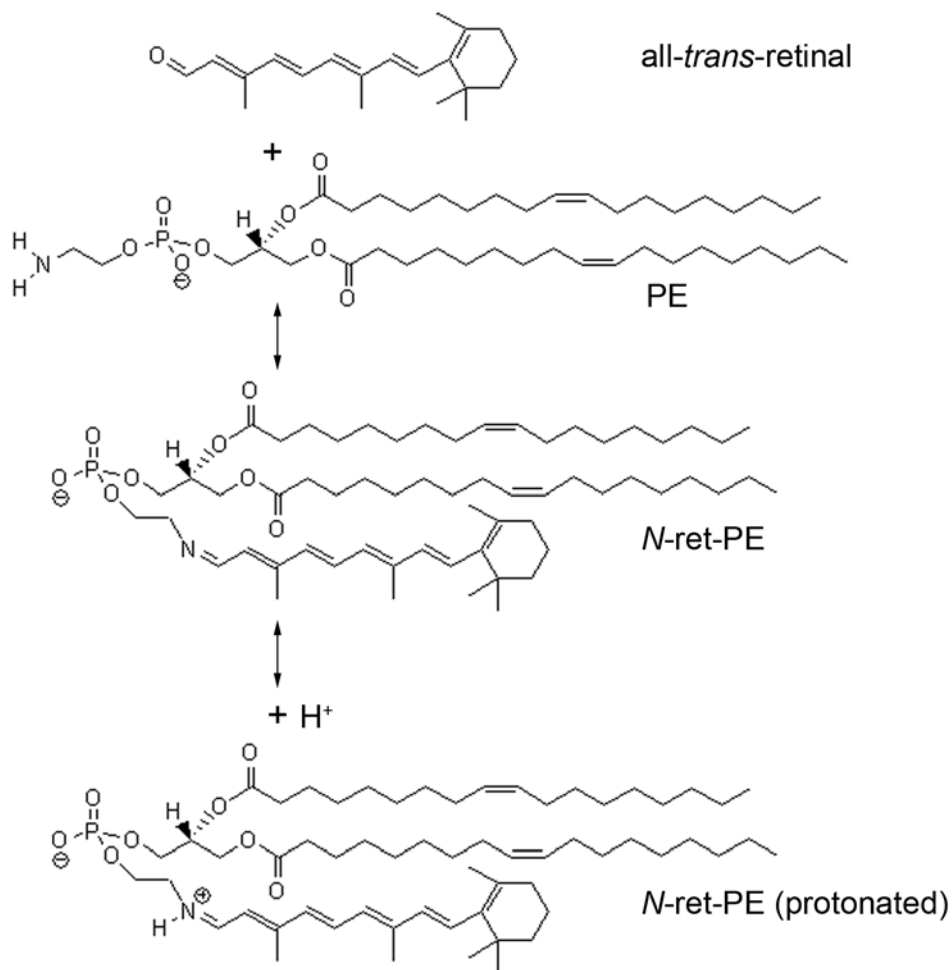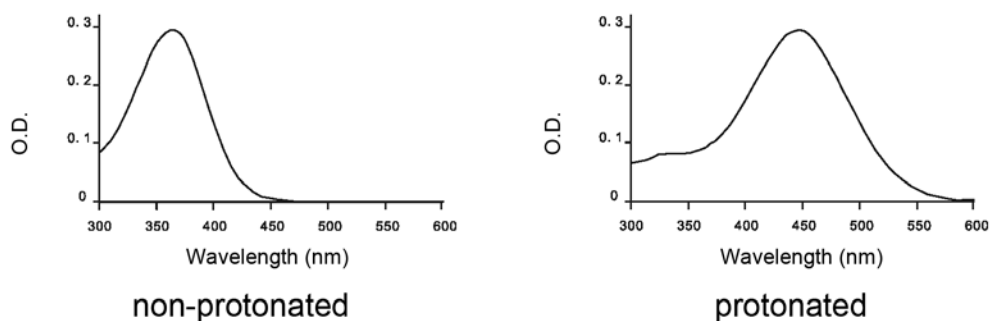
Figure 2.1. Stucture and spectra of *N*-ret-PE. A. The aldehyde group of all-*trans*-retinal reacts with the primary amine of PE to form the Schiff base condensation product *N*-retinylidene-PE (*N*-ret-PE). At lower pH the Schiff base bond is protonated. **B**. Absorption spectra for non-protonated (λ_{max}=370 nm) and protonated (λ_{max}=450 nm) *N*-ret-PE.
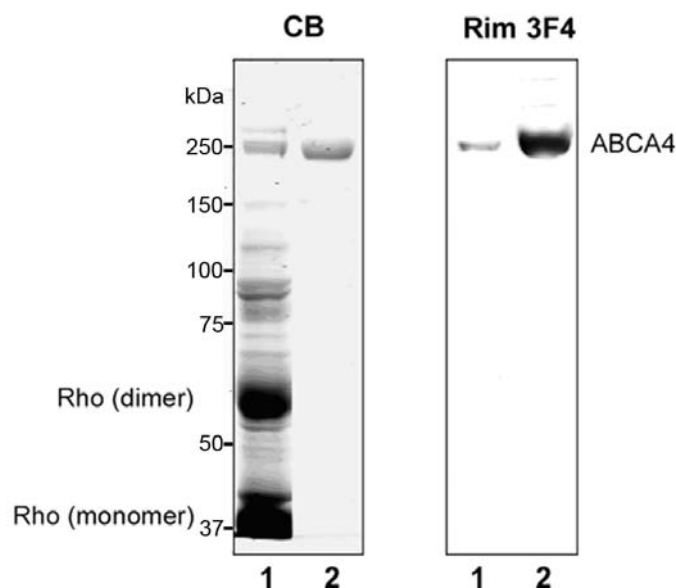
Figure 2.2. Isolation of ABCA4 on an immunoaffinity matrix. Bovine ROS membranes solubilized in CHAPS were added to Rim 3F4-Sepharose matrix. After removing the unbound protein, the bound protein was extracted with SDS for analysis on SDS-PAGE gels stained with Coomassie blue (*CB*) and Western blots were labeled with the anti-ABCA4 monoclonal antibody (*Rim 3F4*). *Lane 1*, ROS membranes; *Lane 2*, bound ABCA4. Band corresponding to the monomer (*Rho monomer*) and dimer (*Rho dimer*) of rhodopsin and ABCA4 are labelled for reference.
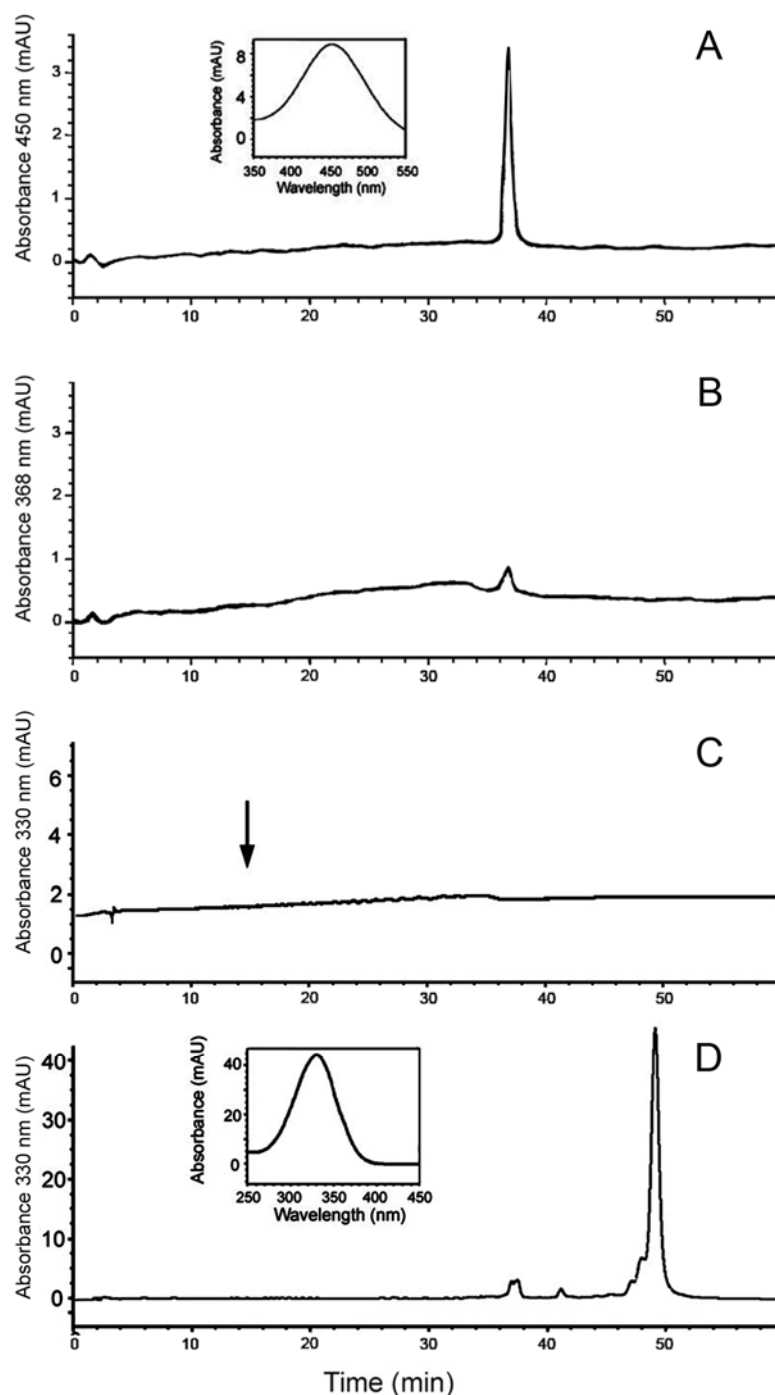
Figure 2.3. HPLC chromatographs and spectra of retinoid compounds bound to ABCA4.
A and **B**, all-*trans*-retinal was added to ABCA4 in the presence of a DOPE/DOPC phospholipid mixture. The HPLC chromatogram of bound retinoid was measured at 450 nm (**A**) (λ_{max} of protonated *N*-ret-PE) and at 368 nm (**B**) (λ_{max} of all-*trans*-retinal). **C**, all-*trans*-retinol was added to ABCA4 in the presence of DOPE, DOPC phospholipid mixture. The HPLC chromatogram was measured at 330 nm (λ_{max} of all-*trans*-retinol); the *arrow* indicates the retention time for all-*trans*-retinol. **D**, *N*-retinyl-PE, the reduced adduct *N*-ret-PE, was added to ABCA4 in the presence of DOPE/DOPC phospholipids mixtures and the bound *N*-retinyl-PE was measured at 330 nm (λ_{max} of *N*-retinyl-PE). Retention times and spectra (*insets*) of major peak in each chromatogram were used to identify the bound retinoid.
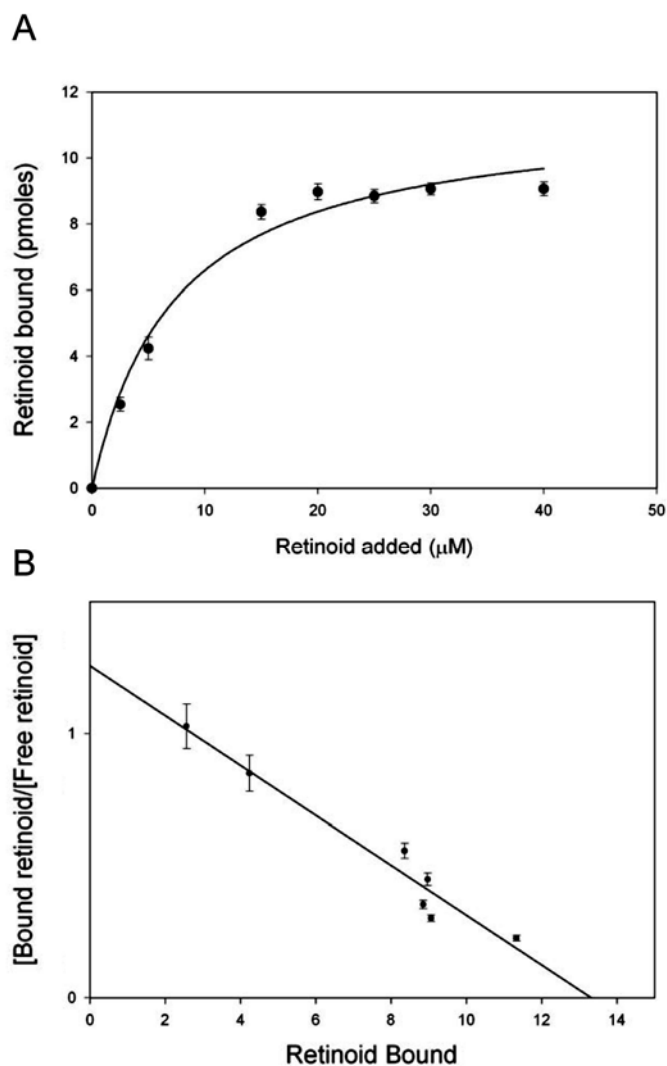
Figure 2.4. Binding of retinoid to ABCA4 using the radiolabeling method. [3H]All-*trans*-retinal was added to ABCA4 or the presence of DOPE/DOPC phopholipid mixture and the bound retinoid was determined after extraction with organic solvent. **A**. Binding of retinoid as a function of added all-*trans*-retinal. The binding curve was fitted with a single apparent K_d of 5.4 μM. **B**. Scatchard plot of the binding data.

A

B
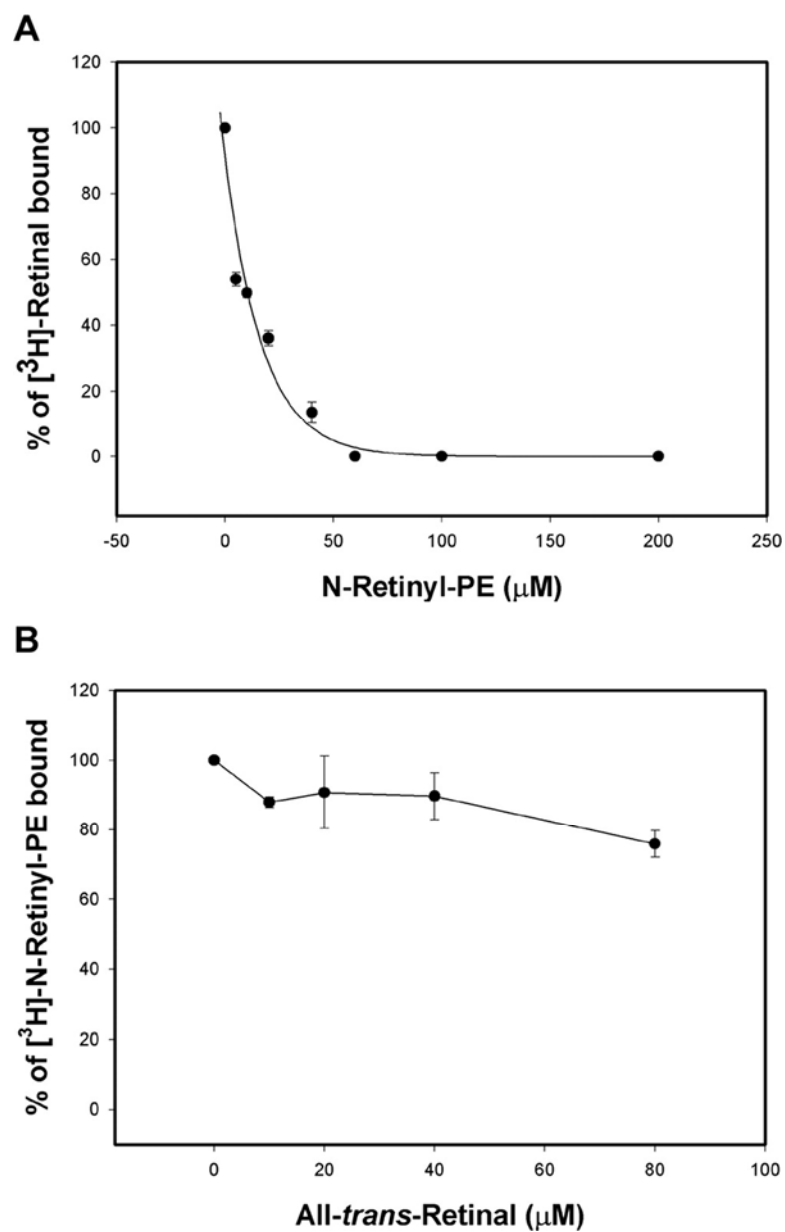
Figure 2.5. Displacement of bound labeled retinoid by unlabeled retinoid. A. The effect of increasing concentrations of *N*-retinyl-PE on [³H]all-*trans*-retinal (in the form of [³H]*N*-ret-PE) bound to ABCA4. **B**. The effect of increasing concentrations of all-*trans*-retinal on [³H]*N*-retinyl-PE bound to ABCA4. Each value is the average of triplicate experiments ± SD.
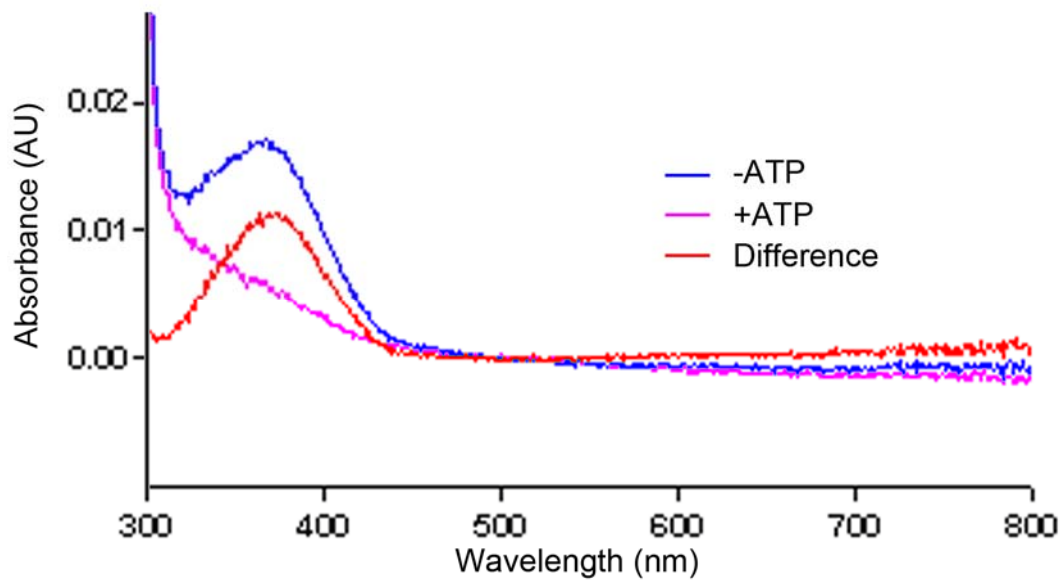
Figure 2.6. Absorption spectra of ABCA4. ABCA4 was immobilized on Rim 3F4-Sepharose beads, treated with buffer or ATP and eluted with specific 3F4 peptide. Absorption spectra were read in a UV-Vis spectrophotometer. Spectrum of the buffer treated ABCA4 is shown in blue, the ATP treated in purple. The difference spectrum of the two is shown in red.
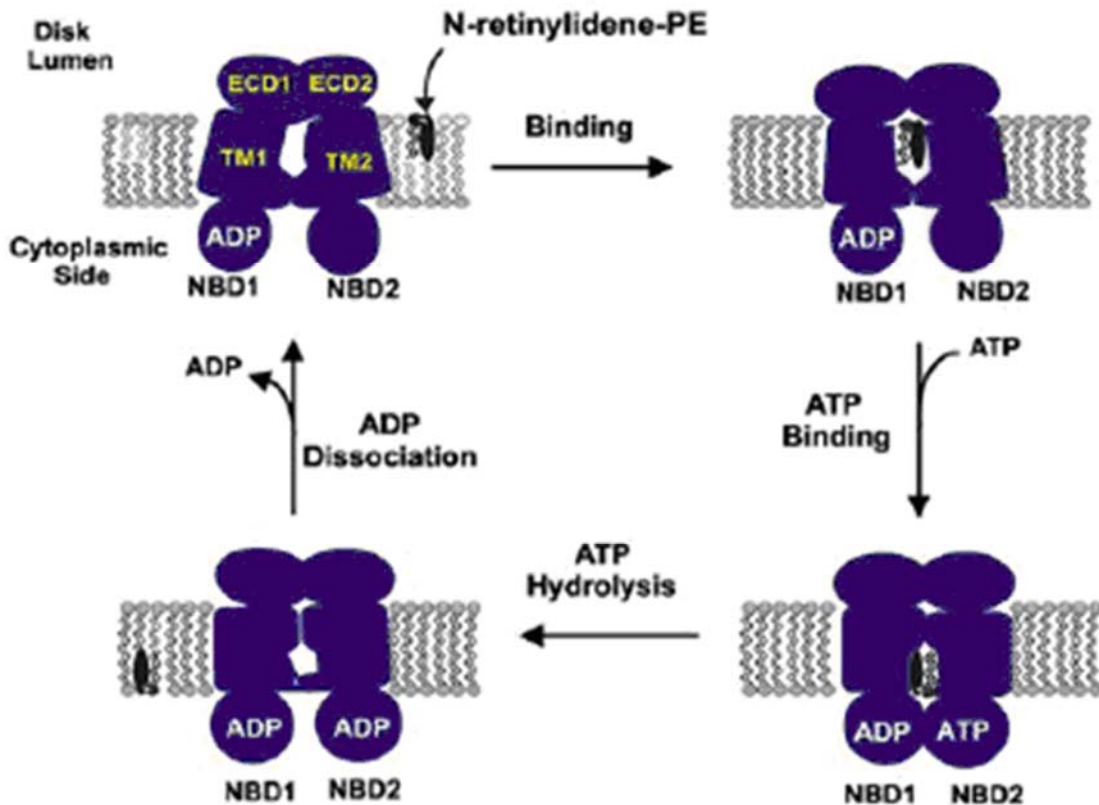
Figure 2.7. Possible mechanism of *N*-retinylidene-PE transport by ABCA4.
N-retinylidene-PE on the lumen side of the disk binds to a high affinity site in ABCA4. ATP binds to nucleotide binding domain 2 (*NBD2*) resulting in a conformational change which promotes a strong interaction of the two NBDs and movement of *N*-retinylidene-PE from a high affinity site on the lumen to a lower affinity site on the cytoplasmic side. ATP hydrolysis disengages the NBDs enabling the *N*-retinylidene-PE to dissociate from ABCA4. In the final step, ADP dissociation from NBD2 returns ABCA4 to its initial state. TM – transmembrane domain, ECD – extracellular domain. (Figure adapted from Molday, 2007)

Table 2.1 The effect of various nucleotides on the release of retinoid from ABCA4.

      Immobilized ABCA4 on Rim 3F4-Sepharose with bound retinoid was suspended in 0.5 ml of column buffer. $10 \times$ ATP, ADP or AMP-PNP solution was added to obtain the final nucleotide concentration of 0.5 mM at 4°C. The filtration device was rotated for 15 min at 4 or 22 °C, after which the beads were washed four times with 0.5 ml column buffer. ABCA4 was eluted with specific 3F4 antibody at 0.2 mg/ml in column buffer. ABCA4 without treatment of nucleotide represented the full binding capacity. Rim 3F4-Sepharose column eluted with no 3F4 peptide was used as zero binding. Molecular extinction coefficient of 33,800 M^{-1} cm^{-1} at 370 nm (Anderson and Maude, 1970) was used to determine the amount of *N*-ret-PE bound.

Compound added	Temperature (°C)	mol *N*-ret-PE/mol ABCA4
None	4	1.08 ± 0.08 (3)
ATP	4	0.23 ± 0.06 (3)
ADP	4	0.88 ± 0.25 (3)
AMP-PNP	4	0.85 ± 0.32 (3)
None	22	0.95 ± 0.07 (3)
ATP	22	0.15 ± 0.01 (3)
ADP	22	0.11 ± 0.19 (3)
AMP-PNP	22	0.22 ± 0.23 (2)

CHAPTER 3: ROLE OF THE C-TERMINUS OF ABCA4 IN PROTEIN FOLDING, FUNCTION AND RETINAL DEGENERATIVE DISEASES [2]

3.1 Introduction

ABCA4, also known as ABCR or the rim protein, is a member of the ABCA subfamily of ATP binding cassette (ABC) transporters expressed in vertebrate photoreceptor cells (Allikmets et al., 1997b; Azarian and Travis, 1997; Illing et al., 1997; Molday et al., 2000). It is localized along the rims and incisures of rod and cone outer segment disks where it has been implicated in the binding and transport of the Schiff base adduct of all-*trans*-retinal and PE known as *N*-retinylidene-PE (*N*-ret-PE) across disk membranes as part of visual cycle (Beharry et al., 2004; Molday et al., 2000; Molday, 2007; Papermaster et al., 1978; Sun et al., 1999; Weng et al., 1999).

To date over 500 different mutations in the *ABCA4* gene are known to cause Stargardt macular degeneration, an early onset, recessive disease characterized by the loss in central vision, the presence of lipofuscin deposits in RPE cells, a delay in dark adaptation, and progressive degeneration of photoreceptor and RPE cells (Allikmets, 2000; Allikmets et al., 1997b; Fishman et al., 1987; Fishman et al., 1991; Gelisken and De Laey, 1985; Rivera et al., 2000; Rozet et al., 1999). Mutations in ABCA4 are also responsible for other related, but more severe retinal degenerative diseases including

---

[2] A version of this chapter has been published.

Zhong, M., Molday, L.L., and Molday, R.S. (2008). Role of the C-terminus of the photoreceptor ABCA4 transporter in protein folding, function and retinal degenerative diseases. J Biol Chem. EPub Date 2008/12/06

autosomal recessive cone-rod dystrophy and retinitis pigmentosa (Brooks-Wilson et al.,
1999b; Cremers et al., 1998; Fishman et al., 2003; Martinez-Mir et al., 1998). Finally,
individuals heterozygous for selected disease-linked mutations in ABCA4 have been
suggested to be at higher risk in developing age related macular degeneration
(Allikmets et al., 1997a). Disease-associated mutations are distributed throughout the
ABCA4 gene and comprise missense, splice-site, and nonsense mutations as well as
small deletion and insertions resulting in a truncated protein. Biochemical studies
indicate that disease-linked mutations in ABCA4 cause a complete or partial loss in
retinal stimulated ATPase activity (Sun et al., 2000).

ABCA4 is most similar to ABCA1, an ABC transporter implicated in the efflux of
cholesterol and phospholipids from cells (Attie, 2007; Brooks-Wilson et al., 1999b; Lawn
et al., 1999). ABCA4 and ABCA1 are over 50% identical in amino acid sequence. Both
proteins have a similar topological organization consisting of two tandem halves each
containing a transmembrane segment followed by a large extracellular domain (ECD) a
membrane spanning domain, and a nucleotide binding domain (NBD) (Bungert et al.,
2001; Fitzgerald et al., 2001). In addition, both transporters contain an extended
C-terminal tail of about 170 amino acids in length downstream from the NBD in the
C-terminal half (NBD2) (Fig. 3.1). The importance of the C-terminus is underscored by
the finding that a mutation in ABCA4 which causes the removal of the C-terminal 30
amino acids of ABCA4 is responsible for cone-rod dystrophy (Stenirri et al., 2006) and a
mutation leading to the deletion of the C-terminal 46 amino acids of ABCA1 is

associated with Tangiers disease, an autosomal recessive disorder characterized by a loss in circulating high density lipoprotein and accumulation of cholesterol esters in peripheral tissues (Brousseau et al., 2000). Fitzgerald et al. (Fitzgerald et al., 2004) have examined several C-terminal deletion mutants of ABCA1 including the Δ46 mutation associated with Tangiers disease. Their studies suggest that a conserved VFVNFA motif present in the cytoplasmic C-terminal domain of ABCA1 interacts with an unknown cytoplasmic protein to orchestrate the binding of apoA-I to ABCA1 and efflux of cholesterol from cells.

The VFVNFA motif is also present within the C-terminal 30 amino acids of ABCA4, but its role in this transporter has not been determined. In this paper, we have characterized a number of C-terminal deletion and chimera mutants of ABCA4 including mutants known to cause cone-rod dystrophy and Stargardt macular degeneration (Fumagalli et al., 2001; Stenirri et al., 2006). Our studies indicate that the VFVNFA motif present within the 30 C-terminal amino acids plays a crucial role in the folding of ABCA4 into a functionally active protein.

3.2 Methods

3.2.1 Reagents and Solutions

All-*trans*-retinal and ATP were purchased from Sigma (St Louis, MO), CHAPS detergent was from Anatrace (Maumee, OH), and lipids including brain polar lipids, DOPE, and DOPC were from Avanti Polar Lipids (Alabaster, AL). Extracti-Gel D detergent removal gel was obtained from Thermo Scientific (Rockford, IL) and

8-azidoadenosine 5'-[α^{32}P] triphosphate was a product of ALT Bioscience (Lexington, KY). All-*trans*-retinal and all-*trans*-retinol were radiolabeled and isolated as described by Garwin and Saari (Garwin and Saari, 2000).

The composition of buffers was as follows: hypotonic buffer: 10 mM HEPES, pH 7.5; column buffer: 50 mM HEPES, pH 7.5, 0.1 M NaCl, 10 mM CHAPS, 1 mM DTT, 3 mM $MgCl_2$, 10% glycerol, 0.32 mg/ml DOPE, and 0.32 mg/ml DOPC; reconstitution buffer: 25 mM HEPES, pH 7.5, 0.14 M NaCl, 1mM EDTA, 1 mM DTT, and 10% glycerol; and solubilization buffer: 50 mM HEPES, pH 7.5, 0.1 M NaCl, 18 mM CHAPS, 1 mM DTT, 3 mM $MgCl_2$, 10% glycerol, 0.32 mg/ml DOPE, and 0.32 mg/ml DOPC. All-*trans*-retinal concentration in ethanol was determined spectrophotometrically using an extinction coefficient of 42,900 $M^{-1}cm^{-1}$.

3.2.2 Monoclonal Antibodies and DNA Constructs

The Rim 3F4 monoclonal antibody directed against a defined epitope near the C terminus of ABCA4 and the Rho 1D4 monoclonal antibody to the nine-amino acid C-terminal sequence of rhodopsin have been described previously (Hodges et al., 1988; Illing et al., 1997; MacKenzie et al., 1984). The purified Rho 1D4 antibody was purchased from UBC-UILO (http://www.uilo.ubc.ca/researcher_Flintbox.asp). C-terminal deletion mutants of ABCA4 containing an added 9 amino acid 1D4 tag (**-T-E-T-S-Q-V-A-P-A**) were generated by PCR using 1) the human ABCA4-1D4 in the pCEP4 plasmid (Invitrogen) as a template; 2) a common forward primer that anneals between nt positions 5808 and 5831 and contains an Afl II site; and 3) unique reverse

primers that anneal between nt 6778 to 6795 (ABCA4-Δ8-1D4), 6751 to 6771 (ABCA4-Δ16-1D4), 6726 to 6747 (ABCA4-Δ24-1D4) and 6710 to 6729 (ABCA4-Δ30-1D4) and contain a Nhe I site and the sequence for 1D4 tag. C-terminal deletion mutants of ABCA1 were also generated by polymerase chain reaction (PCR) using human ABCA1-1D4 in the pCEP4 plasmid as the template, a common forward primer that anneals between nt position 6221 to 6239 of ABCA1 with a BamH I site, and unique reverse primers that anneal to nt positions 6689 to 6711 (ABCA1-Δ24-1D4), 6642 to 6663 (ABCA1-Δ40-1D4), and 6625 to 6645 (ABCA1-Δ46-1D4) and contain a BamH I site and the sequence for 1D4 tag. Chimera constructs ABCA4/A1 with the C-terminus of ABCA4 replaced with the C-terminus of ABCA1 just after the VFVNFA motif and ABCA1/A4 in which the C-terminus of ABCA1 was replaced with the C terminus of ABCA4 were generated by overlapping PCR (Aiyar et al., 1996). Alanine substitution mutants (ABCA4-Ala6 and ABCA1-Ala6) in which the VFVNFA motif in ABCA4 and ABCA1 were replaced with alanine residues (VFVNFA$\rightarrow$AAAAAA) were also generated by overlapping PCR (Aiyar et al., 1996).

3.2.3 Expression of WT and Mutant ABCA4 and ABCA1 in HEK 293T Cells and Extraction of Membrane Proteins

HEK 293-T cells were maintained in Dulbecco's modified Eagle's medium supplemented with 10% fetal bovine serum, 100 units/ml penicillin, 100 µg/ml streptomycin, 2 mM L-glutamine and 1.25 µg/ml fungizone (Invitrogen, Carlsbad, CA). Typically, each 10-cm dish of cells at 30% confluency was transfected with 20 µg of

plasmid DNA using calcium phosphate (Chen and Okayama, 1987). After 48 h, cells from two or three plates were harvested in 1.5 ml hypotonic buffer. Membranes from homogenates of transfected cells were prepared as described previously (Bungert et al., 2001), but in a smaller scale. Briefly, the cell homogenate from two or three 10-cm dishes was passed 5 times through a 26-gauge needle and subsequently applied to a step gradient consisting 5% and 60% (w/v) sucrose. Centrifugation was carried out for 30 min at 77,000 $\times$ g in a TLS 55 swing bucket (Optima TL Ultracentrifuge, Beckman, Palo Alto, CA). Membranes at the interface between the 5% and 60% layers were collected, pelleted at 100,000 $\times$ g and resuspended at a concentration of 5 mg protein/ml in buffer consisting of 10 mM HEPES, pH 7.5, 150 mM NaCl, 1 mM $MgCl_2$, 1 mM $CaCl_2$, 0.1 mM EDTA and 10% glycerol. To compare extractability of the expressed 1D4 tagged ABCA4 mutants, 20 μl of membranes was added to 180 μl CHAPS solubilization buffer at 4 °C. The mixture was stirred for 20 min and subsequently centrifuged at 100,000 x g for 10 min in a TLA55 rotor (Beckman). The supernatant fraction (20 μl) was mixed with 4 $\times$ SDS loading buffer and resolved by SDS-PAGE for analysis by western blotting. To determine the total expression level of each mutant, 2 μl of membranes was mixed with 18 μl water, 10 μl 4 $\times$ SDS loading buffer and resolved by SDS-PAGE gel for quantification by western blotting.

3.2.4 Analysis of Retinoid Binding

Solid phase binding assay using [3H]-labeled all-*trans*-retinal was carried out as described previously (Beharry et al., 2004). All incubations were carried out at 4 °C.

Briefly, transfected HEK 293T cells harvested from one dish were centrifuged at 2800 × *g* for 3 min and resuspended in 0.5 ml of solubilization buffer. The supernatant fraction obtained after centrifugation (100,000 × g for 10 min) was incubated with 12.5 μl Rho 1D4-Sepharose 2B immunoaffinity matrix pre-equilibrated in column buffer. After 1 h, the matrix containing the bound 1D4-tagged protein was washed several times with 0.4 ml column buffer by low speed centrifugation and mixed with 0.25 ml of 20 μM [^{3}H]-labeled all-*trans*-retinal (specific activity of 500 dpm/pmol, 2.5 x 10^6 dpm total) in column buffer for 30 min. The matrix was washed several times with 0.4 ml column buffer to remove unbound [^{3}H]-labeled all-*trans*-retinal and then incubated in the presence or absence of 0.5 mM ATP for 15 min. The matrix was washed 2 more times with 0.4 ml column buffer before being transferred to Ultrafree-MC (0.45 μm filter) spin column (Millipore). The samples containing the immobilized 1D4 tagged ABCA4 proteins with bound labeled retinoid was washed 3 more times before extracting the [^{3}H]-labeled all-*trans*-retinal from the matrix with 0.5 ml of ice-cold ethanol for 15 min at RT by centrifugation. Radiolabeled all-*trans*-retinal in the ethanol extractions was determined by liquid scintillation counting. Assays were carried out in triplicate for each point determination. In general, the procedures were carried out under dim light to prevent any photoreaction of the retinoids. 1D4 tagged Na/K ATPase was treated in the same way and used as a control to monitor for background retinoid binding. The counts in the controls, typically about 20% of the test sample not treated with ATP, were subtracted from the test samples to determine specific retinoid binding. A duplicate

column eluted with 60 μl 1% SDS was used to determine the amount of 1D4-tagged protein immobilized on Rho 1D4 Sepharose affinity matrix.

3.2.5 Reconstitution in Lipid Vesicles

For ATPase assays, 2-3 dishes of transfected HEK 293T cells were solubilized as described for retinoid binding studies. The solubilized protein was incubated with 25 μl Rim 3F4 or Rho 1D4 Sepharose for 1 h at 4 °C in an Ultrafree-MC spin column. The matrix was washed 6 times with 0.4 ml column buffer to remove unbound protein and then eluted with incubation in 37.5 μl of 0.2 mg/ml competing peptide (3F4 (YDLPLHPRTA) or 1D4 (TETSQVAPA) peptide) in column buffer at 7 °C for 20 min. The addition of peptide and elution was repeated and two eluates were combined. The eluted ABCA4 proteins were reconstituted into brain polar lipids using the procedure of Sun *et al* with minor modifications (Sun et al., 1999). Briefly, 9 μl of 25 mg/ml sonicated brain polar lipid extract (33% PE, 18% phosphatidylserine, 13% PC, 4.1% phosphatidylinositol, 31% other lipids) was mixed with 6 μl of 15% *n*-octylglucoside (w/v) in 25 mM HEPES, pH 7.4, 140 mM NaCl, 10% glycerol. Purified ABCA4 protein (60 μl) was added, and the mixture was incubated on ice for 30 min. Reconstitution buffer (180 μl) was added rapidly, and the sample was then passed through 200 μl of Extracti-gel resin pre-equilibrated with reconstitution buffer in a Mobicol mini-column fitted with a 10 μm pore size filter (MoBiTec, Gottingen, Germany). The flow-through containing reconstituted ABCA4 or ABCA1 protein was collected at 0.8 ml/min by applying gentle pressure with a syringe, and 5 mM $MgCl_2$ was added prior to carrying out ATPase

activity measurements.

3.2.6 ATPase Assay

ATP assays were carried out using [α-^{32}P]ATP (PerkinElmer, Waltham, MA) and thin layer chromatography as previously described (Ahn et al., 2000). ATPase assays were carried out in a 10-µl total reaction volume consisting of 8 µl (20-40 ng) of reconstituted protein and 1 µl of 10× retinoid or buffer. The reaction was initiated by the addition of 1µl of a 10× ATP solution (0.2 µCi) to achieve a final concentration of 50 µM. After 30 min at 37°C, 4 µl of 10% SDS were added. One µl of the reaction mixture was spotted onto a polyethyleneimine cellulose plate (Sigma-Aldrich, St Louis, MO) and chromatographed in 0.5 M LiCl/1 M formic acid. The plate was exposed to a storage phosphor screen for 3 h and scanned in a Typhoon Variable Mode Imager (Amersham Biosciences, Pittsburgh, PA). Spots corresponding to ATP and ADP were quantified using ImageQuant TL software. The ratio of the amount of ADP produced to the initial amount of ATP present in the reaction mixture was calculated. Each sample was assayed in triplicate. Buffer blanks were included to determine nonenzymatic ATP hydrolysis, which was subtracted from the total ATP hydrolyzed.

3.2.7 Protein Determination

The amount of protein in detergent extracts and reconstituted vesicles was determined by comparing the intensity of Coomassie Brilliant Blue staining of ABCA4 with that of standard amounts of bovine serum albumin after SDS-polyacrylamide gel electrophoresis.

3.2.8 Western Blot Analysis

Proteins were separated by SDS gel electrophoresis on 8% polyacrylamide gels and transferred to Immobilon FL membranes (Millipore, Billerica, MA) at 13V for 30 min in a semidry transfer apparatus (Bio-Rad) using a buffer consisting of 25 mM Tris, 192 mM glycine, 10% methanol, pH 8.3. The membranes were blocked with 0.5% skim milk in PBS (140 mM NaCl, 3 mM KCl, 10 mM phosphate, pH 7.4) for 30 min, rinsed and incubated with Rho 1D4 monoclonal antibody diluted in 0.5% milk, PBS for 1 h. After extensive washing in PBS containing 0.05% Tween 20 (PBST), the membranes were treated for 30 min with secondary antibody (goat anti-mouse Ig conjugated with IRDye 680 (LI-COR, Lincoln, NE), diluted 1:10,000 in 0.5% milk, 0.02 % SDS, PBST) and washed in PBST prior to analysis with a LI-COR infrared imaging system.

3.2.9 Photoaffinity Labeling of ABCA4

Five μl membrane protein (25 μg protein) in resuspension buffer (25 mM HEPES, pH 7.5, 0.15 M NaCl, 5 mM $MgCl_2$) was mixed with 15 μl of 8-azido [α-^{32}P]ATP (4.5 μM, 0.05 mCi/ml) in the same buffer. The sample was immediately exposed to 254 nm UV at a distance of 10 cm for 10 min. SDS sample buffer (10 μl) was mixed with each sample without heating, and the proteins were resolved by SDS-PAGE and analyzed by autoradiography. Triplicate cell expression samples were carried out for each mutant. The same amount of unlabeled membranes was resolved by SDS-PAGE and subjected to western blotting analysis for protein quantification.

3.2.10 Immunofluorescence Labeling of Cells

Human embryonic kidney cells (HEK293T) were grown on glass coverslips and transfected with the plasmid using calcium phosphate. After 24 h, the cells were washed in 0.1M phosphate buffer, and fixed for 20 min in 4% paraformaldehyde in 0.1M phosphate buffer at 22°C. Cells were then blocked and permeabilized for 30 min at 22 °C in the same buffer containing 10% (v/v) normal goat serum and 0.1% (v/v) Triton X-100. For single labeling experiments, the cells were treated with the Rho 1D4 antibody for 1 h at 22 °C, washed in PBS buffer and treated with goat anti-mouse Ig coupled Cy3 diluted 1:1000 in phosphate buffer and counterstained with the nuclear dye DAPI. For double labeling studies, ABCA4 protein was labeled with Rho 1D4 followed by goat antimouse Ig conjugated to Alexa 488 and calnexin was labeled with a rabbit anti-calnexin polyclonal antibody followed by goat anti-rabbit Ig conjugated to Alexa 594. Immunofluorescence labeling was visualized using a Meta 510 Zeiss Confocal microscope or a Zeiss Axioplan 2 fluorescence microscope.

3.3 RESULTS

3.3.1 C-terminal 1D4 Tag Does Not Affect the ATPase Activity of ABCA4

In previous studies the Rim 3F4 monoclonal antibody coupled to Sepharose was used to purify ABCA4 from bovine rod outer segments and recombinant ABCA4 from transfected cells for structure-function studies (Ahn et al., 2000; Beharry et al., 2004; Illing et al., 1997; Sun et al., 1999; Sun et al., 2000). Since the 3F4 epitope is localized close to the C-terminus (amino acids 2252-2262) of ABCA4, the Rim 3F4 antibody can

not be used to purify ABCA4 C-terminal deletion mutants for biochemical studies. To circumvent this problem, we have added a 9 amino acid 1D4 tag to the C-terminus of WT and mutant ABCA4. This tag recognized by the Rho 1D4 monoclonal antibody (MacKenzie et al., 1984) has been shown previously to be extremely effective for the immunoaffinity purification of membrane proteins for structure-function studies (Loewen et al., 2001; Oprian et al., 1987) .

First, it was necessary to determine if addition of the 1D4 tag has any effect on the biochemical properties of ABCA4. This was determined by expressing ABCA4 and ABCA4-1D4 in HEK 293T cells and purifying the proteins from CHAPS solubilized membranes on a Rim 3F4-Sepharose immunoaffinity matrix. Both proteins expressed at similar levels and were solubilized to the same extent in CHAPS detergent. Elution of the proteins bound to the immunoaffinity matrix with the 3F4 peptide yielded similar amounts of highly pure 250 kDa ABCA4 as quantified on SDS gels stained with Coomassie blue (Fig. 3.2 A,B). After reconstitution into brain lipid vesicles, both ABCA4 and ABCA4-1D4 displayed similar basal and all-*trans*-retinal stimulated ATPase activities (Fig. 3.2C). The basal activities for ABCA4 and ABCA4-1D4 were 54.3 ± 0.9 and 48.9 ± 2.5 nmoles ATP hydrolyzed/min/mg protein, respectively. HEK 293T cells transfected with vector alone were used in control studies. No contaminating proteins or ATPase activity was observed when the detergent solubilized extract from these cells was passed through either a Rim 3F4 or Rho 1D4 immunoaffinity column (data not shown). These results indicate that the C-terminal 1D4 tag does not affect the

expression, purification, or enzymatic activity of ABCA4 and the basal and retinal stimulated ATPase activities are solely due to expressed ABCA4.

3.3.2 1D4-tagged ABCA4 and ABCA1 Mutants

To investigate the importance of the C-terminus on the biochemical properties of ABCA4, we generated four C-terminal deletion mutants and one C-terminal chimera mutant (ABCA4/A1) in which the C-terminal 24 amino acid segment of ABCA4 was replaced with the C-terminal 40 amino acid segment of ABCA1, and one C-terminal mutant in which a conserved VFVNFA motif was replaced with alanine residues (ABCA4-Ala6) (Fig. 3.3). Several related ABCA1 mutants were also constructed for comparative studies. The WT and mutant proteins contained a 1D4 C-terminal tag for detection and purification. For simplicity we have omitted 1D4 in the designation of the various ABCA4 proteins used in this study.

3.3.3 The Effect of C-terminal Deletions on the Expression and Solubilization of ABCA4

The level of expression of WT ABCA4 and the various mutants was determined by directly solubilizing membranes from HEK 293T cells in SDS for analysis by SDS-PAGE and western blotting (Fig. 3.4A). The wild-type and mutants migrated as tightly spaced doublets, presumably arising from differential posttranslational processing of the proteins. The level of expression of the mutants was typically within 75% that of WT ABCA4 with the exception of ABCA4-Δ24 which expressed at only 40% of WT ABCA4. The ability of CHAPS to effectively solubilize the ABCA4 mutants from HEK 293T cell

membranes was also investigated. Fig. 3.4B shows that all CHAPS-solubilized mutants migrated as a sharp single band, but at variable levels. The single bands suggest that CHAPS solubilized only a single class of ABCA4 proteins, presumably nonaggregated proteins having a native-like structure. ABCA4-Δ8 was solubilized in CHAPS at a level comparable to WT ABCA4, whereas the ABCA4-Δ16 and ABCA4-Δ24 mutants on average solubilized at about 75% and 35% of WT ABCA4. The ABCA4-Δ30 and the ABCA4/A1 mutants solubilized at only 10-20% that of WT ABCA4. When CHAPS solubilization of the mutants was normalized to the level of protein expression as determined by SDS solubilization, only the ABCA4-Δ30 and ABCA4/A1 mutants showed significantly reduced levels compared to WT ABCA4 (Fig. 3.4C) suggesting that a major fraction of these mutants (~80-90%) were highly misfolded and possibly aggregated.

3.3.4 8-Azido-ATP Photoaffinity Labeling of ABCA4 Mutants

The capacity of the C-terminal ABCA4 deletion mutants to bind ATP was investigated by photoaffinity labeling. Membranes from transfected HEK 293T cells were treated with 8-azido-[^{32}P]ATP, irradiated with ultraviolet light, and resolved by SDS-PAGE for quantitative analysis of bound radiolabeled azido-ATP on a phosphor imager. As shown in Fig. 3.5 A and 3.5 B, WT ABCA4, ABCA4-Δ8, and ABCA4-Δ16 were labeled to a similar extent. The ABCA4-Δ24 mutant displayed a 3-fold higher level of 8-azido-ATP labeling when normalized for the amount of protein present, while the ABCA4/A1 chimera mutant showed significantly reduced labeling and the ABCA4-Δ30 lacking a conserved VFVNFA motif did not label.

3.3.5 Binding of *N*-ret-PE (*N*-ret-PE) to C-terminal Mutants

In previous studies, we have shown that purified ABCA4 from bovine ROS immobilized on an immunoaffinity matrix specifically bound *N*-ret-PE in the absence of ATP (Beharry et al., 2004). The addition of ATP caused *N*-ret-PE to dissociate from ABCA4. We have used this assay to measure *N*-ret-PE binding to the C-terminal mutants (Fig. 3.6). All mutants except ABCA4-Δ30 bound *N*-ret-PE in the absence of ATP at levels comparable to WT ABCA4. *N*-ret-PE substrate binding was lost upon the addition of ATP. As part of this study, we also determined if purified ABCA1 was capable of binding *N*-ret-PE. As shown in Fig. 3.6, no binding of *N*-ret-PE to ABCA1 was observed.

3.3.6 Immunoaffinity purification of ABCA1 and ABCA4

For analysis of ATPase activities, 1D4-tagged wild-type and mutant ABCA4 and ABCA1 were purified from CHAPS solubilized extracts of HEK293 cells on a Rho 1D4 immunoaffinity matrix. Fig. 3.7A shows representative Coomassie blue stained SDS gels of the protein preparations eluted from the matrix with the competing 1D4 peptide. The ABCA4 and ABCA1 transporters were present as intensely stained bands having an apparent molecular mass of 250 kDa. Another faint protein band running at 65 kDa was often observed in both WT and mutant ABCA4 and ABCA1 preparations. The identity of this protein remains to be determined, but it most likely represents a chaperone protein that is tightly bound to a portion of the ABCA transporters.

3.3.7 The Effect of C-terminal Mutations on Basal and Retinal Activated ATPase Activity

Basal and all-*trans*-retinal stimulated ATPase activity was measured for the immunoaffinity purified C-terminal ABCA4 mutants reconstituted into brain polar lipid vesicles containing PE. All mutants retained varying levels of basal ATPase activity (Fig. 3.7B). The ABCA4-Δ8 and ABCA4-Δ16 mutants exhibit basal ATPase activity that was stimulated by the addition of all-*trans*-retinal at levels similar to WT ABCA4. The ABCA4-Δ24 mutant had reduced basal and all-*trans*-retinal stimulated ATPase activities, whereas the ABCA4-Δ30 mutant lacking the VFVNFA motif displayed low basal activity and no stimulation by all-*trans*-retinal. The ABCA4/A1 chimera mutant exhibited low basal activity and only limited stimulation by all-*trans*-retinal.

To further investigate the importance of the VFVNFA motif in retinal stimulated ATPase activity, we constructed and expressed an ABCA4 mutant in which the 6 amino acids in this motif were replaced with alanine residues (ABCA4-Ala6). As seen in Fig. 3.7C, this mutant, like the ABCA4-Δ30 mutant, was devoid of retinal stimulated ATPase activity.

3.3.8 Differential Effect of C-terminal Deletion and Chimera Mutations on the Basal ATPase Activities of ABCA1 and ABCA4

Although the effect of ABCA1 C-terminal deletion mutations on the efflux cholesterol in the presence and absence of apoA-1 has been reported (Fitzgerald et al., 2004), their effect on the ATPase activity of the purified transporter was not investigated.

As part of our study, we compared the basal ATPase activity of C-terminal deletion mutants of ABCA4 with several C-terminal ABCA1 deletion mutants. A gradual decrease in basal ATPase activity of ABCA4 was observed with increasing deletion of the C-terminus (Fig. 3.8). An opposite trend was observed for ABCA1 deletion mutants, namely, a higher ATPase activity was observed for the deletion mutants in which 40 and 46 amino acids were absent relative to WT ABCA1 and ABCA1-Δ24. In addition two chimera mutants ABCA4/A1 and ABCA1/A4 were examined (Fig. 3.8). Whereas the ABCA4/A1 mutant showed significantly reduced basal ATPase activity relative to WT ABCA4, the ABCA1/A4 mutant showed increased activity relative to WT ABCA1. These results suggest that segments of ABCA4 downstream of the VFVNFA motif enhance the basal ATPase activity of ABCA4 and ABCA1, whereas segments of ABCA1 downstream of this motif reduce the basal ATPase activity of these transporters.

3.3.9 Immunofluorescence Localization of ABCA4 Mutants

Previous studies in our laboratory have shown that WT ABCA4 expressed in COS-1 cells preferentially localizes to intracellular vesicles of varying sizes consistent with the intracellular localization of ABCA4 in photoreceptor cells (Ahn et al., 2003; Illing et al., 1997). In the present study, we have compared the subcellular localization of the 1D4 tagged WT and mutant ABCA4 expressed in HEK 293T cells. WT ABCA4 and deletion mutants ABCA4-Δ8, ABC4-Δ16 and ABCA4-Δ24 all exhibited a similar subcellular distribution with the majority of the protein being localized to intracellular vesicular structures (Fig. 3.9 A-B). In contrast essentially all the ABCA4-Δ30 and

ABCA4-Ala6 mutants deficient in the VFVNFA motif and most of the ABCA4/A1 mutant showed a perinuclear, reticular distribution characteristic of ER retention (Fig 8 C-E). Double labeling using the ER marker calnexin confirmed the localization of ABCA4-Δ30 within the ER of cells (Fig 8C).

These studies suggest that the major fraction of ABCA4-Δ8, ABCA-Δ16 and ABCA4-Δ24 mutants are folded in a native-like conformation that allows the protein to exit the ER and accumulate as intracellular vesicles in HEK 293T cells. In contrast, essentially all of the ABCA4-Δ30 and ABCA4-ala6 mutants are misfolded and retained in the ER by the quality control system of cells.

As part of this study, we also investigated the distribution of the 1D4 tagged WT and mutant ABCA1 proteins expressed in HEK 293 cells. WT-ABCA1 localized to the plasma membrane of HEK293 cells as previously reported (Tamehiro et al., 2008), whereas essentially all of the ABCA1-Δ46 and most of the ABCA1-Ala6 mutant displayed a perinuclear distribution characteristic of retention in the ER (Fig 8F-H). The ABCA1/A4 mutant localized to both the plasma membrane and ER.

3.4 DISCUSSION

In this study we have expressed, purified and characterized a series of C-terminal deletion and chimera mutants of ABCA4 and ABCA1 in order to define the role of the C-terminus of ABCA4 in protein structure and function and to gain insight into the molecular basis for retinal degenerative diseases associated with mutations in this segment of the transporter. Our studies indicate that a conserved VFVNFA motif is

required for the production of a functional protein. The ABCA4-Δ30 mutant lacking the VFVNFA motif failed to bind the substrate *N*-ret-PE, was not labeled with 8-azido ATP, and showed limited basal and no retinal stimulated ATPase activity. Similarly, the ABCA4-ala6 mutant in which the VFVNFA motif was replaced with six alanine residues was not stimulated by retinal. In contrast the ABCA4-Δ8, ABCA4-Δ16, and ABCA4-Δ24 mutants which have the VFVNFA motif retain these functional properties.

Our results showing that the VFVNFA motif is required for the production of a functionally active ABCA4 protein is in general agreement with the studies of Fitzgerald et al (Fitzgerald et al., 2004) showing that this conserved motif is critical for the function of ABCA1 in apoA-1 binding and cholesterol efflux from cells (Fitzgerald et al., 2004). However, the VFVNFA motif may play distinct mechanistic roles for each transporter. In the case of ABCA1, the VFVNFA motif has been suggested to interact with an unidentified cytoplasmic protein to induce apoA-1 binding to an extracellular domain of ABCA1 and promote cholesterol efflux from cells (Fitzgerald et al., 2004). Our studies on ABCA4 indicate that the VFVNFA motif plays a crucial role in proper folding of the protein into a functionally active conformation. First, no candidate interacting proteins were found to differentially co-immunoprecipitate with WT ABCA4 and ABCA4-Δ30 as analyzed on Coomassie blue stained SDS gels. Second, the ABCA4-Δ30 mutant lacking the VFVNFA motif solubilized poorly in CHAPS detergent relative to WT and other ABCA4 deletion mutants suggesting that most of the expressed protein was misfolded and possibly aggregated. Even the protein that was solubilized was functionally inactive

except for residual basal ATPase activity. This was true also for the ABCA4-Ala6 mutant which also lacks the VFVNFA motif. Third, the subcellular distribution of ABCA4-Δ30 and ABCA4-ala6 differed significantly from that of WT ABCA4 and the other active deletion mutants as revealed by immunofluorescence labeling of cells. In particular, WT ABCA4, ABCA4-Δ8, ABCA4-Δ16 and ABCA4-Δ24 mutants all preferentially localized to large intracellular vesicular structures in HEK 293T cells, a distribution previously observed for heterologously expressed peripherin/rds and rom-1, two photoreceptor proteins that co-localize with ABCA4 along the rim region of rod and cone photoreceptors (Ahn et al., 2003; Goldberg et al., 1995; Moritz and Molday, 1996). In contrast, the ABCA4-Δ30 and ABCA4-Ala6 mutants localized in a diffuse perinuclear pattern characteristic of retention of these proteins in the ER. Together, these studies indicate that VFVNFA motif of ABCA4 is required for the proper folding of ABCA4 into its native, functional state.

Our studies, however, also suggest that the VFVNFA motif is important in the proper folding of ABCA1. The ABCA1-Δ46 and ABCA1-Ala6 mutants lacking the VFVNFA motif, which were previously reported to be devoid of cholesterol efflux activity (Fitzgerald et al., 2004), are retained in the ER suggesting that the loss of function of these mutants may be primarily due to protein misfolding and not a deficiency in protein-protein interactions.

Some differences in the role of VFVNFA in ABCA4 and ABCA1, however, are evident in the relative basal ATPase activity of the deletion mutants. The ABCA1 C-terminal deletion mutant, ABCA1-Δ46, lacking the VFVNFA motif and downstream

amino acids, displayed a significantly higher ATPase activity than WT ABCA1, whereas the equivalent ABCA4-Δ30 mutant showed a marked reduction in ATPase activity compared to WT ABCA4 (Fig. 3.8). However, the basal activity may not be an accurate measure of the function of these transporters.

While the VFVNFA motif is critical for functional activity of ABCA4 through its effect on protein folding, segments just downstream of this motif appear to play a role in modulating the functional properties of ABCA4. ABCA4-Δ24 exhibited 3-fold higher 8-azido ATP labeling, but lower basal and retinal stimulated ATPase activity. This suggests that amino acids just downstream of the VFVNFA motif may directly or indirectly interact with the NBDs to modify ATP binding and hydrolysis in NBD2 (Ahn et al., 2003). The importance of downstream sequences is further supported in the expression and functional analysis of the ABCA4/A1 chimera mutant in which the C-terminal 24 amino acids of ABCA4 is replaced with the C-terminal segment of ABCA1. This mutant retained its ability to bind *N*-ret-PE, but showed a marked reduction in both azido-ATP labeling and retinal stimulated ATPase activity. Furthermore, this mutant solubilized poorly with CHAPS and exhibited a subcellular distribution consistent with a major fraction of the protein being retained in the ER. These results suggest that the ABCA1 C-terminal segment interferes with efficient folding of ABCA4 and has a negative effect on nucleotide binding and hydrolysis activities. Interestingly, an opposite effect was observed for the reverse chimera mutant ABCA1/A4 in which the C-terminal segment of ABCA1 was replaced with that of ABCA4. In our study, the basal ATPase

activity of this mutant was twice the activity of WT ABCA1 (Fig. 3.8) and in an earlier published study (Fitzgerald et al., 2004), a higher cholesterol efflux activity in the presence or absence of apoA-1 was observed for this mutant relative to WT ABCA1. Hence, the C-terminus of ABCA4 appears to contain residues that enhance the functional activity of ABCA1, possibly through interactions with the NBDs, whereas the C-terminus of ABCA1 has residues that inhibit the folding of ABCA4 and diminish its functional activity.

Alignment of C-terminal ABCA4 sequences from various species show a conserved KQQ(T/N)E region just downstream of the VFVNFA motif which may contribute to enhanced ATPase activity of the ABCA1/A4 chimera mutant (Fig. 3.10). ABCA1 orthologues also contain a conserved region (KDQSDD) just downstream of the VFVNFA motif. Additional mutational studies should further define the importance of these conserved regions in modulating the nucleotide dependent activities of these ABCA transporters.

Mutations in the ABCA4 gene have been shown to cause a number of retinal degenerative diseases of varying severity. A model has been proposed in which the severity of the disease phenotype is inversely proportional to the level of residual functional activity displayed by the mutant ABCA4 proteins (Maugeri et al., 1999; Shroyer et al., 1999). Retinitis pigmentosa, the most severe disease phenotype with complete loss in vision, would arise when mutations in both alleles cause the complete loss in function such as for the case of frameshift mutations causing severely truncated

proteins. At the other end of the spectrum, age-related macular degeneration, the mildest phenotype can occur in individuals who are heterozygous for selected disease-linked mutations in ABCA4. These individuals retain a significant proportion of ABCA4 functional activity from the wild-type allele. Cone rod dystrophy and Stargardt macular degeneration are intermediate in severity with the former resulting from mutations that cause a significant, but not complete, loss in ABCA4 function and the latter resulting from mutations which result in only partial loss in activity. Our studies on C-terminal deletion mutants are consistent with this model and provide mechanistic insight into the different phenotypes displayed by two patients with deletion mutations in the C-terminus of ABCA4. A patient with cone-rod dystrophy was reported to be compound heterozygous for a 6730-16del44 mutation which causes the loss in the C-terminal 29 amino acids of ABCA4 including the VFVNFA motif and a R212C missense mutation (Stenirri et al., 2006). The relatively severe phenotype of this patient is consistent with the complete loss in functional activity observed for the ABCA4-Δ30 mutant. The R212C missense mutation appears to retain some of its activity at least with respect to azido-ATP photoaffinity labeling (Sun et al., 2000). Another patient diagnosed with a mild form of Stargardt macular degeneration was found to be compound heterozygous for a 6748delA mutation in one allele and a S1066P missense mutation in the other allele (Fumagalli et al., 2001). The 6748delA mutant protein is comparable to the ABCA4-Δ24 mutant studied here in that the amino acid content after the VFVNFA motif is altered. As shown in our study, the ABCA4-Δ24 mutant retains significant

functional activity. The functional consequence of the S1066P mutation in ABCA4 has not been examined. However, based on analysis of other disease-linked missense mutation in the ECD1 region of ABCA4 (Sun et al., 2000), it is likely that this mutant also retains at least some functional activity. Hence, together these mutations are likely to provide sufficient functional activity to generate the milder phenotype of Stargardt macular degeneration.

In summary, we have shown that the VFVNFA motif is required for proper folding of ABCA4 into a functionally active protein. Segments downstream of this motif appear to modulate the activity of ABCA4 possibly through direct or indirect interaction with the NBD domains of ABCA4. Functional analysis of the C-terminal deletion mutants provides a molecular based rationale for the phenotype displayed by patients with disease-associated mutations in this region of ABCA4.
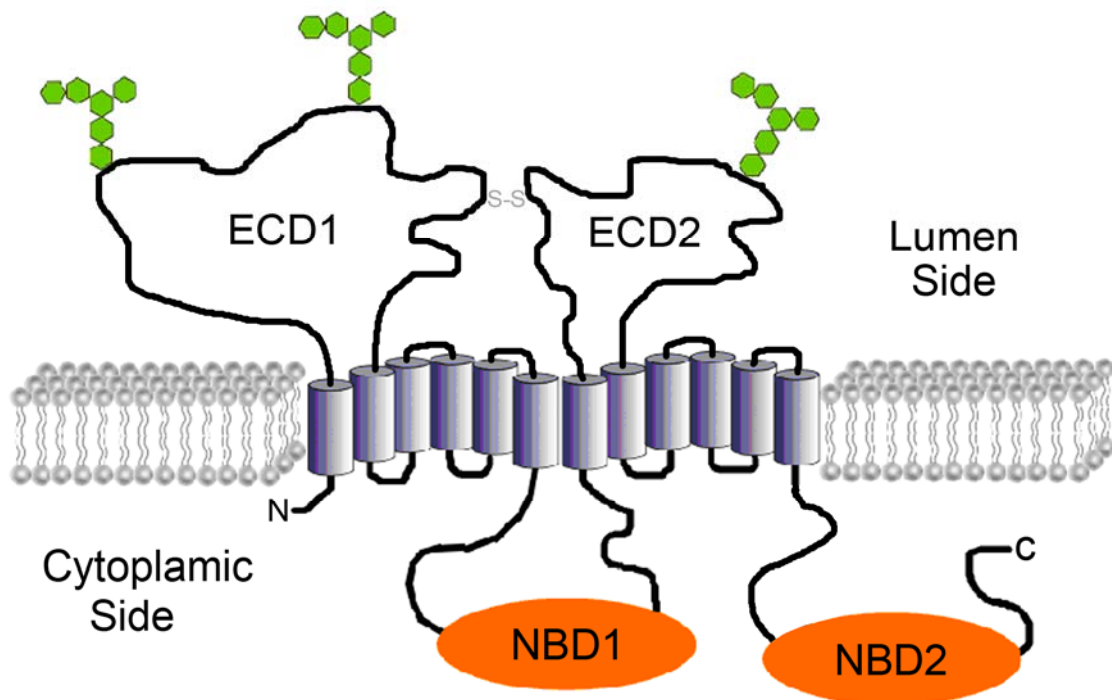
Figure 3.1. Membrane topological model for ABCA4. The homologous N and C half of the transporter each harbors an extracellular domain (*ECD*) and an nucleotide binding domain (*NBD*). N-linked oligosaccharide chains are shown with hexagons in ECD1 and ECD2.
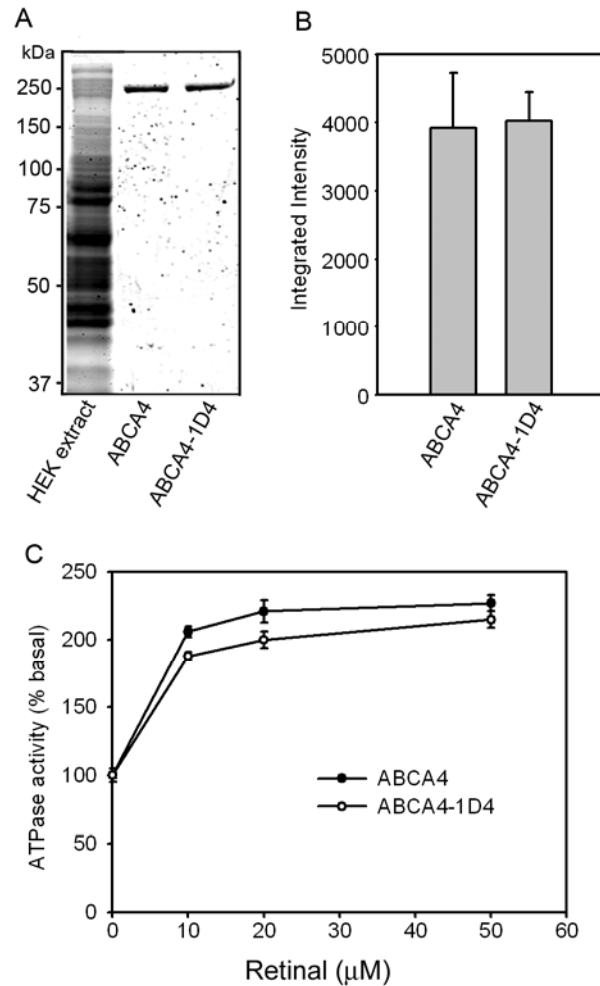
Figure 3.2. Expression and ATPase activity of ABCA4 and ABCA4-1D4. ABCA4 and ABCA4-1D4 containing a 9 amino acid 1D4 epitope were expressed in HEK 293T cells, solubilized in CHAPS detergent, purified on a Rim 3F4-Sepharose immunoaffinity matrix and reconstituted into liposomes for determination of basal and all-*trans*-retinal stimulated ATPase activity measurements. **A**. SDS gel stained with Coomassie blue showing a typical membrane extract from HEK 293T cells expressing ABCA4 (lane 1), immunoaffinity purified ABCA4 (lane 2), and immunoaffinity purified ABCA4-1D4 (lane 3). **B**. Relative expression levels of ABCA4 and ABCA4-1D4 quantified from Coomassie blue stained proteins. **C**. ATPase activity of purified and reconstituted ABCA4 and ABCA4-1D4 as a function of added all-*trans*-retinal. Data show the average value for 3 experiments ± SD.
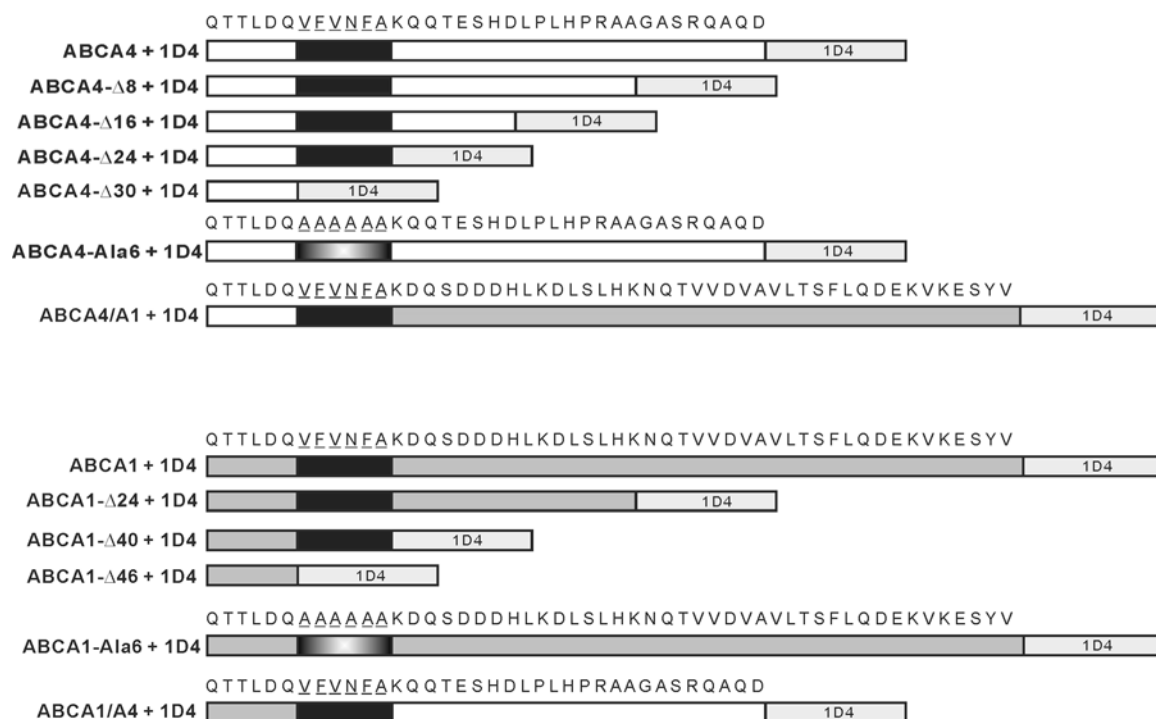
Figure 3.3. Schematic showing the sequence of the various C-terminal deletion and chimera mutants of 1D4 tagged ABCA4 and ABCA1 used in this study. Only the C-terminal 36 and 52 amino acids are shown for full-length ABCA4 and ABCA1, respectively. The 9 amino acid 1D4 epitope (TETSQVAPA) is shown in light gray; ABCA4 in white; ABCA1 in darker gray; and the VFVNFA motif in black.
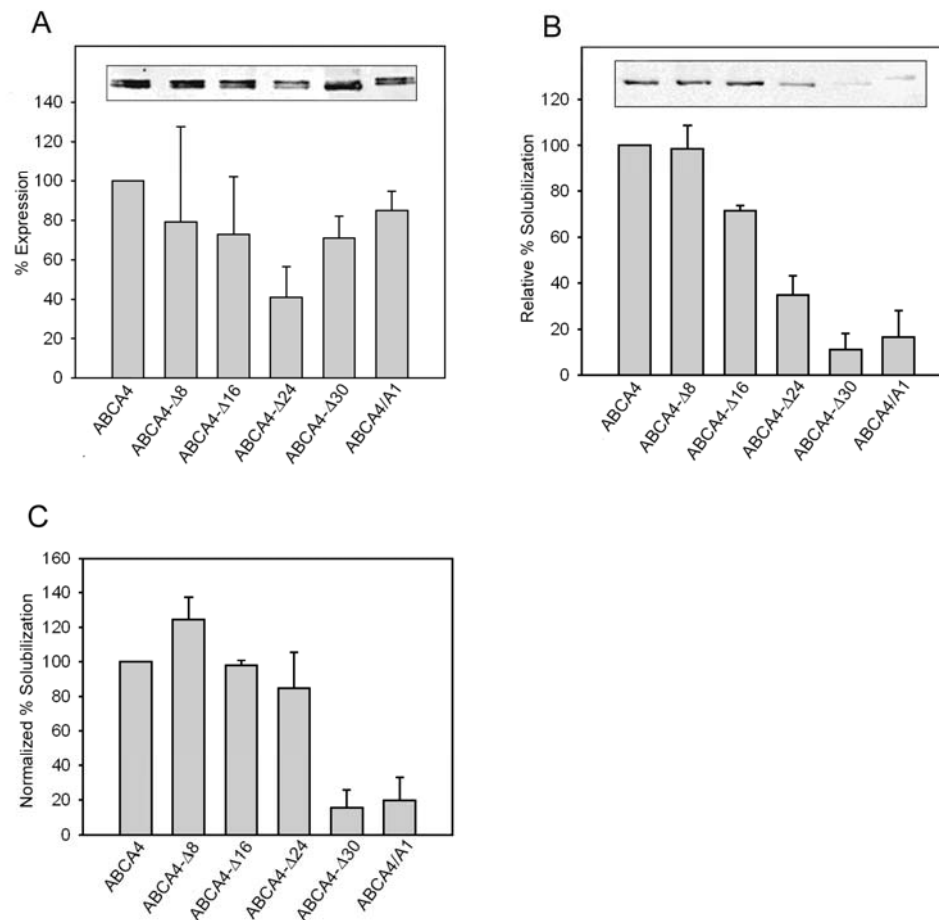
Figure 3.4. Expression and solubilization of ABCA4 C-terminal mutants. Membranes from HEK 293T cells expressing WT and mutant ABCA4 and containing the 1D4 tag were treated with detergent and the amount of ABCA4 was quantified on Western blots labeled with the Rho 1D4 antibody. **A**. Relative expression of ABCA4 mutants was determined from membranes solubilized with SDS; **B**. Relative solubilization was determined by solubilizing membranes in 18 mM CHAPS and removing unsolubilized material by centrifugation prior to SDS gel electrophoresis and Western blotting. **C**. Normalized solubilization was determined from the ratio of CHAPS solubilization to the level of expression determined from SDS solubilized membranes and expressed as % of WT ABCA4. Inserts show representative examples of western blots of the ABCA4 mutants. A doublet band was present in SDS solubilized samples and a single sharp band was observed for CHAPS solubilized samples suggesting that poorly processed ABCA4 was not solubilized by CHAPS. Quantitative data are an average from 3 or more independent experiments ± SD.

A

Rho 1D4

Azido-ATP

WT ABCA4 | ABCA4-Δ8 | ABCA4-Δ16 | ABCA4-Δ24 | ABCA4-Δ30 | ABCA4/A1

B

% Azido-ATP Labeling

ABCA4 | ABCA4-Δ8 | ABCA4-Δ16 | ABCA4-Δ24 | ABCA4-Δ30 | ABCA4/A1
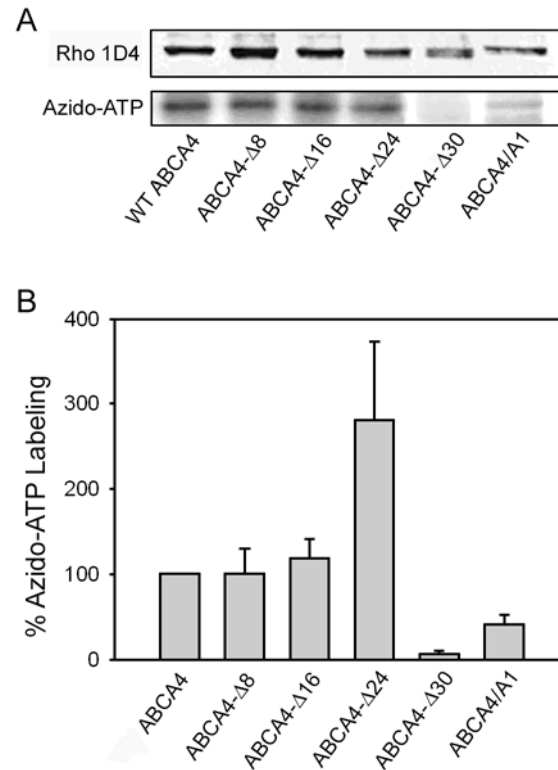
Figure 3.5. Azido-ATP photoaffinity labeling of ABCA4 mutants. Membranes from HEK 293T cells expressing the ABCA4 mutants tagged with the 1D4 epitope were photoaffinity labeled with 8-azido-adenosine 5'-[α ^{32}P] triphosphate prior to analysis on SDS gels. **A**. Representative western blots of 1D4 tagged ABCA4 proteins labeled with the Rho 1D4 antibody and azido-ATP labeling analyzed on a phosphor imager. **B**. Quantitative analysis of azido-ATP labeling of mutants relative to WT ABCA4 after normalization for the amount of ABCA4. Data represent an average of 3 experiments $\pm$ SD.
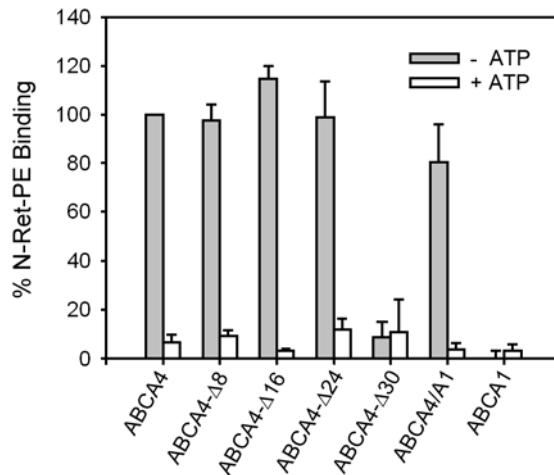
Figure 3.6. Binding of *N*-ret-PE to ABCA4 mutants in the absence and presence of ATP. WT and mutant ABCA4 tagged with the 1D4 epitope were immobilized on a Rho 1D4-Sepharose matrix and incubated with [^{3}H]-labeled all-*trans*-retinal in the presence of PE. The matrix was washed to remove unbound substrate and incubated in the absence or presence of 0.5 mM ATP. The bound *N*-ret-PE was eluted with ethanol and quantified by scintillation counting. Data represent the average of 3 or more experiments ± SD.
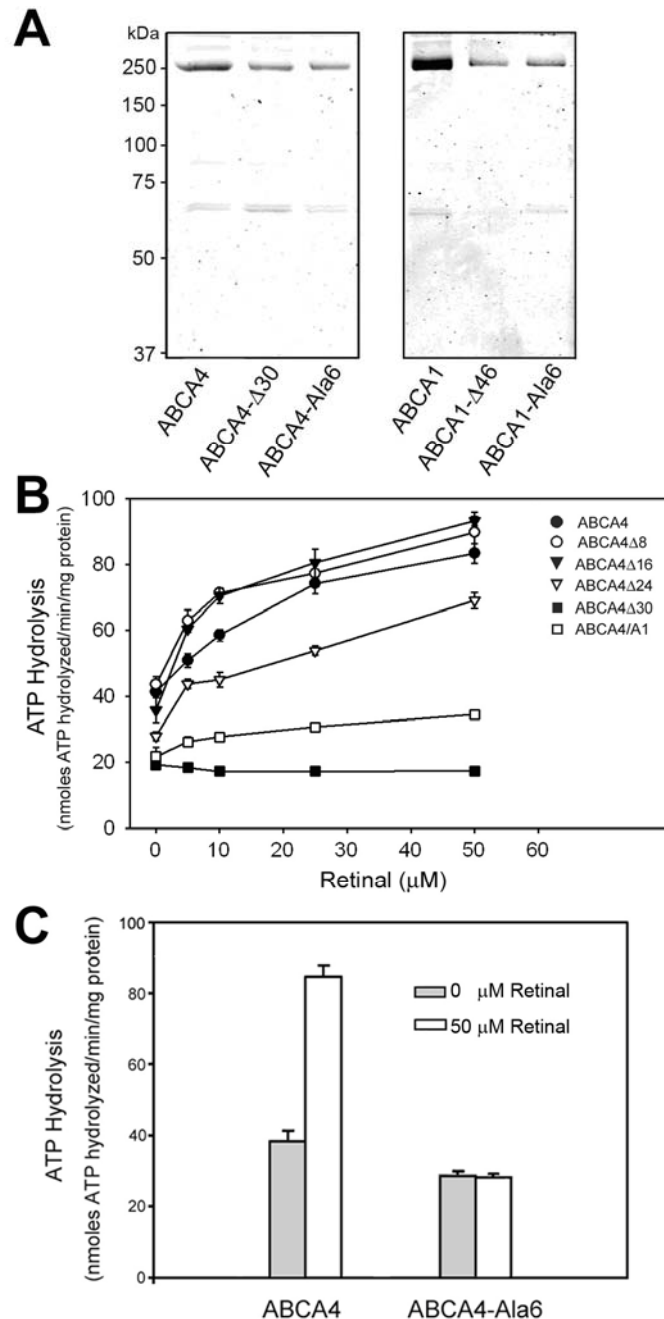
Figure 3.7. Purification of WT and mutant ABCA4 and ABCA1 and analysis of retinal stimulated ATPase activities of ABCA4 mutants. ABCA4 and ABCA1 proteins were expressed in HEK 293T cells, purified on Rho1D4-Sepharose matrix, and reconstituted into brain lipid vesicles. The ATPase activity of ABCA4 mutants was measured as a function of increasing all-*trans*-retinal concentrations. **A**. Coomassie blue stained SDS gels showing the intense 250 kDa ABCA4 or ABCA1 transporters and an additional faint 65 kDa band co-immunoprecipitating protein band. **B**. Retinal stimulated ATPase activity of purified and reconstituted ABCA4 proteins. Data represent an average of 3 experiments $\pm$ SD. **C**. ATPase activity of wild-type ABCA4 and the ABCA4-Ala6 mutant in which the VFVNFA motif was replaced with six alanine residues. Data represent an average of 3 experiments $\pm$ SD.
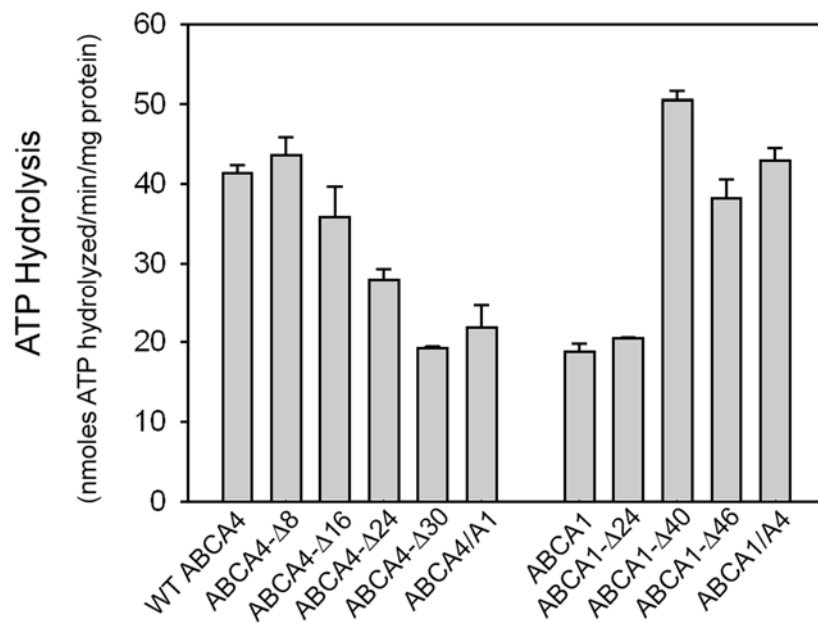
Figure 3.8. Basal ATPase activity of ABCA4 and ABCA1 mutants. ABCA4 and ABCA1 mutants were expressed in HEK 293T cells, immunoaffinity purified on a Rho 1D4-Sepharose matrix and reconstituted into brain lipid vesicles for analysis of basal ATPase activity.
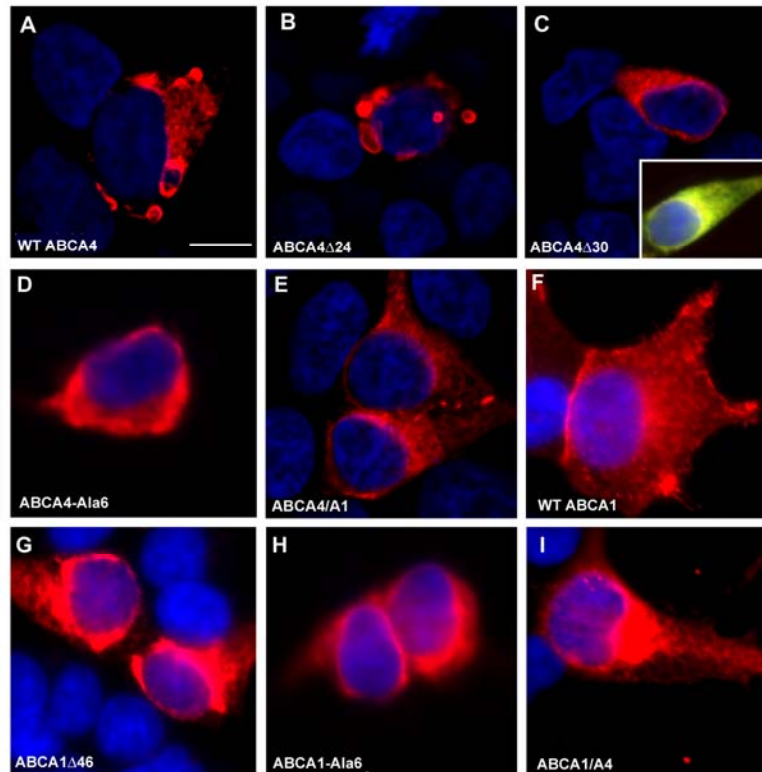
Figure 3.9. Immunofluorescence microscopy of HEK 293T cells expressing ABCA4 mutants. HEK 293T cells transfected with WT or mutant ABCA4 plasmids were fixed in paraformaldehyde, permeabilized in 0.1% Triton X-100, labeled with the Rho 1D4 antibody and Cy3-tagged goat anti-mouse Ig, and counterstained with DAPI nuclear stain. **A-B**. WT and ABCA4-Δ24 mutants are localized to large intracellular vesicular structures. A similar labeling pattern was observed for the ABCA4-Δ8 and ABCA4-Δ16 mutants (data not shown). **C-D**. ABCA4-Δ30 and ABCA4-Ala6 mutants labeling shows a perinuclear pattern characteristic of ER localization. Inset in C shows a merged image of a cell double labeled for ABCA4-Δ30 (red) and the ER marker calnexin (green). Colocalization is indicated by a yellow color. **E**. ABCA4/A1 mutants show primarily a perinuclear pattern characteristic of ER although some intravesicular labeling is observed. **F**. WT ABCA1 mutant shows a pattern of labeling characteristic of plasma membrane localization. **G-H**. ABCA1-Δ46 and ABCA1-Ala6 mutants show a perinuclear pattern of labeling characteristic of ER localization. **I**. ABCA1/A4 mutant shows strong perinuclear labeling along with some plasma membrane labeling. Bar = 5 μm.

ABCA4 C-terminal sequences

```
Human:          VFVNFAKQQTESHDLPLHPRAAGASRQAQD
Monkey:         VFVNFAKQQNEIHDLPLHPRAAGASRQAQD
Bovine:         VFVNFAKQQNETYDLPLHPRTAGASRQAKEVDKGNSAPQG
Dog:            VFVNFAKQQTETHDLPLHPRAAGASRQAKV
Mouse:          VFVNFAKQQTETYDLPLHPRAAGASWQAKLEEKSGRLQTQEPLPAGSEQLANGSNPTAAEDKHTRSPQ
X.laevis        VFVNFAKQQTDDEDIHLHPRAAGATRDVKVAPAPPPKTPAQ
X.tropicalis    VFVNFAKQQTEDEDIHLHPRAAGATRDMKVAPAPPPKTPAQ
                *********.:   *: ****:***:  :  :
```

ABCA1 C-terminal sequences

```
Human:          VFVNFAKDQSDDDHLKDLSLHKNQTVVDVAVLTSFLQDEKVKESYV
Mouse:          VFVNFAKDQSDDDHLKDLSLHKNQTVVDVAVLTSFLQDEKVKESYV
Chicken:        VFVNFAKDQSDDDHTKDLSLHKNQTVVDIAILNSFLQDEKVKESCV
                **************  **************:*:*.*********** *
```

Figure 3.10. Sequence alignments of the C-terminal segments from several ABCA4 and ABCA1 orthologues. The VFVNFA motif shown in bold type is underlined. Sequences just downstream of the VFVNFA are conserved for ABCA4 and ABCA1 and may contribute in modulating the functional activities of these transporters. "*" marks identical residues in all sequences. ":" and "." means conserved and semi-conserved substitutions respectively.

CHAPTER 4: INTERACTION OF ABCA4 WITH RHODOPSIN AND ARRESTIN

4.1 Introduction

ABCA4 is a member of the ATP Binding Cassette (ABC) transporter superfamily (Allikmets et al., 1997b; Azarian and Travis, 1997; Illing et al., 1997), which are membrane proteins that translocate a wide variety of substrates across extra- and intracellular membranes (Borst and Elferink, 2002; Higgins, 1992). It is exclusively expressed in the retina and is specifically localized to the rim region of the disks in photoreceptor cell outer segments (Illing et al., 1997; Papermaster et al., 1978). Mutations in ABCA4 are known to cause Stargardt disease, a form of inherited juvenile macular degeneration (Allikmets et al., 1997b). Biochemical studies and research on *abca4* knockout mice suggest that ABCA4 translocates a retinoid substrate, *N*-ret-PE, across the disk membrane. When ABCA4 function is compromised, the buildup of this compound leads to toxicity and photoreceptor death (Beharry et al., 2004; Molday et al., 2000; Molday, 2007; Sun et al., 1999; Weng et al., 1999).

In this study, proteins that co-purify with ABCA4 by immunoaffinity chromatography were analyzed by mass spectrometry. Major components of the visual cascade, rhodopsin, and arrestin (including a splice variant of arrestin, p[44]) were identified. Their identities were confirmed by western blotting techniques. Rhodopsin is one of the best studied G protein-coupled receptors (GPCRs). As the visual pigment in rod photoreceptor cells, it triggers the phototransduction cascade. The shutoff of the visual cascade starts with deactivation of Meta II rhodopsin. This is achieved by

phosphorylation of activated rhodopsin, catalyzed by rhodopsin kinase (RK), and subsequent binding of arrestin (Mendez et al., 2000). In this study we have found that the association of rhodopsin / arrestin complex to ABCA4 only takes place in bleached ROS but not dark adapted ROS, and all-*trans*-retinal is a key regulator of the interaction.

The identification of rhodopsin and arrestin as protein binding partners of ABCA4 provides a new lead for the investigation of potential regulatory mechanisms of ABCA4. A better understanding of the regulation of ABCA4 will help elucidate the physiological and pathological role of ABCA4 in the visual cycle and Stargardt disease.

4.2 Methods

4.2.1 Reagents and Solutions

All-*trans*-retinal, all-*trans*-retinol, soybean phospholipids, and CHAPS were purchased from Sigma. The phospholipids (DOPE and DOPC) were from Avanti Polar Lipids (Alabaster, AL). Complete Protease Inhibitor was from Roche Applied Sciences (Indianapolis, IN). All organic solvents (chloroform, hexane, and methanol) were HPLC grade and water was distilled and deionized. The Rim 3F4 monoclonal antibody directed against a defined epitope near the C-terminus of ABCA4 and the Rho 1D4 antibody to the nine-amino acid C-terminal sequence of rhodopsin have been described previously (Hodges et al., 1988; Illing et al., 1997; MacKenzie et al., 1984). Monoclonal antibody Sct-128 against arrestin was a kind gift from Dr. Paul Hargrave (University of Florida).

The composition of buffers was as follows: hypotonic buffer: 10 mM HEPES, pH 7.5; solubilization buffer: 50 mM HEPES, pH 7.5, 0.1 M NaCl, 18 mM CHAPS, 1 mM

DTT, 3 mM MgCl$_2$, 10% glycerol, 0.32 mg/ml DOPE, and 0.32 mg/ml DOPC; column buffer: 50 mM HEPES, pH 7.5, 0.1 M NaCl, 10 mM CHAPS, 1 mM DTT, 3 mM MgCl$_2$, 10% glycerol, 0.32 mg/ml DOPE, and 0.32 mg/ml DOPC; reconstitution buffer: 25 mM HEPES, pH 7.5, 0.14 M NaCl, 1mM EDTA, 1 mM DTT, and 10% glycerol. All-*trans*-retinal concentration in ethanol was determined spectrophotometrically using an extinction coefficient of 42,900 M^{-1}cm^{-1}.

4.2.2 Immunoaffinity Purification of ABCA4 from Bleached or Dark-adapted ROS Membranes

The Rim-3F4 monoclonal antibody was purified and coupled to CNBr-activated Sepharose 2B matrix as described in Section 2.2.2. one mg of dark adapted ROS preparation was washed in the dark with 1.5 ml hypotonic buffer by centrifugation at 20,000 $\times$ g for 10 min and resuspended with 1.5 ml same buffer. Resuspended ROS were either wrapped in aluminum to be kept dark adapted or exposed to a 60 W light bulb placed 10 cm away. The bleaching was carried out on ice for 30 min. The following steps before elution were carried out under dim red light. All incubations were done in light proof containers. The membranes were washed 3 times with 1.5 ml of hypotonic buffer, solubilized in 0.5 ml of solubilization buffer, and incubated with 50 μl packed Rim 3F4-Sepharose 2B beads for 1 h at 4°C. The beads were washed 6 times with 0.4 ml of column buffer. Bound proteins were eluted with 65 μl of 1% SDS or column buffer containing 0.2 mg/ml 3F4 peptide. Thirty μl of the sample was mixed with 10 μl of 4$\times$ loading dye for analysis by SDS-PAGE.

4.2.3 SDS Gel Electrophoresis and Western Blotting

Protein samples were separated on 8% SDS polyacrylamide gels and transferred onto Immobilon-FL membranes with a semi-dry blotting apparatus as described in Section 3.2.8. Gels that were not transferred for blotting were stained with Coomassie blue. The Coomassie stain contained 0.025% R250 Coomassie dye, 25% isopropanol, and 10% acetic acid. Gels were destained with 10% acetic acid.

4.2.4 MALDI-TOF Mass Spectrometry

In-gel digestion of immunoprecipitated proteins was performed by punching out the Coomassie-stained bands from a Nu-Page (Invitrogen) SDS gradient gel with a glass Pasteur pipette. The gel plugs were washed with water several times to remove acetic acid and incubated 3 times for 15 min each with a 1:1 mixture of 100 mM ammonium bicarbonate and 100% acetonitrile for destaining. After incubating with 100% acetonitrile, the gels were dried and subsequently incubated with 10 mM DTT in 100 mM ammonium bicarbonate at 56°C for 1 hr and 50 mM iodoacetamide in the same buffer in the dark for 30 min. The samples were then washed with ammonium bicarbonate and dehydrated with 100% acetonitrile. The gel pieces containing the samples were incubated with porcine trypsin (Promega, Madison, WI) at 10 ng/µl in 50 mM ammonium bicarbonate and 5 mM $CaCl_2$ for 15 min. The protease solution was removed, and the gel pieces were overlaid with 50 mM ammonium bicarbonate and 5 mM $CaCl_2$. The samples were digested for 18 h at 37°C. The supernatant was collected in a separate tube, and the gel pieces were re-extracted with 50 mM ammonium bicarbonate/66%

acetonitrile (basic extraction) and with 5% formic acid/66% acetonitrile (acidic extraction). The extractions were pooled, dried in a Speedvac (Thermo Electron, Waltham, MA) and resuspended in 10 µl of 50 mM ammonium bicarbonate. Trypsin-digested samples (2 µl) were applied to H4 chips (Ciphergen, Fremont, CA). The sample was dried and washed with two quick rinses of water before applying 20% α-cyanohydroxycinnamic acid (CHCA) matrix in a solvent containing 50% acetonitrile and 0.1% trifluoroacetic acid. Samples were analyzed on a Ciphergen MALDI-TOF mass spectrometer. Masses obtained were average masses and mined against a mammalian data base using Profound server.

4.2.5 Chemical Treatment of ROS Membranes

To remove free all-*trans*-retinal, bleached ROS membranes were incubated with 2 mM NADPH or 20 mM hydroxylamine in 10 mM HEPES at 30°C for 30 min under an incandescent light bulb (60 W). NADPH is the cofactor needed by retinol dehydrogenase to reduce all-*trans*-retinal to all-*trans*-retinol. Hydroxylamine reacts with all-*trans*-retinal and converts it to inert retinal-oxime. To add all-*trans*-retinal or *N*-retinyl-PE, the reduction product of *N*-ret-PE, to dark-adapted ROS membranes, 5 mM stock in ethanol was added in the dark to achieve a final concentration of 25 µM. Incubation was continued at 30°C in the dark for 30 min. The treated membranes were washed 3 times with 1.5 ml of hypotonic buffer and solubilized as described in Section 4.3.1.

4.2.6 Extraction of Rhodopsin from ABCA4 / rhodopsin / Arrestin Complex

Three mg of ROS was solubilized in 1.5 ml solubilization buffer and incubated with 150 μl Rim 3F4-Sepharose beads for 30 min at 4°C. The beads were eluted with 240 μl 3F4 peptide (0.2 mg/ml in column buffer) 2 times at RT. The eluted proteins were combined and 160 μl of this fraction was incubated with 50 μl Rho 1D4-Sepharose beads for 30 min at 4°C. The flow through fraction of the Rho 1D4-Sepharose beads was also collected for analysis. After 6 washes with 0.3 ml column buffer, the Rho 1D4-Sepharose beads were eluted with 80 μl 2% SDS solution containing 50 mM NaHepes, pH 7.5, 0.1 mM NaCl and 5 mM $MgCl_2$. The elutions from Rim 3F4-Sepharose 2B beads, Rho 1D4-Sepharose 2B beads and flow through from the latter (30 μl each) each were mixed with 4 $\times$ gel cocktail and resolved by SDS-PAGE.

4.2.7 Addition of soluble ROS proteins to Immobilized ABCA4

Extraction of soluble proteins (containing endogenous arrestin) from dark-adapted ROS was carried out under dim red light. 4 mg of ROS suspended in homogenizing buffer containing sucrose as previously described (Section 2.2.2) was spun down in an Optima ultracentrifuge (Beckman, Palo Alto, CA) at 100,000 $\times$ g for 10 min. The resulting pellet was resuspended in 250 μl extraction buffer (2 mM NaHEPES, 2 mM $MgCl_2$, 0.1 mM EDTA and complete protease inhibitor) and incubated on ice for 1 h with occasional vortexing. The membrane was centrifuged down and the supernatant was collected. The extraction was repeated and the supernatants from both extractions were pooled and diluted with solubilization buffer 1:1.

ROS were kept dark adapted or bleached and solubilized as described in Section 4.2.1. One mg of dark-adapted ROS was solubilized under dim red light and incubated with 50 μl of Rim 3F4-Sepharose beads in the dark. A duplicate column was prepared as previously described. After thorough washing to remove unbound proteins, soluble ROS proteins supplemented with detergent (500 μl) were incubated with one column. The duplicate column was incubated with same buffer containing no soluble proteins. After washing, the bound proteins were eluted with 80 μl of 3F4 peptide twice and the two elutions were pooled. One mg of ROS was exposed to light, solubilized and incubated with the third Rim 3F4-Sepharose column. This column was washed and incubated with buffer containing no ROS soluble proteins, as a positive control for rhodopsin / arrestin binding to ABCA4. Bound proteins were eluted with 0.2 mg/ml 3F4 peptide in column buffer and analyzed by SDS-PAGE.

4.2.8 Reconstitution and ATPase Activity Assay

ABCA4 with large amount of rhodopsin / arrestin complex bound (purified from bleached ROS) or with little rhodopsin / arrestin complex (from dark-adapted ROS) were reconstituted into brain polar lipids using the procedure of Sun *et al* with minor modifications (Sun et al., 1999). Briefly 9 μl of 25 mg/ml brain polar phospholipids were mixed with 6 μl of 15% *n*-octylglucoside (w/v) in 25 mM HEPES, pH 7.4, 140 mM NaCl, 10% glycerol. 48 μl of purified ABCA4 complex (containing 20–40 ng/μl ABCA4) was added and the mixture was incubated 30 min on ice. The sample was rapidly diluted with the addition of 180 μl reconstitution buffer, and then passed through 200 μl

Extracti-gel resin (Thermo Scientific, Waltham, MA) pre-equilibrated with reconstitution buffer in a Mobicol mini-column fitted with 10 µm pore size filter(MoBiTec, Gottingen, Germany). The flow-through containing reconstituted ABCA4 was collected and 5 mM $MgCl_2$ was added prior to measuring ATPase activity.

ATPase activity assays were carried out using [α-^{32}P]ATP (PerkinElmer) and thin layer chromatography as described (Ahn et al., 2000). ATPase assays were carried out in a 10-µl total reaction volume. Reconstituted sample (8 µl) was mixed with 1 µl of 10× retinal or buffer. The final concentration of retinal was 50 µM. The reaction was initiated by the addition of 1 µl of a 10× ATP solution to achieve final concentration of 50 µM or 0.5 mM with 0.2 µCi [α -^{32}P] ATP. After 30 min at 37°C, 4 µl of 10% SDS was added. ATP hydrolysis was visualized by thin layer chromatography.

4.3 Results

4.3.1 Light Sensitive Association of Protein Interactors to ABCA4

ROS preparations were kept dark-adapted or bleached before being solubilized and incubated with Rim 3F4-Sepharose beads (in the dark) to pull down ABCA4 and protein interaction partners. As revealed with Commassie stained SDS-PAGE gel (Fig. 4.1), a faint band (36 kDa) was seen when ABCA4 was purified from dark adapted ROS (Fig. 4.1, *lane Bound (D)*); three distinctive protein bands with apparent molecular weight of approximately 48 kDa, 44 kDa and 36 k Da co-purified with ABCA4 when the protein was purified from bleached ROS (Fig. 4.1, *lane Bound (L)*).

4.3.2 ABCA4 Binds Rhodopsin / arrestin Complex

Mass spectrometric peptide mapping identified the proteins that co-purified with ABCA4 as arrestin, its shorter splice variant (p^{44}) and rhodopsin. The identification of these proteins were confirmed by western blotting experiments with specific monoclonal antibody Sct-128 against arrestin and p^{44}, and Rho-1D4 against rhodopsin (Fig 4.2).

4.3.3 Association of Rhodopsin / arrestin Complex with ABCA4 is Dependant on All-*trans*-retinal

All-*trans*-retinal is released from rhodopsin when ROS are bleached. To determine the role of all-*trans*-retinal in promoting the binding of rhodopsin / arrestin complex to ABCA4, NADPH or hydroxylamine was added to bleached ROS preparations to remove all-*trans*-retinal. NADPH is a cofactor for endogenous retinol dehydrogenase to reduce all-*trans*-retinal to all-*trans*-retinol. Hydroxylamine reacts with all-*trans*-retinal to form inert retinal-oxime. Membrane proteins were then solubilized with CHAPS and incubated with Rim 3F4-Sepharose matrix. Proteins retained on the column were separated by SDS-page and analyzed by western blotting. The removal of all-*trans*-retinal in ROS membranes reversed binding of arrestin/rhodopsin complex to ABCA4 (Fig. 4.3A). Whereas addition of all-*trans*-retinal to dark-adapted ROS encouraged association of rhodopsin / arrestin complex to ABCA4 to the same extent as bleached ROS (Fig. 4.3B). Neither all-*trans*-retinol nor *N*-retinyl-PE had any effect. Since *N*-retinyl-PE binds ABCA4 at the same site as the natural substrate *N*-ret-PE but with a higher affinity, this result suggests that all-*trans*-retinal promotes the association

of these proteins via interaction with rhodopsin and not though *N*-ret-PE binding to ABCA4.

4.3.4 ABCA4 Binds Rhodopsin / arrestin Complex through Arrestin

To study in more detail the binding of rhodopsin / arrestin to ABCA4, the protein complex purified on Rim 3F4-Sepharose matrix was eluted with 3F4 peptides and subsequently incubated with Rho 1D4-Sepharose matrix (Fig. 4.4). Analysis of the flow through (unbound) fraction from the 1D4-column indicated that about 50% of ABCA4 and arrestin did not bind the 1D4 column. Most rhodopsin was removed. A very similar arrestin/ABCA4 ratio remained, compared to the elution from 3F4 beads. In the SDS elution from 1D4 beads, arrestin/ABCA4 ratio remained similar and more rhodopsin was eluted. This result indicated that a fraction of ABCA4 has only arrestin bound. Another fraction of ABCA4 is associated with the rhodopsin / arrestin complex. The existence ABCA4/arrestin complex suggests a binding site on arrestin/p[44] for ABCA4.

4.3.5 Extracted Endogenous Arrestin Does not Re-bind Immobilized ABCA4

Duplicate Rim 3F4-Sepharose columns with ABCA4 purified from dark-adapted ROS were incubated with either buffer or soluble protein extracted from ROS (supplemented with 8 mM CHAPS). After thorough washing, the bound proteins were eluted with 0.2 mg/ml 3F4 peptide in column buffer. As shown in Fig. 4.5, ABCA4 purified from dark-adapted ROS had only a small amount of arrestin bound (*lane 1*, rhodopsin was not labeled). Incubation with extracted soluble protein (containing arrestin) didn't increase the amount of arrestin bound to ABCA4 to the level of the

ABCA4 purified from bleached ROS (*lane 2* and *3*). The last two lanes show the arrestin labeling in the extracted soluble ROS proteins and the flow-through fraction after incubation with immobilized ABCA4.

4.3.6 Association of Rhodopsin / arrestin Complex with ABCA4 Does Not Affect ATPase Activity of ABCA4 in Reconstituted Lipid Vesicles

ABCA4 purified from dark-adapted ROS had much less arrestin/rhodopsin complex bound (about 1/4) compared to ABCA4 purified from bleached ROS. Protein complexes were reconstituted into lipid vesicles and subjected to ATPase activity assays. Binding of arrestin/rhodopsin complex showed no significant effect on the basal or retinal stimulated ATPase activity of ABCA4 (Fig. 4.6).

4.4 DISCUSSION

In this study, three proteins co-purified with ABCA4 from bleached ROS on Rim 3F4 immunoaffinity column. Mass spectrometric analysis identified these proteins to be rhodopsin, visual arrestin and the splice variant of arrestin, p^{44}. Identification of these proteins was confirmed by western blotting. Since both of rhodopsin and arrestin are abundant proteins in ROS, we wanted to ensure that these interactions were specific. The finding that visual arrestin and rhodopsin binding to ABCA4 is regulated by light has provided strong evidence that they are indeed binding partners.

As a downstream event of rhodopsin photolysis, free all-*trans*-retinal is released from rhodopsin. To investigate the role of all-*trans*-retinal in the association of rhodopsin / arrestin complex to ABCA4, it was incubated with dark adapted ROS membranes, and

ABCA4 was purified under dim red light (without bleaching ROS). All-*trans*-retinal restored the interaction to the same level of ABCA4 purified from bleached ROS. Treatment with chemicals that remove free retinal diminished the binding in bleached ROS. These results together suggest that all-*trans*-retinal is a key regulator of this interaction. *N*-retinyl-PE, the reduced adduct of *N*-ret-PE was shown to bind at ABCA4 to the same site as the substrate (Section 2.3.5). Addition of *N*-retinyl-PE to the membrane did not promote the interaction of ABCA4 with rhodopsin and arrestin. This indicates the effect of all-*trans*-retinal is through binding to rhodopsin and not ABCA4. All-*trans*-retinal likely binds to rhodopsin on a different site than that occupied by the covalently bound 11-*cis*-retinal.

To determine which of the two proteins, rhodopsin or arrestin, binds to ABCA4 directly, the protein complex purified on Rim 3F4-Sephorase beads was eluted with specific 3F4 peptide and then passed through Rho 1D4-Sephorase beads. About 50% of ABCA4 / arrestin did not bind the 1D4-Sephorase column (compare *lane 1D4 FT* and *3F4 peptide* in Fig. 4.4A). This fraction contained almost no rhodopsin. The fraction recovered on the 1D4-Sephorase column had similar arrestin/ABCA4 ratio compared to that of the flow-through fraction or the initial material. A higher rhodopsin / ABCA4 ratio was also seen in this fraction. These results suggest that a significant fraction of arrestin that co-purifies with ABCA4 is not associated with rhodopsin and that arrestin binds to ABCA4 directly.

To further study the possible direct interaction between ABCA4 and arrestin,

soluble proteins (containing large amounts of the full-length arrestin but not p[44]) were extracted from ROS and incubated with ABCA4 purified on Rim 3F4-Sepharose from dark-adapted ROS. The extracted arrestin did not bind to immobilized ABCA4. One possible explanation is that arrestin needs to be activated to bind ABCA4. Crystal structure of the bovine rod arrestin (Hirsch et al., 1999) shows an elongated molecule with two domains (N-terminal and C-terminal) and an extended C-terminal tail that makes a strong contact with the body of the N-terminal domain. Upon binding to the C-terminus of rhodopsin, arrestin is activated and experiences a significant conformational change (Ascano and Robinson, 2006; Gurevich and Gurevich, 2006), which involves the release of the arrestin C-terminal tail from N-terminal domain (Hanson et al., 2006; Palczewski et al., 1991).

To determine if the association of rhodopsin / arrestin complex with ABCA4 has any effect on the ATPase activity of ABCA4, ABCA4 was purified from dark adapted or bleached ROS. ABCA4 with very little or a large amount of rhodopsin / arrestin complex bound was reconstituted and subjected ATPase activity assay. However, no significant difference of the activity was observed. It is possible that the regulative effect of rhodopsin / arrestin complex on the activity of ABCA4 was lost during purification and reconstitution.

Rhodopsin belongs to the large protein superfamily of G protein-coupled receptors (GPCR). GPCRs mediate transmembrane signaling by hormones, neurotransmitters, light, odors, and other factors. The signal from the activated GPCRs

is transmitted via trimeric coupling proteins, G proteins, to cellular targets that include membrane ion channels, phosphodiesterases, phospholipases, and adenylate cyclases etc. (Birnbaumer, 1990; Gilman, 1995). The shutoff of the visual cascade is initiated by phosphorylation of activated rhodopsin, catalyzed by rhodopsin kinase (RK), and subsequent binding of arrestin (Mendez et al., 2000). This process represents one common mechanism of GPCR desensitization: the receptors are inactivated by phosphorylation catalyzed by G protein-receptor kinases (GRKs) and binding of the arrestins. Another prototypic GPCR is the adenylyl cyclase-coupled β_2-adrenergic receptor (β_2-AR). Desensitization of this receptor involves phosphorylation of the activated receptors by β-adrenergic receptor kinase (β-ARK or GRK2) and following binding of β-arrestin 1 and 2.

In human genome hundreds of GPCRs are known (Takeda et al., 2002). In contrast, only 7 genes of GRKs (Reiter and Lefkowitz, 2006) and 4 arrestins (Gurevich and Gurevich, 2006) have been identified. Among the 7 GRKs, GRK1 and 7 are expressed specifically in retinal rods and cones, respectively. The 4 arrestins include arrestin 1 (also called visual or rod arrestin), arrestin 2 (also known as β-arrestin or β-arrestin 1), arrestin 3 (β-arrestin 2) and arrestin 4 (cone arrestin or X-arrestin).

The role of β-arrestin has shifted as a result of new findings. Arrestins are soluble, predominantly cytoplasmic proteins. Binding to phosphorylated active GPCRs and termination of G-protein-mediated signaling (receptor desensitization) was the first arrestin function described. The role of arrestin as the silencer of GPCR signaling is the

classic paradigm. Early evidence that β-arrestins have larger roles in GPCR biology than just desensitization came from the discovery that they also function as endocytic adaptors, linking receptors to the components of the internalization machinery – clathrin (Goodman et al., 1996) and AP2 (Laporte et al., 1999). This was interpreted as a natural extension of their desensitizing function and also described as receptor-mediated endocytosis pathway. Subsequent discoveries indicates that receptor-bound β-arrestins interact with numerous signaling proteins, linking GPCRs to a variety of alternative signaling pathways (Gurevich and Gurevich, 2006; Lefkowitz and Shenoy, 2005). β-arrestins serve as adaptors, scaffolds, and/or signal transducers, and they connect the activated receptors with diverse signaling pathways within the cell. The stimulus-dependent receptor recruitment of β-arrestins may provide a general strategy used by GPCRs. The interaction of rhodopsin / arrestin complex with ABCA4 may lead to discovery of novel functions of visual arrestin in phototransduction or visual cycle.

The small numbers of kinases and arrestins indicate they must possess broad specificity to account for the stereotypical inactivation of the GPCRs. Alternatively, a group of homologous but distinct proteins can be generated from a single gene by alternative mRNA splicing or posttranslational modification. For the visual arrestin, in addition to the full-length protein one truncated splice variant was also indentified in bovine (p^{44}) and human (Smith, 1996; Smith et al., 1994). The amino acid sequence of bovine p^{44} was found to be identical with arrestin, except that the C-terminal 35 residues (positions 370-404) are replaced by a single alanine. Several lines of evidence suggest

p^{44} can play an important and distinct role from arrestin in shaping the rod light response: (1) p^{44} is present in the rod at 1/10 the concentration of arrestin (Smith et al., 1994). (2) Functionally, p^{44} binds to phosphorylated (K_D = 12 nM) or unphosphorylated (K_D = 0.24 μM) photolyzed rhodopsin, while arrestin only binds to phosphorylated photolyzed rhodopsin (K_D = 20 nM) (Pulvermuller et al., 1997). (3) p^{44} is associated with membranes (Palczewski et al., 1994) and is permanently present in ROS (Smith et al., 1994); while arrestin is a soluble protein and immunohistochemical studies have shown that arrestin undergoes a massive translocation from the rod inner segment to the ROS upon illumination of the rod (Mangini and Pepperberg, 1988). Despite the much higher abundance of the visual arrestin in ROS, almost an equal amount of p^{44} co-purify with ABCA4 from bleach ROS. This may be explained by its membrane localization. Whether the p^{44} plays a special role in the regulation of ABCA4 remains to be elucidated.

In summary, rhodopsin / arrestin complex has been found to co-purify with ABCA4 from bleached ROS. All-*trans*-retinal is a key regulator for this interaction in ROS. Arrestin is likely to be the protein that directly binds to ABCA4. This interaction provides a new clue to study the regulation of ABCA4 via protein-protein interaction and may lead to discovery of a novel function of arrestin in the visual system.
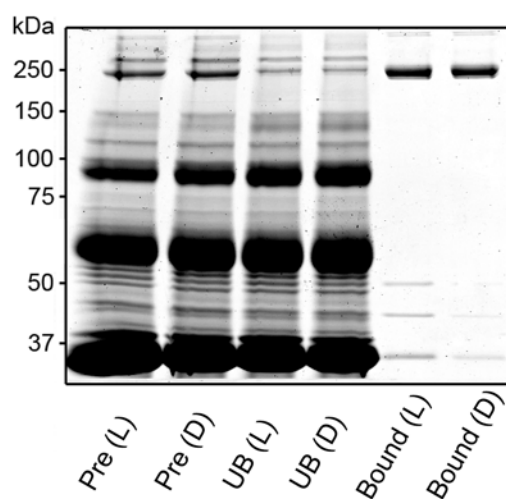
Figure 4.1. ABCA4 purification from light exposed or dark-adapted ROS. ROS membranes were exposed to light (*L*) or kept in the dark (*D*) before being solubilized in CHAPS and incubated with Rim 3F4-Sepharose matrix in the dark. The pre-column fractions (*Pre (L)* and (*Pre (D)*)), unbound fractions (*UB (L)* and *UB (D)*), and the bound fractions (*Bound (L)* and *Bound (D)*) from both columns are shown. The 250 kDa band is ABCA4. Proteins with apparent molecular weights of 48, 44 and 36 kDa co-purify with ABCA4 from light exposed ROS. A faint band of 36 kDa is visible in the bound fraction from dark adapted ROS besides the ABCA4 band.
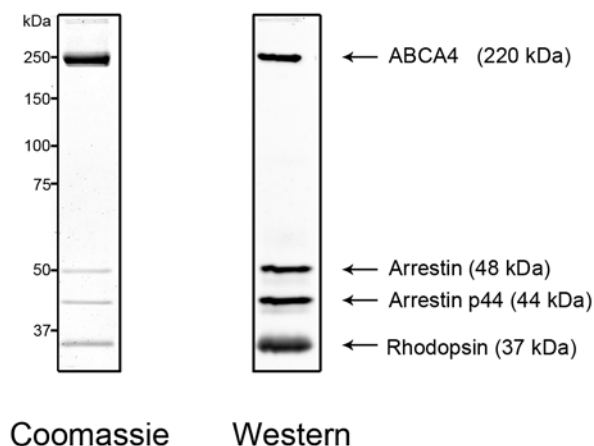
Figure 4.2. Identification of proteins co-purified with ABCA4. Membrane proteins from bleached ROS were solubilized in CHAPS and purified on Rim 3F4-Sepharose matrix. Bound proteins were separated on SDS-PAGE gels. Duplicate lanes were prepared for Coomassie blue staining and Western blot analysis. Protein bands were excised and analyzed by mass spectrometry. *B,* Western blot was labeled with a mixture of monoclonal antibodies, Rim 3F4 (anti ABCA4), Sct-128 (anti arrestin) and Rho-1D4 (anti rhodopsin). Protein name and theoretical molecular weights are placed beside each protein band.
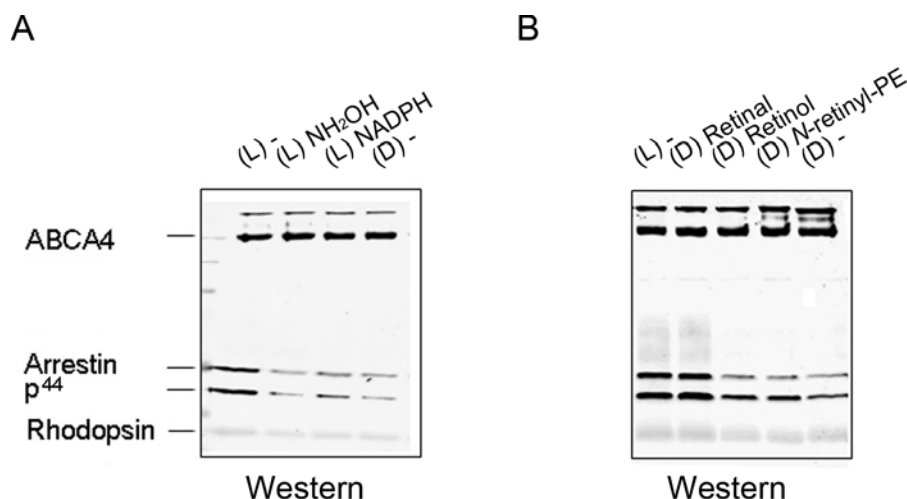
Figure 4.3. Effect of all-*trans*-retinal on rhodopsin / arrestin binding of ABCA4.
A. Bleached ROS membranes were incubated with NH_2OH or NADPH. Treated ROS membranes were then solubilized and ABCA4 was purified on Rim-3F4 Sepharose matrix. Purified proteins were separated by SDS-PAGE, transferred to immobilon-FL membrane for western blotting analysis using specific antibodies Rim-3F4, Arrestin SCT-128 and Rho-1D4. The chemical treatment removed free all-*trans*-retinal and decreased the amount of rhodopsin / arrestin bound to ABCA4 to the level of ABCA4 purified from dark adapted ROS. **B**. Retinal, retinol or *N*- retinyl-PE was added to dark adapted ROS. Treated ROS membranes were then solubilized and ABCA4 was purified in the dark and analyzed by western blotting. Addition of all-*trans*-retinal to dark adapted ROS promoted binding of rhodopsin / arrestin to ABCA4 to the level of ABCA4 purified from light exposed ROS. *(L)* and *(D)* indicate light exposed and dark adapted ROS respectively.
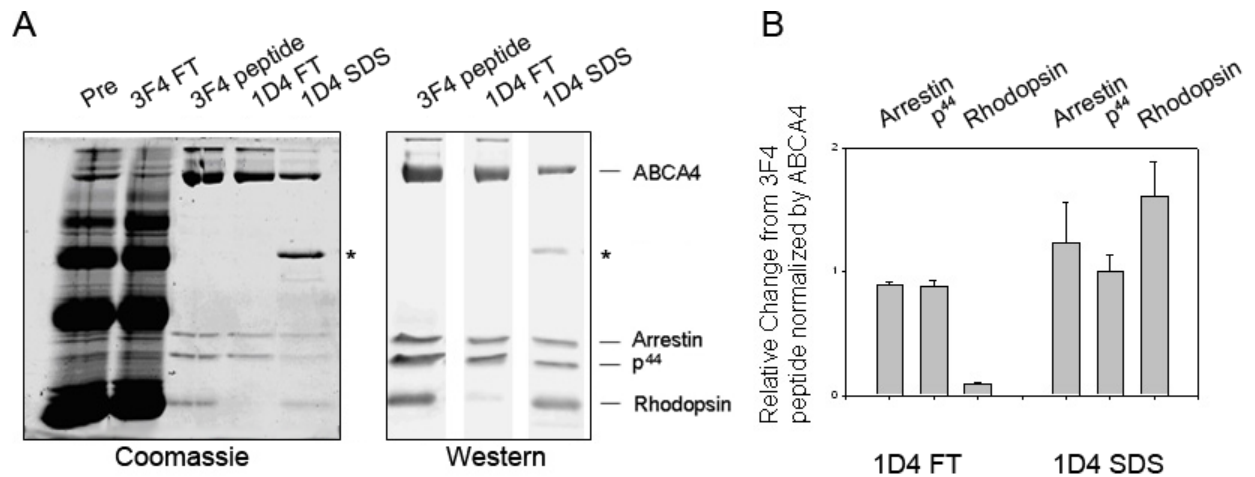
Figure 4.4. Passing ABCA4 / rhodopsin / arrestin complex through Rho 1D4-Sepharose matrix. A. ROS proteins solubilized in CHAPS (*Pre*) were purified on rim-3F4 Sepharose. Proteins eluted by 3F4 peptide (*3F4 peptide*) were incubated with Rho-1D4 Sepharose matrix. Flow through fraction (*1D4 FT*) and SDS eluted fraction (*1D4 SDS*) were collected. About 50% of ABCA4 / Arrestin do not bind to the 1D4 column, indicating that a significant fraction of ABCA4 / Arresin is not associated with rhodopsin. (* indicates the antibody leached off the Rho-1D4 Sepharose column.) **B**. The amounts of arrestin, p^{44} and rhodopsin (relative to ABCA4) from *1D4 FT* and *1D4 SDS* fractions are compared to those from *3F4 peptide* elution (set to 1). For the *1D4 FT* fraction, removal of ~90% rhodopsin maintains a similar ratio of Arr/ABCA4, suggesting a binding site on arrestin/p^{44} for ABCA4.
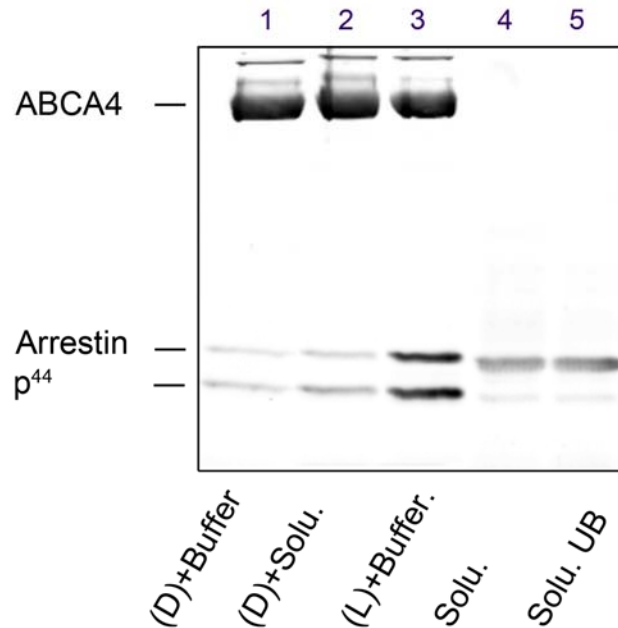
Figure 4.5. Absence of binding of arrestin to immobilized ABCA4. Buffer or ROS soluble proteins containing endogenous arrestin was added to ABCA4 purified on Rim 3F4-Sepharose beads from dark adapted ROS. After incubation, bound proteins were eluted, separated on SDS-PAGE and transferred to immobilon FL membrane. The membrane was labeled with Rim 3F4 and Sct-128 antibody against ABCA4 and arrestin, respectively. ABCA4 purified from bleached ROS is shown in lane 3. Extracted soluble protein before and after incubation with immobilized ABCA4 are shown in lane 4 and 5. Arrestin didn't bind to immobilized ABCA4.
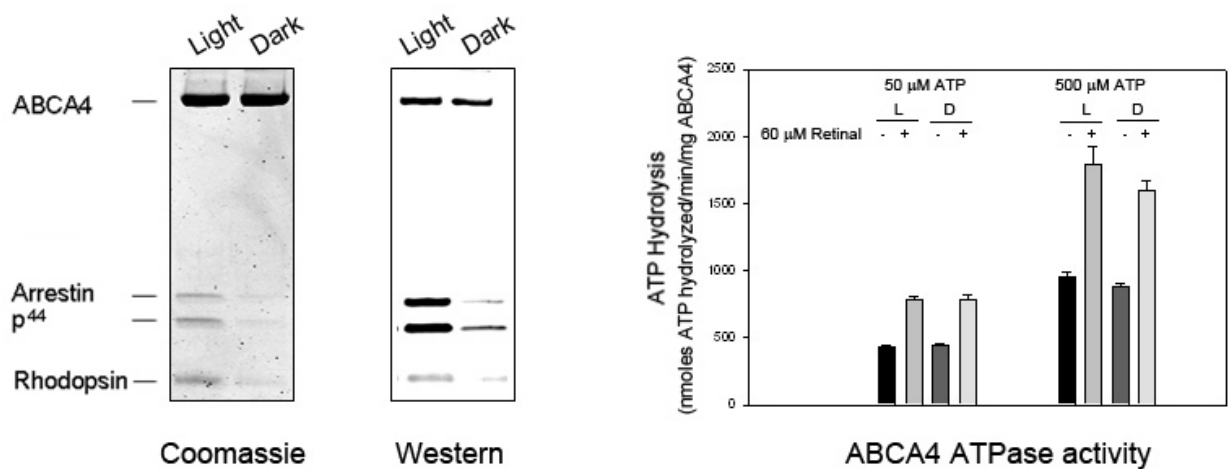
Figure 4.6. ATPase activity. A. ABCA4 was purified from bleached (*LIGHT*) or dark adapted ROS (*DARK*). Less Arrestin/Rhodopsin co-purified in the dark (about 1/4 compared to light sample). **B**. Protein complexes were reconstituted into lipid vesicles and the ATPase activity was measured at 50 μM or 500 μM ATP. Binding of Arrestin/Rhodopsin complex shows no significant effect on the basal and retinal stimulated ATPase activity.

CHAPTER 5: SUMMARY AND FUTURE DIRECTIONS

5.1 Summary

The work from this thesis focused on various aspects of the structure and function of the photoreceptor transporter ABCA4. The second chapter investigated the interactions between small molecules and ABCA4. *N*-ret-PE, the Schiff base conjugate of all-*trans*-retinal and PE, was found to bind ABCA4. ATP binding was shown to promote the dissociation of *N*-ret-PE from ABCA4. These results provided the first direct biochemical evidence that *N*-ret-PE is the preferred retinoid substrate of ABCA4. This agrees with the model for the function of ABCA4 based on a study of the abca4 knockout mouse (Weng et al., 1999) and biochemical studies showing that all-*trans*-retinal stimulates the ATPase activity of ABCA4 in the presence of PE (Ahn et al., 2000; Sun et al., 1999).

The third chapter dealt with the role of the C-terminus on the functional properties of ABCA4. The results showed that the C-terminal deletion mutant lacking a conserved VFVNFA motif (ABCA4-Δ30) does not bind *N*-ret-PE or ATP and is devoid of all-*trans*-retinal stimulated ATPase activity. This study demonstrated the importance of the C-terminus of ABCA4. Mutations in this region can cause a global effect that impairs the function of NBDs (ATP hydrolysis) and MSDs (retinoid substrate binding). Decreased solubility by the detergent CHAPS and ER retention revealed by immunocytochemistry indicate that ABCA4-Δ30 is not properly folded. The functional analysis of the C-terminal deletion mutants provides a molecular based rationale for the

phenotype displayed by patients with mutations in this region of ABCA4.

The fourth chapter described protein-protein interactions between ABCA4 and rhodopsin / arrestin complex. This study identified the binding partners and confirmed the specificity of this interaction by showing that the association takes place in bleached but not in dark adapted ROS. It was also determined that all-*trans*-retinal is a key regulator of this interaction. This finding provides a valuable lead for studying the regulation of ABCA4 through protein-protein interactions and may lead to the discovery of new roles for arrestin in the visual system.

While the work of this thesis provides new knowledge to the structural and functional properties of ABCA4, some questions remain to be answered such as the direction of transport of ABCA4. The direction of transport proposed in the current model is from the lumenal to the cytoplasmic side of the disk membrane. This is in the opposite direction suggested for ABCA1 and other eukaryotic ABC transporters such as P-glycoprotein which transport substrates from the cytoplasmic to the extracellular or lumenal side of membranes. A true transport assay needs to be developed to provide solid evidence for that ABCA4 is an "inward" flippase. Determination of whether structurally similar transporters can operate in different directions will provide valuable insights into the mechanism of transport.

The study of the C-terminus of ABCA4 showed that the VFVNFA motif is important for the correct folding of the protein. This suggests an intramolecular interaction between the C-terminus and another domain of ABCA4. Further studies are needed to

confirm this intramolecular interaction and to map the binding site. Answers to these questions will help explain how one relatively small segment of the C-terminus can affect the folding of the whole protein with multiple domains. The C-terminus of ABCA1 containing the conservative VFVNFA motif has been suggested to be involved in protein-protein interaction (Fitzgerald et al., 2004). The possibility that the C-terminus of ABCA4 is involved in both intramolecular interaction and protein-protein interaction (with rhodopsin / arrestin for example) needs further investigation.

The details of the interaction between rhodopsin / arrestin complex and ABCA4 remain to be studied. These include the stoichiometry of the interaction, identification of the binding sites, and the role of all-*trans*-retinal. The function of this interaction remains an intriguing question.

5.2 Future Directions

A true transport or flippase assay needs to be developed to determine the direction of transport for ABCA4. A flippase assay measures the protein driven redistribution of a certain lipid species across the two leaflets of lipid bilayer. A number of assays have been developed to demonstrate and characterize flippase activities. Most of the assays are based on the use of lipid analogues that possess a certain degree of water-solubility. The analogues are also tagged by fluorescence (Ruetz and Gros, 1994), radiolabel (Chen and Huestis, 1997) or spin-label (Seigneuret and Devaux, 1984) so as to be able to track them through the assay procedure.

A flippase assay for ABCA4 would involve reconstitution of ABCA4 in unilamellar

liposomes. Preliminary experiments have been set up to test whether ABCA4 is a flippase of PE using 1,2-dimyristoyl-*sn*-glycero-3-phosphoethanolamine-*N*-(7-nitro-2-1,3-benzoxadiazole-4-yl) (NBD-PE) (Fig. 5.1A). The fluorescent based assay was chosen for its simple principle and procedure. Sodium dithionite is added to selectively quench the fluorescence from outer leaflet of the vesicles. The flippase activity can be determined by the difference of distribution of NBD-PE in the two layers of the vesicles incubated with ATP or ADP. To test the flipping of *N*-ret-PE, the fluorescent assay can not be used since all-*trans*-retinal has been shown to interfere with the fluorescence of NBD (data not shown). Alternatively, proof of concept experiment is required to test whether free all-*trans*-retinal can be selectively absorbed by BSA from the outer leaflet of liposomes (Fig. 5.1B). The removal of free all-*trans*-retinal will lead to breakdown of *N*-ret-PE to free retinal and PE (an equilibrium exists between *N*-ret-PE and free all-*trans*-retinal). The amount of extracted all-*trans*-retinal should reflect the quantity of *N*-ret-PE in the outer leaflet. ATP or ADP incubated proteoliposome should show different amount of extractable retinal if ABCA4 flips *N*-ret-PE across the lipid membrane. Eventually, intact ROS disks should be utilized to study the transportation of *N*-ret-PE by ABCA4.

Development of a flippase assay for ABCA4 presents challenges. One is its much lower activity compared to P-glycoprotein. Another one is that PE is required to be present at a certain concentration to maintain the activity of ABCA4 (Ahn et al., 2000). This can dilute labeled PE and make the detection of the transport more difficult.

The study of the role of C-terminal VFVNFA motif in ABCA4 emphasizes that a very small part of a soluble domain can have profound effects on the folding of a multi-domain membrane protein. A panel of ABCA4 variants associated with human retinopathies have been biochemically characterized (Sun et al., 2000). Unsurprisingly, mutations causing small deletions (delVVAIC1681 and delPAL1761) or introducing charged amino acids into predicted transmembrane domains (G851D and G1886E) produce significantly reduced amounts of protein, presumably due to misfolding of the transporter. However, missense mutations in the two soluble NBD domains, including R1108C, R1129L, L2027F, and R2038W (located outside the Walker A, B motif and the signature (C) motif), also result in very low protein yields with diminished ATP binding (Sun et al., 2000). These findings make the above variations good candidates for misfolding mutants. Studies involving binding assays and immunocytochemistry will reveal retinoid substrate binding effect on the TMD and localization of the protein. Mutation within a soluble domain that causes the whole membrane protein to misfold is not only found in ABCA4. Deletion of Phe508 located between the Walker A motif and the signature (C) motif within NBD1 of CFTR is a common disease mutation (observed in as many as 90% of cystic fibrosis patients) that causes misfolding and degradation of the CFTR channel (Thibodeau et al., 2005; Wang et al., 2008). Furthermore deletion of Arg1392 and Met1393 located between the Walker A motif and the signature (C) motif within NBD2 of multidrug-resistance protein 2 (MRP2, also known as ABCC2) has been shown to lead to defective folding of MRP2 and result in Dubin-Johnson syndrome

(Keitel et al., 2000). It seems that improper folding arising from mutations in soluble domains of ABC transporters can be a factor in causing disease and highlight the need to develop drugs specific for patients carrying these mutations.

Although many structural properties of ABCA4 have been characterized, a complete high resolution structure remains to be determined. This will be important in further defining the mechanism of transport. The crystal structure will also be able to identify intramolecular interactions within ABCA4 and shed light on how the folding of each domain is dependant on the others.

Another important unresolved issue is the regulation of ABCA4. The protein-protein interactions between ABCA4 and the rhodopsin / arrestin complex may provide clues for possible regulatory mechanisms. Although arrestin, but not rhodopsin, most probably binds to ABCA4, extracted endogenous arrestin does not bind to ABCA4 immobilized on an immunoaffinity column. Perhaps only the "activated" arrestin binds ABCA4 since arrestin has been shown to bind to synthetic phosphorylated peptides from the carboxyl-terminal region of rhodopsin and adopt an activated conformation (Kisselev et al., 2004; Liu et al., 2004; McDowell et al., 2001; McDowell et al., 1999; Puig et al., 1995). Developing an assay to test binding of arrestin activated by phosphorylated rhodopsin C-terminal peptide to immobilized ABCA4 will be the first step to dissect the interaction between ABCA4 and rhodopsin / arrestin complex.

The interaction of rhodopsin / arrestin complex with ABCA4 may reveal novel functions of visual arrestin in photoreceptor cells. The role of arrestins as the silencer of

GPCR signaling is the classic paradigm. However, studies on β-arrestins revealed they also function as endocytic adaptors, linking receptors to the components of the internalization machinery (Goodman et al., 1996; Laporte et al., 1999). Subsequent discoveries further indicates that receptor-bound β-arrestins interact with numerous signaling proteins, linking GPCRs to a variety of alternative signaling pathways (Gurevich and Gurevich, 2006; Lefkowitz and Shenoy, 2005). The functional significance of the linkage of ABCA4 to rhodopsin by visual arrestin remains to be elucidated.

The study of interaction between rhodopsin / arrestin complex and ABCA4 provides exciting evidence of crosstalk between GPCRs and ABC transporters. The GPCR superfamily comprises one of the largest and most diverse protein families in nature and play important roles in a variety of biological and pathological processes. The ligands that bind and activate these receptors include light-sensitive compounds, odors, pheromones, hormones, and neurotransmitters. While ABC transporters function in the movement of a wide variety of compounds across cell membranes including amino acids, peptides, ions, metabolites, vitamins, fatty acid derivatives, steroids, organic anions, phospholipids, drugs and other compounds. However, signaling pathways involved in regulation of ABCA4 and other ABC transporters are still largely unknown. The possibility of GPCR as a signaling molecule upstream of ABC transporters can lead to new directions for understanding disease mechanism involving GPCR signaling and transport activity of ABC transporters.
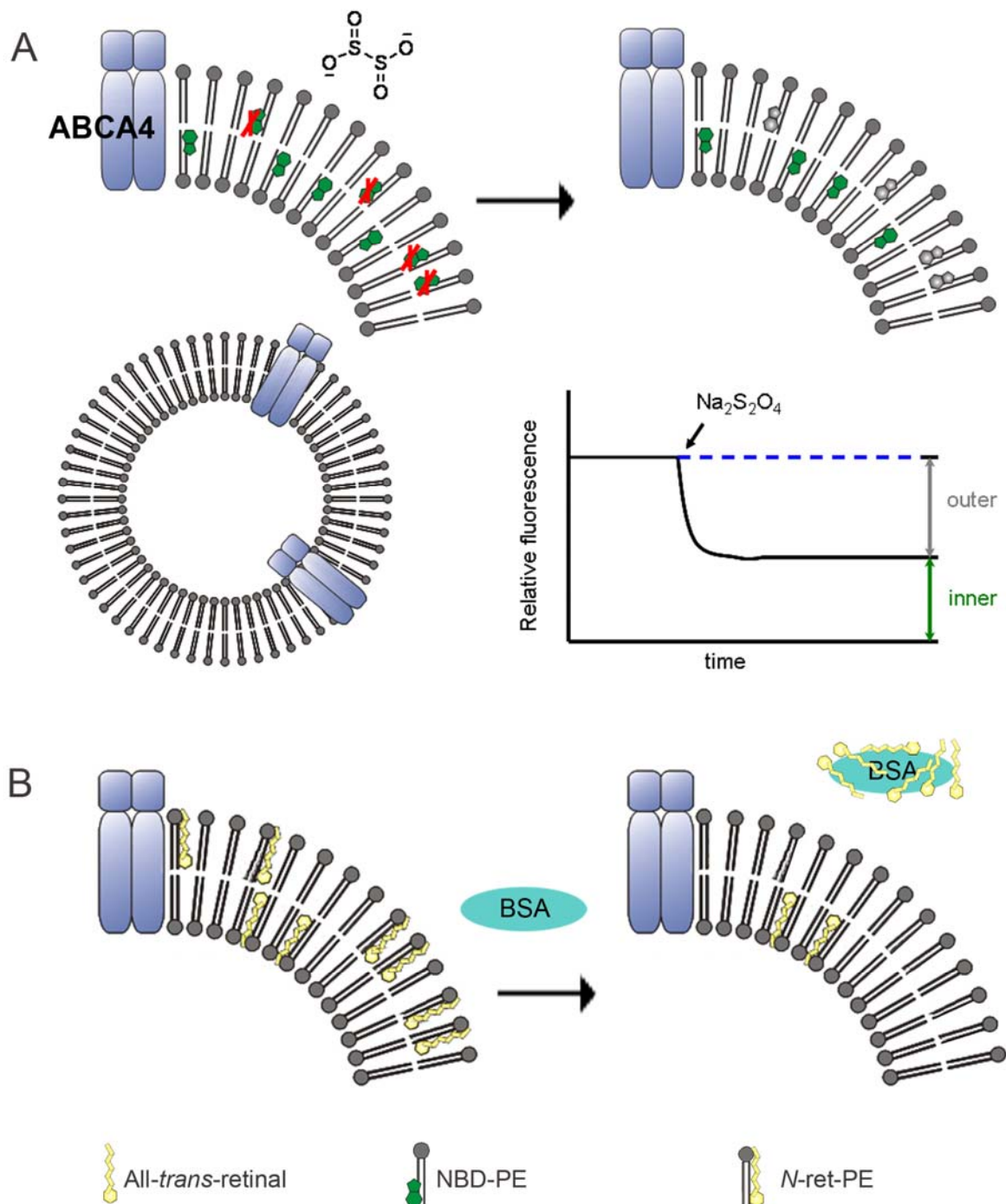
Figure 5.1. Flippase assay. A. To test whether ABCA4 is a flippase of PE, small amount of NBD-labeled PE is incorporated in proteoliposomes. The NBD-PE in the outer leaflet of the liposome can be selectively quenched by the membrane impermeable reagent sodium dithionite. The distribution of the labeled lipid can be determined by measuring the change in fluorescence intensity. Flippase activity is measured as ATP driven re-distribution of the labeled lipid. **B**. Proof of concept experiment is required for setting up an assay to determine whether ABCA4 is a flippase for *N*-retinylidene-PE. BSA is used to selectively extract all-*trans*-retinal from the outer leaflet of the liposome and promote the dissociation of all-*trans*-retinal from PE. Extracted retinal can be quantified by spectrophotometry or HPLC. If ABCA4 is a flippase for *N*-retinylidene-PE, different amount of retinal should be extractable by BSA from ATP or ADP incubated proteoliposomes.

REFERENCES

Abele, R., and Tampe, R. (1999). Function of the transport complex TAP in cellular immune recognition. Biochim Biophys Acta *1461*, 405-419.

Acland, G.M., Aguirre, G.D., Ray, J., Zhang, Q., Aleman, T.S., Cideciyan, A.V., Pearce-Kelling, S.E., Anand, V., Zeng, Y., Maguire, A.M.*, et al.* (2001). Gene therapy restores vision in a canine model of childhood blindness. Nat Genet *28*, 92-95.

Ahn, J., Beharry, S., Molday, L.L., and Molday, R.S. (2003). Functional interaction between the two halves of the photoreceptor-specific ATP binding cassette protein ABCR (ABCA4). Evidence for a non-exchangeable ADP in the first nucleotide binding domain. J Biol Chem *278*, 39600-39608.

Ahn, J., and Molday, R.S. (2000). Purification and characterization of ABCR from bovine rod outer segments. Methods Enzymol *315*, 864-879.

Ahn, J., Wong, J.T., and Molday, R.S. (2000). The effect of lipid environment and retinoids on the ATPase activity of ABCR, the photoreceptor ABC transporter responsible for Stargardt macular dystrophy. J Biol Chem *275*, 20399-20405.

Aiyar, A., Xiang, Y., and Leis, J. (1996). Site-directed mutagenesis using overlap extension PCR. Methods Mol Biol *57*, 177-191.

Ali, R.R., Sarra, G.M., Stephens, C., Alwis, M.D., Bainbridge, J.W., Munro, P.M., Fauser, S., Reichel, M.B., Kinnon, C., Hunt, D.M.*, et al.* (2000). Restoration of photoreceptor ultrastructure and function in retinal degeneration slow mice by gene therapy. Nat Genet *25*, 306-310.

Allikmets, R. (2000). Simple and complex ABCR: genetic predisposition to retinal disease. Am J Hum Genet *67*, 793-799.

Allikmets, R., Shroyer, N.F., Singh, N., Seddon, J.M., Lewis, R.A., Bernstein, P.S., Peiffer, A., Zabriskie, N.A., Li, Y., Hutchinson, A.*, et al.* (1997a). Mutation of the Stargardt disease gene (ABCR) in age-related macular degeneration. Science *277*, 1805-1807.

Allikmets, R., Singh, N., Sun, H., Shroyer, N.E., Hutchinson, A., Chidambaram, A., Gerrard, B., Baird, L., Stauffer, D., Peiffer, A.*, et al.* (1997b). A photoreceptor cell-specific ATP-binding transporter gene (ABCR) is mutated in recessive Stargardt macular dystrophy. Nat Genet *15*, 236-246.

Allocca, M., Doria, M., Petrillo, M., Colella, P., Garcia-Hoyos, M., Gibbs, D., Kim, S.R., Maguire, A., Rex, T.S., Di Vicino, U.*, et al.* (2008). Serotype-dependent packaging of large genes in adeno-associated viral vectors results in effective gene delivery in mice. J Clin Invest *118*, 1955-1964.

Ambudkar, S.V., Lelong, I.H., Zhang, J., Cardarelli, C.O., Gottesman, M.M., and Pastan, I. (1992). Partial purification and reconstitution of the human multidrug-resistance pump: characterization of the drug-stimulatable ATP hydrolysis. Proc Natl Acad Sci U S A *89*, 8472-8476.

Anderson, M.P., Gregory, R.J., Thompson, S., Souza, D.W., Paul, S., Mulligan, R.C., Smith, A.E., and Welsh, M.J. (1991). Demonstration that CFTR is a chloride channel by alteration of its anion selectivity. Science *253*, 202-205.

Anderson, R.E., and Maude, M.B. (1970). Phospholipids of bovine outer segments. Biochemistry *9*, 3624-3628.

Arikawa, K., Molday, L.L., Molday, R.S., and Williams, D.S. (1992). Localization of peripherin/rds in the disk membranes of cone and rod photoreceptors: relationship to disk membrane morphogenesis and retinal degeneration. J Cell Biol *116*, 659-667.

Ascano, M., and Robinson, P.R. (2006). Differential phosphorylation of the rhodopsin cytoplasmic tail mediates the binding of arrestin and its splice variant, p44. Biochemistry *45*, 2398-2407.

Attie, A.D. (2007). ABCA1: at the nexus of cholesterol, HDL and atherosclerosis. Trends Biochem Sci *32*, 172-179.

Azarian, S.M., and Travis, G.H. (1997). The photoreceptor rim protein is an ABC transporter encoded by the gene for recessive Stargardt's disease (ABCR). FEBS Lett *409*, 247-252.

Bascom, R.A., Manara, S., Collins, L., Molday, R.S., Kalnins, V.I., and McInnes, R.R. (1992). Cloning of the cDNA for a novel photoreceptor membrane protein (rom-1) identifies a disk rim protein family implicated in human retinopathies. Neuron *8*, 1171-1184.

Bavik, C.O., Levy, F., Hellman, U., Wernstedt, C., and Eriksson, U. (1993). The retinal pigment epithelial membrane receptor for plasma retinol-binding protein. Isolation and cDNA cloning of the 63-kDa protein. J Biol Chem *268*, 20540-20546.

Beharry, S., Zhong, M., and Molday, R.S. (2004). N-retinylidene-phosphatidylethanolamine is the preferred retinoid substrate for the photoreceptor-specific ABC transporter ABCA4 (ABCR). J Biol Chem *279*, 53972-53979.

Bessant, D.A., Ali, R.R., and Bhattacharya, S.S. (2001). Molecular genetics and prospects for therapy of the inherited retinal dystrophies. Curr Opin Genet Dev *11*, 307-316.

Birnbaumer, L. (1990). G proteins in signal transduction. Annu Rev Pharmacol Toxicol *30*, 675-705.

Bodzioch, M., Orso, E., Klucken, J., Langmann, T., Bottcher, A., Diederich, W., Drobnik, W., Barlage, S., Buchler, C., Porsch-Ozcurumez, M*., et al.* (1999). The gene encoding ATP-binding cassette transporter 1 is mutated in Tangier disease. Nat Genet *22*, 347-351.

Bok, D., Ong, D.E., and Chytil, F. (1984). Immunocytochemical localization of cellular retinol binding protein in the rat retina. Invest Ophthalmol Vis Sci *25*, 877-883.

Borst, P., and Elferink, R.O. (2002). Mammalian ABC transporters in health and disease. Annu Rev Biochem *71*, 537-592.

Brooks-Wilson, A., Marcil, M., Clee, S.M., Zhang, L.H., Roomp, K., van Dam, M., Yu, L., Brewer, C., Collins, J.A., Molhuizen, H.O*., et al.* (1999a). Mutations in ABC1 in Tangier disease and familial high-density lipoprotein deficiency. Nat Genet *22*, 336-345.

Brooks-Wilson, A., Marcil, M., Clee, S.M., Zhang, L.H., Roomp, K., van Dam, M., Yu, L., Brewer, C., Collins, J.A., Molhuizen, H.O*., et al.* (1999b). Mutations in ABC1 in Tangier disease and familial high-density lipoprotein deficiency. Nat Genet *22*, 336-345.

Brousseau, M.E., Schaefer, E.J., Dupuis, J., Eustace, B., Van Eerdewegh, P., Goldkamp, A.L., Thurston, L.M., FitzGerald, M.G., Yasek-McKenna, D., O'Neill, G*., et al.* (2000). Novel mutations in the gene encoding ATP-binding cassette 1 in four tangier disease kindreds. J Lipid Res *41*, 433-441.

Bungert, S., Molday, L.L., and Molday, R.S. (2001). Membrane topology of the ATP binding cassette transporter ABCR and its relationship to ABC1 and related ABCA transporters: identification of N-linked glycosylation sites. J Biol Chem *276*, 23539-23546.

Chang, G. (2003). Structure of MsbA from Vibrio cholera: a multidrug resistance ABC transporter homolog in a closed conformation. J Mol Biol *330*, 419-430.

Chang, G., and Roth, C.B. (2001). Structure of MsbA from E. coli: a homolog of the multidrug resistance ATP binding cassette (ABC) transporters. Science *293*, 1793-1800.

Chen, C., and Okayama, H. (1987). High-efficiency transformation of mammalian cells by plasmid DNA. Mol Cell Biol *7*, 2745-2752.

Chen, C.J., Chin, J.E., Ueda, K., Clark, D.P., Pastan, I., Gottesman, M.M., and Roninson, I.B. (1986). Internal duplication and homology with bacterial transport proteins in the mdr1 (P-glycoprotein) gene from multidrug-resistant human cells. Cell *47*, 381-389.

Chen, J.Y., and Huestis, W.H. (1997). Role of membrane lipid distribution in

chlorpromazine-induced shape change of human erythrocytes. Biochim Biophys Acta *1323*, 299-309.

Cideciyan, A.V., Aleman, T.S., Boye, S.L., Schwartz, S.B., Kaushal, S., Roman, A.J., Pang, J.J., Sumaroka, A., Windsor, E.A., Wilson, J.M*., et al.* (2008). Human gene therapy for RPE65 isomerase deficiency activates the retinoid cycle of vision but with slow rod kinetics. Proc Natl Acad Sci U S A *105*, 15112-15117.

Cohen, A.I. (1963). Vertebrate retinal cells and their organization. Biol Rev Cambridge Phil Soc *38*, 427-459.

Comer, G.M., Ciulla, T.A., Criswell, M.H., and Tolentino, M. (2004). Current and future treatment options for nonexudative and exudative age-related macular degeneration. Drugs Aging *21*, 967-992.

Connell, G., Bascom, R., Molday, L., Reid, D., McInnes, R.R., and Molday, R.S. (1991). Photoreceptor peripherin is the normal product of the gene responsible for retinal degeneration in the rds mouse. Proc Natl Acad Sci U S A *88*, 723-726.

Cook, N.J., Molday, L.L., Reid, D., Kaupp, U.B., and Molday, R.S. (1989). The cGMP-gated channel of bovine rod photoreceptors is localized exclusively in the plasma membrane. J Biol Chem *264*, 6996-6999.

Cremers, F.P., van de Pol, D.J., van Driel, M., den Hollander, A.I., van Haren, F.J., Knoers, N.V., Tijmes, N., Bergen, A.A., Rohrschneider, K., Blankenagel, A*., et al.* (1998). Autosomal recessive retinitis pigmentosa and cone-rod dystrophy caused by splice site mutations in the Stargardt's disease gene ABCR. Hum Mol Genet *7*, 355-362.

Cuatrecasas, P. (1970). Protein purification by affinity chromatography. Derivatizations of agarose and polyacrylamide beads. J Biol Chem *245*, 3059-3065.

Dawson, R.J., and Locher, K.P. (2006). Structure of a bacterial multidrug ABC transporter. Nature *443*, 180-185.

De Pont, J.J., Daemen, F.J., and Bonting, S.L. (1970). Biochemical aspects of the visual process. VII. Equilibrium conditions in the formation of retinylidene imines. Arch Biochem Biophys *140*, 267-274.

Dean, M., and Allikmets, R. (2001). Complete characterization of the human ABC gene family. J Bioenerg Biomembr *33*, 475-479.

Dean, M., and Annilo, T. (2005). Evolution of the ATP-binding cassette (ABC) transporter superfamily in vertebrates. Annu Rev Genomics Hum Genet *6*, 123-142.

Deigner, P.S., Law, W.C., Canada, F.J., and Rando, R.R. (1989). Membranes as the energy source in the endergonic transformation of vitamin A to 11-cis-retinol. Science

244, 968-971.

Doyle, L.A., Yang, W., Abruzzo, L.V., Krogmann, T., Gao, Y., Rishi, A.K., and Ross, D.D. (1998). A multidrug resistance transporter from human MCF-7 breast cancer cells. Proc Natl Acad Sci U S A *95*, 15665-15670.

Eldred, G.E., and Lasky, M.R. (1993). Retinal age pigments generated by self-assembling lysosomotropic detergents. Nature *361*, 724-726.

Eter, N., Krohne, T.U., and Holz, F.G. (2006). New pharmacologic approaches to therapy for age-related macular degeneration. BioDrugs *20*, 167-179.

Ewart, G.D., Cannell, D., Cox, G.B., and Howells, A.J. (1994). Mutational analysis of the traffic ATPase (ABC) transporters involved in uptake of eye pigment precursors in Drosophila melanogaster. Implications for structure-function relationships. J Biol Chem *269*, 10370-10377.

Fishman, G.A., Farber, M., Patel, B.S., and Derlacki, D.J. (1987). Visual acuity loss in patients with Stargardt's macular dystrophy. Ophthalmology *94*, 809-814.

Fishman, G.A., Farbman, J.S., and Alexander, K.R. (1991). Delayed rod dark adaptation in patients with Stargardt's disease. Ophthalmology *98*, 957-962.

Fishman, G.A., Stone, E.M., Eliason, D.A., Taylor, C.M., Lindeman, M., and Derlacki, D.J. (2003). ABCA4 gene sequence variations in patients with autosomal recessive cone-rod dystrophy. Arch Ophthalmol *121*, 851-855.

Fitzgerald, M.E., Tolley, E., Frase, S., Zagvazdin, Y., Miller, R.F., Hodos, W., and Reiner, A. (2001). Functional and morphological assessment of age-related changes in the choroid and outer retina in pigeons. Vis Neurosci *18*, 299-317.

Fitzgerald, M.L., Morris, A.L., Rhee, J.S., Andersson, L.P., Mendez, A.J., and Freeman, M.W. (2002). Naturally occurring mutations in the largest extracellular loops of ABCA1 can disrupt its direct interaction with apolipoprotein A-I. J Biol Chem *277*, 33178-33187.

Fitzgerald, M.L., Okuhira, K., Short, G.F., 3rd, Manning, J.J., Bell, S.A., and Freeman, M.W. (2004). ATP-binding cassette transporter A1 contains a novel C-terminal VFVNFA motif that is required for its cholesterol efflux and ApoA-I binding activities. J Biol Chem *279*, 48477-48485.

Forrester, J.V., Dick, A.D., McMenamin, P.G., and Lee, W.R. (2002). The Eye: Basic Sciences in Practice (WB Saunders).

Foxman, S.G., Heckenlively, J.R., Bateman, J.B., and Wirtschafter, J.D. (1985). Classification of congenital and early onset retinitis pigmentosa. Arch Ophthalmol *103*, 1502-1506.

Fumagalli, A., Ferrari, M., Soriani, N., Gessi, A., Foglieni, B., Martina, E., Manitto, M.P., Brancato, R., Dean, M., Allikmets, R., *et al.* (2001). Mutational scanning of the ABCR gene with double-gradient denaturing-gradient gel electrophoresis (DG-DGGE) in Italian Stargardt disease patients. Hum Genet *109*, 326-338.

Garwin, G.G., and Saari, J.C. (2000). High-performance liquid chromatography analysis of visual cycle retinoids. Methods Enzymol *316*, 313-324.

Gelisken, O., and De Laey, J.J. (1985). A clinical review of Stargardt's disease and/or fundus flavimaculatus with follow-up. Int Ophthalmol *8*, 225-235.

Gilman, A.G. (1995). Nobel Lecture. G proteins and regulation of adenylyl cyclase. Biosci Rep *15*, 65-97.

Goldberg, A.F., and Molday, R.S. (1996). Subunit composition of the peripherin/rds-rom-1 disk rim complex from rod photoreceptors: hydrodynamic evidence for a tetrameric quaternary structure. Biochemistry *35*, 6144-6149.

Goldberg, A.F., Moritz, O.L., and Molday, R.S. (1995). Heterologous expression of photoreceptor peripherin/rds and Rom-1 in COS-1 cells: assembly, interactions, and localization of multisubunit complexes. Biochemistry *34*, 14213-14219.

Gonzalez-Fernandez, F., Baer, C.A., and Ghosh, D. (2007). Module structure of interphotoreceptor retinoid-binding protein (IRBP) may provide bases for its complex role in the visual cycle - structure/function study of Xenopus IRBP. BMC Biochem *8*, 15.

Gonzalez-Fernandez, F., and Ghosh, D. (2008). Focus on Molecules: interphotoreceptor retinoid-binding protein (IRBP). Exp Eye Res *86*, 169-170.

Goodman, O.B., Jr., Krupnick, J.G., Santini, F., Gurevich, V.V., Penn, R.B., Gagnon, A.W., Keen, J.H., and Benovic, J.L. (1996). Beta-arrestin acts as a clathrin adaptor in endocytosis of the beta2-adrenergic receptor. Nature *383*, 447-450.

Gorczyca, W.A., Polans, A.S., Surgucheva, I.G., Subbaraya, I., Baehr, W., and Palczewski, K. (1995). Guanylyl cyclase activating protein. A calcium-sensitive regulator of phototransduction. J Biol Chem *270*, 22029-22036.

Gottesman, M.M., Hrycyna, C.A., Schoenlein, P.V., Germann, U.A., and Pastan, I. (1995). Genetic analysis of the multidrug transporter. Annu Rev Genet *29*, 607-649.

Gu, S.M., Thompson, D.A., Srikumari, C.R., Lorenz, B., Finckh, U., Nicoletti, A., Murthy, K.R., Rathmann, M., Kumaramanickavel, G., Denton, M.J., *et al.* (1997). Mutations in RPE65 cause autosomal recessive childhood-onset severe retinal dystrophy. Nat Genet *17*, 194-197.

Guan, L., and Kaback, H.R. (2006). Lessons from lactose permease. Annu Rev Biophys

Biomol Struct *35*, 67-91.

Gurevich, E.V., and Gurevich, V.V. (2006). Arrestins: ubiquitous regulators of cellular signaling pathways. Genome Biol *7*, 236.

Haines, J.L., Hauser, M.A., Schmidt, S., Scott, W.K., Olson, L.M., Gallins, P., Spencer, K.L., Kwan, S.Y., Noureddine, M., Gilbert, J.R*., et al.* (2005). Complement factor H variant increases the risk of age-related macular degeneration. Science *308*, 419-421.

Hamel, C.P., Tsilou, E., Pfeffer, B.A., Hooks, J.J., Detrick, B., and Redmond, T.M. (1993). Molecular cloning and expression of RPE65, a novel retinal pigment epithelium-specific microsomal protein that is post-transcriptionally regulated in vitro. J Biol Chem *268*, 15751-15757.

Hanson, S.M., Francis, D.J., Vishnivetskiy, S.A., Kolobova, E.A., Hubbell, W.L., Klug, C.S., and Gurevich, V.V. (2006). Differential interaction of spin-labeled arrestin with inactive and active phosphorhodopsin. Proc Natl Acad Sci U S A *103*, 4900-4905.

Hauswirth, W., Aleman, T.S., Kaushal, S., Cideciyan, A.V., Schwartz, S.B., Wang, L., Conlon, T., Boye, S.L., Flotte, T.R., Byrne, B*., et al.* (2008). Phase I Trial of Leber Congenital Amaurosis due to RPE65 Mutations by Ocular Subretinal Injection of Adeno-Associated Virus Gene Vector: Short-Term Results. Hum Gene Ther.

He, W., Cowan, C.W., and Wensel, T.G. (1998). RGS9, a GTPase accelerator for phototransduction. Neuron *20*, 95-102.

Higgins, C.F. (1992). ABC transporters: from microorganisms to man. Annu Rev Cell Biol *8*, 67-113.

Higgins, C.F., and Linton, K.J. (2004). The ATP switch model for ABC transporters. Nat Struct Mol Biol *11*, 918-926.

Hirsch, J.A., Schubert, C., Gurevich, V.V., and Sigler, P.B. (1999). The 2.8 A crystal structure of visual arrestin: a model for arrestin's regulation. Cell *97*, 257-269.

Hodges, R.S., Heaton, R.J., Parker, J.M., Molday, L., and Molday, R.S. (1988). Antigen-antibody interaction. Synthetic peptides define linear antigenic determinants recognized by monoclonal antibodies directed to the cytoplasmic carboxyl terminus of rhodopsin. J Biol Chem *263*, 11768-11775.

Hollenstein, K., Frei, D.C., and Locher, K.P. (2007). Structure of an ABC transporter in complex with its binding protein. Nature *446*, 213-216.

Hsu, S.C., and Molday, R.S. (1991). Glycolytic enzymes and a GLUT-1 glucose transporter in the outer segments of rod and cone photoreceptor cells. J Biol Chem *266*, 21745-21752.

Hu, G., and Wensel, T.G. (2002). R9AP, a membrane anchor for the photoreceptor GTPase accelerating protein, RGS9-1. Proc Natl Acad Sci U S A *99*, 9755-9760.

Hvorup, R.N., Goetz, B.A., Niederer, M., Hollenstein, K., Perozo, E., and Locher, K.P. (2007). Asymmetry in the structure of the ABC transporter-binding protein complex BtuCD-BtuF. Science *317*, 1387-1390.

Illing, M., Molday, L.L., and Molday, R.S. (1997). The 220-kDa rim protein of retinal rod outer segments is a member of the ABC transporter superfamily. J Biol Chem *272*, 10303-10310.

Ishiguro, S., Suzuki, Y., Tamai, M., and Mizuno, K. (1991). Purification of retinol dehydrogenase from bovine retinal rod outer segments. J Biol Chem *266*, 15520-15524.

Jakobsdottir, J., Conley, Y.P., Weeks, D.E., Mah, T.S., Ferrell, R.E., and Gorin, M.B. (2005). Susceptibility genes for age-related maculopathy on chromosome 10q26. Am J Hum Genet *77*, 389-407.

Jardetzky, O. (1966). Simple allosteric model for membrane pumps. Nature *211*, 969-970.

Juliano, R.L., and Ling, V. (1976). A surface glycoprotein modulating drug permeability in Chinese hamster ovary cell mutants. Biochim Biophys Acta *455*, 152-162.

Kadaba, N.S., Kaiser, J.T., Johnson, E., Lee, A., and Rees, D.C. (2008). The high-affinity E. coli methionine ABC transporter: structure and allosteric regulation. Science *321*, 250-253.

Kajiwara, K., Berson, E.L., and Dryja, T.P. (1994). Digenic retinitis pigmentosa due to mutations at the unlinked peripherin/RDS and ROM1 loci. Science *264*, 1604-1608.

Kanda, A., Chen, W., Othman, M., Branham, K.E., Brooks, M., Khanna, R., He, S., Lyons, R., Abecasis, G.R., and Swaroop, A. (2007). A variant of mitochondrial protein LOC387715/ARMS2, not HTRA1, is strongly associated with age-related macular degeneration. Proc Natl Acad Sci U S A *104*, 16227-16232.

Keen, T.J., and Inglehearn, C.F. (1996). Mutations and polymorphisms in the human peripherin-RDS gene and their involvement in inherited retinal degeneration. Hum Mutat *8*, 297-303.

Keitel, V., Kartenbeck, J., Nies, A.T., Spring, H., Brom, M., and Keppler, D. (2000). Impaired protein maturation of the conjugate export pump multidrug resistance protein 2 as a consequence of a deletion mutation in Dubin-Johnson syndrome. Hepatology *32*, 1317-1328.

Kennan, A., Aherne, A., and Humphries, P. (2005). Light in retinitis pigmentosa. Trends

Genet *21*, 103-110.

Keppler, D., Leier, I., Jedlitschky, G., and Konig, J. (1998). ATP-dependent transport of glutathione S-conjugates by the multidrug resistance protein MRP1 and its apical isoform MRP2. Chem Biol Interact *111-112*, 153-161.

Kim, S.R., Jang, Y.P., Jockusch, S., Fishkin, N.E., Turro, N.J., and Sparrow, J.R. (2007). The all-trans-retinal dimer series of lipofuscin pigments in retinal pigment epithelial cells in a recessive Stargardt disease model. Proc Natl Acad Sci U S A *104*, 19273-19278.

Kisselev, O.G., McDowell, J.H., and Hargrave, P.A. (2004). The arrestin-bound conformation and dynamics of the phosphorylated carboxy-terminal region of rhodopsin. FEBS Lett *564*, 307-311.

Klein, I., Sarkadi, B., and Varadi, A. (1999). An inventory of the human ABC proteins. Biochim Biophys Acta *1461*, 237-262.

Kliffen, M., van der Schaft, T.L., Mooy, C.M., and de Jong, P.T. (1997). Morphologic changes in age-related maculopathy. Microsc Res Tech *36*, 106-122.

Kolb, H., and Gouras, P. (1974). Electron microscopic observations of human retinitis pigmentosa, dominantly inherited. Invest Ophthalmol *13*, 487-498.

Kong, J., Kim, S.R., Binley, K., Pata, I., Doi, K., Mannik, J., Zernant-Rajang, J., Kan, O., Iqball, S., Naylor, S.*, et al.* (2008). Correction of the disease phenotype in the mouse model of Stargardt disease by lentiviral gene therapy. Gene Ther *15*, 1311-1320.

Laporte, S.A., Oakley, R.H., Zhang, J., Holt, J.A., Ferguson, S.S., Caron, M.G., and Barak, L.S. (1999). The beta2-adrenergic receptor/betaarrestin complex recruits the clathrin adaptor AP-2 during endocytosis. Proc Natl Acad Sci U S A *96*, 3712-3717.

Lawn, R.M., Wade, D.P., Garvin, M.R., Wang, X., Schwartz, K., Porter, J.G., Seilhamer, J.J., Vaughan, A.M., and Oram, J.F. (1999). The Tangier disease gene product ABC1 controls the cellular apolipoprotein-mediated lipid removal pathway. J Clin Invest *104*, R25-31.

Leber, T. (1869). Uber retinitis pigmentosa and angeborene amaurose. Graefes Arch Klin Exp Ophthalmol *15*, 13-20.

Lefkowitz, R.J., and Shenoy, S.K. (2005). Transduction of receptor signals by beta-arrestins. Science *308*, 512-517.

Lewin, A.S., Drenser, K.A., Hauswirth, W.W., Nishikawa, S., Yasumura, D., Flannery, J.G., and LaVail, M.M. (1998). Ribozyme rescue of photoreceptor cells in a transgenic rat model of autosomal dominant retinitis pigmentosa. Nat Med *4*, 967-971.

Liu, P., Roush, E.D., Bruno, J., Osawa, S., and Weiss, E.R. (2004). Direct binding of visual arrestin to a rhodopsin carboxyl terminal synthetic phosphopeptide. Mol Vis *10*, 712-719.

Liu, X., Seno, K., Nishizawa, Y., Hayashi, F., Yamazaki, A., Matsumoto, H., Wakabayashi, T., and Usukura, J. (1994). Ultrastructural localization of retinal guanylate cyclase in human and monkey retinas. Exp Eye Res *59*, 761-768.

Locher, K.P., Lee, A.T., and Rees, D.C. (2002). The E. coli BtuCD structure: a framework for ABC transporter architecture and mechanism. Science *296*, 1091-1098.

Loewen, C.J., and Molday, R.S. (2000). Disulfide-mediated oligomerization of Peripherin/Rds and Rom-1 in photoreceptor disk membranes. Implications for photoreceptor outer segment morphogenesis and degeneration. J Biol Chem *275*, 5370-5378.

Loewen, C.J., Moritz, O.L., and Molday, R.S. (2001). Molecular characterization of peripherin-2 and rom-1 mutants responsible for digenic retinitis pigmentosa. J Biol Chem *276*, 22388-22396.

MacKenzie, D., Arendt, A., Hargrave, P., McDowell, J.H., and Molday, R.S. (1984). Localization of binding sites for carboxyl terminal specific anti-rhodopsin monoclonal antibodies using synthetic peptides. Biochemistry *23*, 6544-6549.

Makino, E.R., Handy, J.W., Li, T., and Arshavsky, V.Y. (1999). The GTPase activating factor for transducin in rod photoreceptors is the complex between RGS9 and type 5 G protein beta subunit. Proc Natl Acad Sci U S A *96*, 1947-1952.

Mangini, N.J., and Pepperberg, D.R. (1988). Immunolocalization of 48K in rod photoreceptors. Light and ATP increase OS labeling. Invest Ophthalmol Vis Sci *29*, 1221-1234.

Marlhens, F., Bareil, C., Griffoin, J.M., Zrenner, E., Amalric, P., Eliaou, C., Liu, S.Y., Harris, E., Redmond, T.M., Arnaud, B.*, et al.* (1997). Mutations in RPE65 cause Leber's congenital amaurosis. Nat Genet *17*, 139-141.

Martinez-Mir, A., Paloma, E., Allikmets, R., Ayuso, C., del Rio, T., Dean, M., Vilageliu, L., Gonzalez-Duarte, R., and Balcells, S. (1998). Retinitis pigmentosa caused by a homozygous mutation in the Stargardt disease gene ABCR. Nat Genet *18*, 11-12.

Mata, N.L., Tzekov, R.T., Liu, X.R., Weng, J., Birch, D.G., and Travis, G.H. (2001). Delayed. dark-adaptation and lipofuscin accumulation in abcr+/- mice: Implications for involvement of ABCR in age-related macular degeneration. Invest Ophth Vis Sci *42*, 1685-1690.

Mata, N.L., Weng, J., and Travis, G.H. (2000a). Biogenesis of lipofuscin in retina and RPE of ABCR-knockout mice and humans with ABCR-mediated macular degenerations. Invest Ophth Vis Sci *41*, S144-S144.

Mata, N.L., Weng, J., and Travis, G.H. (2000b). Biosynthesis of a major lipofuscin fluorophore in mice and humans with ABCR-mediated retinal and macular degeneration. P Natl Acad Sci USA *97*, 7154-7159.

Maugeri, A., van Driel, M.A., van de Pol, D.J., Klevering, B.J., van Haren, F.J., Tijmes, N., Bergen, A.A., Rohrschneider, K., Blankenagel, A., Pinckers, A.J.*, et al.* (1999). The 2588G-->C mutation in the ABCR gene is a mild frequent founder mutation in the Western European population and allows the classification of ABCR mutations in patients with Stargardt disease. Am J Hum Genet *64*, 1024-1035.

McBee, J.K., Kuksa, V., Alvarez, R., de Lera, A.R., Prezhdo, O., Haeseleer, F., Sokal, I., and Palczewski, K. (2000). Isomerization of all-trans-retinol to cis-retinols in bovine retinal pigment epithelial cells: dependence on the specificity of retinoid-binding proteins. Biochemistry *39*, 11370-11380.

McDowell, J.H., Robinson, P.R., Miller, R.L., Brannock, M.T., Arendt, A., Smith, W.C., and Hargrave, P.A. (2001). Activation of arrestin: requirement of phosphorylation as the negative charge on residues in synthetic peptides from the carboxyl-terminal region of rhodopsin. Invest Ophthalmol Vis Sci *42*, 1439-1443.

McDowell, J.H., Smith, W.C., Miller, R.L., Popp, M.P., Arendt, A., Abdulaeva, G., and Hargrave, P.A. (1999). Sulfhydryl reactivity demonstrates different conformational states for arrestin, arrestin activated by a synthetic phosphopeptide, and constitutively active arrestin. Biochemistry *38*, 6119-6125.

McIlwain, J.T. (1996). Introduction to the Biology of Vision (Cambridge, UK, Cambridge University Press).

Mendez, A., Burns, M.E., Roca, A., Lem, J., Wu, L.W., Simon, M.I., Baylor, D.A., and Chen, J. (2000). Rapid and reproducible deactivation of rhodopsin requires multiple phosphorylation sites. Neuron *28*, 153-164.

Michaelides, M., Hunt, D.M., and Moore, A.T. (2003). The genetics of inherited macular dystrophies. J Med Genet *40*, 641-650.

Moiseyev, G., Chen, Y., Takahashi, Y., Wu, B.X., and Ma, J.X. (2005). RPE65 is the isomerohydrolase in the retinoid visual cycle. Proc Natl Acad Sci U S A *102*, 12413-12418.

Moiseyev, G., Takahashi, Y., Chen, Y., Gentleman, S., Redmond, T.M., Crouch, R.K., and Ma, J.X. (2006). RPE65 is an iron(II)-dependent isomerohydrolase in the retinoid

visual cycle. J Biol Chem *281*, 2835-2840.

Molday, L.L., Rabin, A.R., and Molday, R.S. (2000). ABCR expression in foveal cone photoreceptors and its role in Stargardt macular dystrophy. Nat Genet *25*, 257-258.

Molday, R.S. (1998). Photoreceptor membrane proteins, phototransduction, and retinal degenerative diseases. The Friedenwald Lecture. Invest Ophthalmol Vis Sci *39*, 2491-2513.

Molday, R.S. (2007). ATP-binding cassette transporter ABCA4: molecular properties and role in vision and macular degeneration. J Bioenerg Biomembr *39*, 507-517.

Molday, R.S., Hicks, D., and Molday, L. (1987). Peripherin. A rim-specific membrane protein of rod outer segment discs. Invest Ophthalmol Vis Sci *28*, 50-61.

Molday, R.S., and Molday, L.L. (1987). Differences in the protein composition of bovine retinal rod outer segment disk and plasma membranes isolated by a ricin-gold-dextran density perturbation method. J Cell Biol *105*, 2589-2601.

Monaco, J.J., Cho, S., and Attaya, M. (1990). Transport protein genes in the murine MHC: possible implications for antigen processing. Science *250*, 1723-1726.

Moritz, O.L., and Molday, R.S. (1996). Molecular cloning, membrane topology, and localization of bovine rom-1 in rod and cone photoreceptor cells. Invest Ophthalmol Vis Sci *37*, 352-362.

Nakatani, K., and Yau, K.W. (1988). Calcium and magnesium fluxes across the plasma membrane of the toad rod outer segment. J Physiol *395*, 695-729.

Oldham, M.L., Khare, D., Quiocho, F.A., Davidson, A.L., and Chen, J. (2007). Crystal structure of a catalytic intermediate of the maltose transporter. Nature *450*, 515-521.

Oprian, D.D., Molday, R.S., Kaufman, R.J., and Khorana, H.G. (1987). Expression of a synthetic bovine rhodopsin gene in monkey kidney cells. Proc Natl Acad Sci U S A *84*, 8874-8878.

Oram, J.F. (2002). ATP-binding cassette transporter A1 and cholesterol trafficking. Curr Opin Lipidol *13*, 373-381.

Osterberg, G. (1935). Topography of the layer of rods and cones in the human retina. Acta Ophthalmol (Copenh) *6*, 1-102.

Palczewski, K. (1994). Is vertebrate phototransduction solved? New insights into the molecular mechanism of phototransduction. Invest Ophthalmol Vis Sci *35*, 3577-3581.

Palczewski, K., Buczylko, J., Ohguro, H., Annan, R.S., Carr, S.A., Crabb, J.W., Kaplan,

M.W., Johnson, R.S., and Walsh, K.A. (1994). Characterization of a truncated form of arrestin isolated from bovine rod outer segments. Protein Sci *3*, 314-324.

Palczewski, K., Kumasaka, T., Hori, T., Behnke, C.A., Motoshima, H., Fox, B.A., Le Trong, I., Teller, D.C., Okada, T., Stenkamp, R.E.*, et al.* (2000). Crystal structure of rhodopsin: A G protein-coupled receptor. Science *289*, 739-745.

Palczewski, K., Pulvermuller, A., Buczylko, J., and Hofmann, K.P. (1991). Phosphorylated rhodopsin and heparin induce similar conformational changes in arrestin. J Biol Chem *266*, 18649-18654.

Papermaster, D.S., and Dreyer, W.J. (1974). Rhodopsin content in the outer segment membranes of bovine and frog retinal rods. Biochemistry *13*, 2438-2444.

Papermaster, D.S., Schneider, B.G., Zorn, M.A., and Kraehenbuhl, J.P. (1978). Immunocytochemical localization of a large intrinsic membrane protein to the incisures and margins of frog rod outer segment disks. J Cell Biol *78*, 415-425.

Parish, C.A., Hashimoto, M., Nakanishi, K., Dillon, J., and Sparrow, J. (1998). Isolation and one-step preparation of A2E and iso-A2E, fluorophores from human retinal pigment epithelium. Proc Natl Acad Sci U S A *95*, 14609-14613.

Pinkett, H.W., Lee, A.T., Lum, P., Locher, K.P., and Rees, D.C. (2007). An inward-facing conformation of a putative metal-chelate-type ABC transporter. Science *315*, 373-377.

Poetsch, A., Molday, L.L., and Molday, R.S. (2001). The cGMP-gated channel and related glutamic acid-rich proteins interact with peripherin-2 at the rim region of rod photoreceptor disc membranes. J Biol Chem *276*, 48009-48016.

Poincelot, R.P., Millar, P.G., Kimbel, R.L., Jr., and Abrahamson, E.W. (1969). Lipid to protein chromophore transfer in the photolysis of visual pigments. Nature *221*, 256-257.

Pugh, E.N., Jr., and Lamb, T.D. (1993). Amplification and kinetics of the activation steps in phototransduction. Biochim Biophys Acta *1141*, 111-149.

Puig, J., Arendt, A., Tomson, F.L., Abdulaeva, G., Miller, R., Hargrave, P.A., and McDowell, J.H. (1995). Synthetic phosphopeptide from rhodopsin sequence induces retinal arrestin binding to photoactivated unphosphorylated rhodopsin. FEBS Lett *362*, 185-188.

Pulvermuller, A., Maretzki, D., Rudnicka-Nawrot, M., Smith, W.C., Palczewski, K., and Hofmann, K.P. (1997). Functional differences in the interaction of arrestin and its splice variant, p44, with rhodopsin. Biochemistry *36*, 9253-9260.

Radu, R.A., Mata, N.L., Nusinowitz, S., Liu, X.R., Sieving, P.A., and Travis, G.H. (2003). Treatment with isotretinoin inhibits lipofuscin accumulation in a mouse model of

recessive Stargardt's macular degeneration. P Natl Acad Sci USA *100*, 4742-4747.

Ramachandra, M., Ambudkar, S.V., Chen, D., Hrycyna, C.A., Dey, S., Gottesman, M.M., and Pastan, I. (1998). Human P-glycoprotein exhibits reduced affinity for substrates during a catalytic transition state. Biochemistry *37*, 5010-5019.

Rando, R.R. (1991). Membrane phospholipids as an energy source in the operation of the visual cycle. Biochemistry *30*, 595-602.

Rattner, A., Smallwood, P.M., and Nathans, J. (2000). Identification and characterization of all-trans-retinol dehydrogenase from photoreceptor outer segments, the visual cycle enzyme that reduces all-trans-retinal to all-trans-retinol. J Biol Chem *275*, 11034-11043.

Redmond, T.M., Yu, S., Lee, E., Bok, D., Hamasaki, D., Chen, N., Goletz, P., Ma, J.X., Crouch, R.K., and Pfeifer, K. (1998). Rpe65 is necessary for production of 11-cis-vitamin A in the retinal visual cycle. Nat Genet *20*, 344-351.

Reid, D.M., Friedel, U., Molday, R.S., and Cook, N.J. (1990). Identification of the sodium-calcium exchanger as the major ricin-binding glycoprotein of bovine rod outer segments and its localization to the plasma membrane. Biochemistry *29*, 1601-1607.

Reiter, E., and Lefkowitz, R.J. (2006). GRKs and beta-arrestins: roles in receptor silencing, trafficking and signaling. Trends Endocrinol Metab *17*, 159-165.

Reyes, C.L., and Chang, G. (2005). Structure of the ABC transporter MsbA in complex with ADP.vanadate and lipopolysaccharide. Science *308*, 1028-1031.

Riordan, J.R., Rommens, J.M., Kerem, B., Alon, N., Rozmahel, R., Grzelczak, Z., Zielenski, J., Lok, S., Plavsic, N., Chou, J.L.*, et al.* (1989). Identification of the cystic fibrosis gene: cloning and characterization of complementary DNA. Science *245*, 1066-1073.

Rivera, A., White, K., Stohr, H., Steiner, K., Hemmrich, N., Grimm, T., Jurklies, B., Lorenz, B., Scholl, H.P., Apfelstedt-Sylla, E.*, et al.* (2000). A comprehensive survey of sequence variation in the ABCA4 (ABCR) gene in Stargardt disease and age-related macular degeneration. Am J Hum Genet *67*, 800-813.

Rodieck, R.W. (1998). The First Steps in Seeing (Sunderland, Massachusetts, USA, Sinauer Associates, Inc.).

Rozet, J.M., Gerber, S., Souied, E., Ducroq, D., Perrault, I., Ghazi, I., Soubrane, G., Coscas, G., Dufier, J.L., Munnich, A.*, et al.* (1999). The ABCR gene: a major disease gene in macular and peripheral retinal degenerations with onset from early childhood to the elderly. Mol Genet Metab *68*, 310-315.

Ruetz, S., and Gros, P. (1994). Phosphatidylcholine translocase: a physiological role for

the mdr2 gene. Cell *77*, 1071-1081.

Saari, J.C. (2000). Biochemistry of visual pigment regeneration: the Friedenwald lecture. Invest Ophthalmol Vis Sci *41*, 337-348.

Saari, J.C., and Bredberg, D.L. (1989). Lecithin:retinol acyltransferase in retinal pigment epithelial microsomes. J Biol Chem *264*, 8636-8640.

Sanyal, S., and Jansen, H.G. (1981). Absence of receptor outer segments in the retina of rds mutant mice. Neurosci Lett *21*, 23-26.

Sarkadi, B., Price, E.M., Boucher, R.C., Germann, U.A., and Scarborough, G.A. (1992). Expression of the human multidrug resistance cDNA in insect cells generates a high activity drug-stimulated membrane ATPase. J Biol Chem *267*, 4854-4858.

Schlichtenbrede, F.C., da Cruz, L., Stephens, C., Smith, A.J., Georgiadis, A., Thrasher, A.J., Bainbridge, J.W., Seeliger, M.W., and Ali, R.R. (2003). Long-term evaluation of retinal function in Prph2Rd2/Rd2 mice following AAV-mediated gene replacement therapy. J Gene Med *5*, 757-764.

Schneider, E., and Hunke, S. (1998). ATP-binding-cassette (ABC) transport systems: functional and structural aspects of the ATP-hydrolyzing subunits/domains. FEMS Microbiol Rev *22*, 1-20.

Seddon, J.M., George, S., and Rosner, B. (2006). Cigarette smoking, fish consumption, omega-3 fatty acid intake, and associations with age-related macular degeneration: the US Twin Study of Age-Related Macular Degeneration. Arch Ophthalmol *124*, 995-1001.

Seigneuret, M., and Devaux, P.F. (1984). ATP-dependent asymmetric distribution of spin-labeled phospholipids in the erythrocyte membrane: relation to shape changes. Proc Natl Acad Sci U S A *81*, 3751-3755.

Shapiro, A.B., and Ling, V. (1994). ATPase activity of purified and reconstituted P-glycoprotein from Chinese hamster ovary cells. J Biol Chem *269*, 3745-3754.

Shroyer, N.F., Lewis, R.A., Allikmets, R., Singh, N., Dean, M., Leppert, M., and Lupski, J.R. (1999). The rod photoreceptor ATP-binding cassette transporter gene, ABCR, and retinal disease: from monogenic to multifactorial. Vision Res *39*, 2537-2544.

Sivaprasad, S., and Chong, N.V. (2006). The complement system and age-related macular degeneration. Eye *20*, 867-872.

Smith, W.C. (1996). A splice variant of arrestin from human retina. Exp Eye Res *62*, 585-592.

Smith, W.C., Milam, A.H., Dugger, D., Arendt, A., Hargrave, P.A., and Palczewski, K.

(1994). A splice variant of arrestin. Molecular cloning and localization in bovine retina. J Biol Chem *269*, 15407-15410.

Sparrow, J.R., Fishkin, N., Zhou, J., Cai, B., Jang, Y.P., Krane, S., Itagaki, Y., and Nakanishi, K. (2003). A2E, a byproduct of the visual cycle. Vision Res *43*, 2983-2990.

Sparrow, J.R., Kim, S.R., Cuervo, A.M., and Bandhyopadhyayand, U. (2008). A2E, a pigment of RPE lipofuscin, is generated from the precursor, A2PE by a lysosomal enzyme activity. Adv Exp Med Biol *613*, 393-398.

Stargardt, K. (1909). Uber familiare, progressive degeenration under makulagegend des augen. Albrecht von Graefes Arch Ophthalmol *71*, 534-550.

Stenirri, S., Battistella, S., Fermo, I., Manitto, M.P., Martina, E., Brancato, R., Ferrari, M., and Cremonesi, L. (2006). De novo deletion removes a conserved motif in the C-terminus of ABCA4 and results in cone-rod dystrophy. Clin Chem Lab Med *44*, 533-537.

Sun, H., Molday, R.S., and Nathans, J. (1999). Retinal stimulates ATP hydrolysis by purified and reconstituted ABCR, the photoreceptor-specific ATP-binding cassette transporter responsible for Stargardt disease. J Biol Chem *274*, 8269-8281.

Sun, H., and Nathans, J. (2001). Mechanistic studies of ABCR, the ABC transporter in photoreceptor outer segments responsible for autosomal recessive Stargardt disease. J Bioenerg Biomembr *33*, 523-530.

Sun, H., Smallwood, P.M., and Nathans, J. (2000). Biochemical defects in ABCR protein variants associated with human retinopathies. Nat Genet *26*, 242-246.

Sung, C.H., Makino, C., Baylor, D., and Nathans, J. (1994). A rhodopsin gene mutation responsible for autosomal dominant retinitis pigmentosa results in a protein that is defective in localization to the photoreceptor outer segment. J Neurosci *14*, 5818-5833.

Takeda, S., Kadowaki, S., Haga, T., Takaesu, H., and Mitaku, S. (2002). Identification of G protein-coupled receptor genes from the human genome sequence. FEBS Lett *520*, 97-101.

Tam, B.M., Moritz, O.L., Hurd, L.B., and Papermaster, D.S. (2000). Identification of an outer segment targeting signal in the COOH terminus of rhodopsin using transgenic Xenopus laevis. J Cell Biol *151*, 1369-1380.

Tamehiro, N., Zhou, S., Okuhira, K., Benita, Y., Brown, C.E., Zhuang, D.Z., Latz, E., Hornemann, T., von Eckardstein, A., Xavier, R.J.*, et al.* (2008). SPTLC1 binds ABCA1 to negatively regulate trafficking and cholesterol efflux activity of the transporter. Biochemistry *47*, 6138-6147.

Teller, D.C., Okada, T., Behnke, C.A., Palczewski, K., and Stenkamp, R.E. (2001). Advances in determination of a high-resolution three-dimensional structure of rhodopsin, a model of G-protein-coupled receptors (GPCRs). Biochemistry *40*, 7761-7772.

Thibodeau, P.H., Brautigam, C.A., Machius, M., and Thomas, P.J. (2005). Side chain and backbone contributions of Phe508 to CFTR folding. Nat Struct Mol Biol *12*, 10-16.

Travis, G.H., Brennan, M.B., Danielson, P.E., Kozak, C.A., and Sutcliffe, J.G. (1989). Identification of a photoreceptor-specific mRNA encoded by the gene responsible for retinal degeneration slow (rds). Nature *338*, 70-73.

Tutulan-Cunita, A.C., Mikoshi, M., Mizunuma, M., Hirata, D., and Miyakawa, T. (2005). Mutational analysis of the yeast multidrug resistance ABC transporter Pdr5p with altered drug specificity. Genes Cells *10*, 409-420.

Urbatsch, I.L., al-Shawi, M.K., and Senior, A.E. (1994). Characterization of the ATPase activity of purified Chinese hamster P-glycoprotein. Biochemistry *33*, 7069-7076.

van Helvoort, A., Smith, A.J., Sprong, H., Fritzsche, I., Schinkel, A.H., Borst, P., and van Meer, G. (1996). MDR1 P-glycoprotein is a lipid translocase of broad specificity, while MDR3 P-glycoprotein specifically translocates phosphatidylcholine. Cell *87*, 507-517.

Wabbels, B., Demmler, A., Paunescu, K., Wegscheider, E., Preising, M.N., and Lorenz, B. (2006). Fundus autofluorescence in children and teenagers with hereditary retinal diseases. Graefes Arch Clin Exp Ophthalmol *244*, 36-45.

Wang, X., Koulov, A.V., Kellner, W.A., Riordan, J.R., and Balch, W.E. (2008). Chemical and biological folding contribute to temperature-sensitive DeltaF508 CFTR trafficking. Traffic *9*, 1878-1893.

Ward, A., Reyes, C.L., Yu, J., Roth, C.B., and Chang, G. (2007). Flexibility in the ABC transporter MsbA: Alternating access with a twist. Proc Natl Acad Sci U S A *104*, 19005-19010.

Weng, J., Mata, N.L., Azarian, S.M., Tzekov, R.T., Birch, D.G., and Travis, G.H. (1999). Insights into the function of Rim protein in photoreceptors and etiology of Stargardt's disease from the phenotype in abcr knockout mice. Cell *98*, 13-23.

Winston, A., and Rando, R.R. (1998). Regulation of isomerohydrolase activity in the visual cycle. Biochemistry *37*, 2044-2050.

Yamada, E. (1969). Some structural features of the fovea centralis in the human retina. Arch Ophthalmol *82*, 151-159.

Yang, Z., Camp, N.J., Sun, H., Tong, Z., Gibbs, D., Cameron, D.J., Chen, H., Zhao, Y., Pearson, E., Li, X.*, et al.* (2006). A variant of the HTRA1 gene increases susceptibility to

age-related macular degeneration. Science *314*, 992-993.

Young, R.W. (1971). THE RENEWAL OF ROD AND CONE OUTER SEGMENTS IN THE RHESUS MONKEY. Journal of Cell Biology *49*, 303.

Young, R.W. (1976). Visual cells and the concept of renewal. Invest Ophthalmol Vis Sci *15*, 700-725.

Young, R.W. (1987). Pathophysiology of age-related macular degeneration. Surv Ophthalmol *31*, 291-306.

Zaman, G.J., Flens, M.J., van Leusden, M.R., de Haas, M., Mulder, H.S., Lankelma, J., Pinedo, H.M., Scheper, R.J., Baas, F., Broxterman, H.J*., et al.* (1994). The human multidrug resistance-associated protein MRP is a plasma membrane drug-efflux pump. Proc Natl Acad Sci U S A *91*, 8822-8826.

Zhong, M., Molday, L.L., and Molday, R.S. (2008). Role of the C-terminus of the photoreceptor ABCA4 transporter in protein folding, function and retinal degenerative diseases. J Biol Chem.

Zhou, Z., White, K.A., Polissi, A., Georgopoulos, C., and Raetz, C.R. (1998). Function of Escherichia coli MsbA, an essential ABC family transporter, in lipid A and phospholipid biosynthesis. J Biol Chem *273*, 12466-12475.